DESIGN AND FABRICATION OF MICROSTRIP ANTENNAS FOR IOT ENABLED DEVICES FOR WIRELESS APPLICATIONS

Thesis Submitted for the Award of the Degree of

DOCTOR OF PHILOSOPHY

in

Electronics and Communication Engineering

By

Rashmi Roges

Registration Number: 11919226

Supervised By

Dr Praveen Kumar Malik (23314)

Professor

School of Electrical and Electronics Engineering

Lovely Professional University

LOVELY PROFESSIONAL UNIVERSITY, PUNJAB

2023

DECLARATION

I, hereby declare that the presented work in the thesis entitled "**Design and Fabrication of Microstrip Antennas for IoT Enabled Devices for Wireless Applications**" in fulfilment of the degree of **Doctor of Philosophy (Ph. D.)** is the outcome of research work carried out by me under the supervision Prof. Dr. Praveen Kumar Malik, working as Professor, in the School of Electronics and Electrical Engineering of Lovely Professional University, Punjab, India. In keeping with the general practice of reporting scientific observations, due acknowledgments have been made whenever the work described here has been based on the findings of other investigators. This work has not been submitted in part or full to any other University or Institute for the award of any degree.

Name of the Scholar: Rashmi Roges

Registration No: 11919226

Department/School: Electronics and Communication Engineering

Lovely Professional University,

Punjab, India

CERTIFICATE

This is to certify that the work reported in the Ph. D. thesis entitled "**Design and Fabrication of Microstrip Antennas for IoT Enabled Devices for Wireless Applications** " submitted in fulfillment of the requirement for the reward of degree of **Doctor of Philosophy (Ph.D.)** in the School of Electronics and Electrical Engineering, is a research work carried out by **Rashmi Roges**, 11919226, is bonafide record of his/her original work carried out under my supervision and that no part of thesis has been submitted for any other degree, diploma or equivalent course.

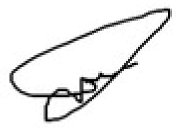

Name of the Supervisor: Dr. Praveen Kumar Malik

Designation: Professor

Department/School: School of Electronics and Electrical Engineering

Lovely Professional University

Jalandhar, Punjab

ABSTRACT

During the initial years of the 21st century, the Internet was limited to desktops, laptops, and smartphones. But for some time now, practically all electronic gadgets can be connected to the internet and controlled remotely. This is IoT. IoT is already influencing and shaping our lives in many ways. An IoT system can provide an enhanced response, along with tracking and logical capabilities, and it is now being embraced in almost all industrial scopes and opens the door to innumerable applications. When the internet helped to connect people, share information and ideas, and perform better, the Internet of Things is enabling the same for the things and the gadgets around us. The combination of IoT with other recent technologies like Machine Learning Cloud Computing and Artificial Intelligence is ever more promising in this era.

Consider a practical example of an IoT system, in which some household electronic gadgets relate to a car. When the person opens the car door while reaching home, the home door unlocks and the air conditioner is set per the room temperature, the coffee pot and the water heater are turned on by themselves. The system is very appealing but to implement such a system, there should exist efficient communication between these devices and the data received should be processed and interpreted correctly. It is a melodious interoperation of many components.

An IoT system architecture basically includes IoT devices, which are either electronic gadgets like home appliances or sensors and actuators. The IoT devices collect the data and share them. The data is shared and exchanged through gateways and this layer sets all the rules for data collection. Then comes the processing engine or the event processing layer which processes the data collected. Finally comes the application layer which acts as an interface between the application and the user.

The devices are connected to the network through gateways and gateways must transfer the information to the cloud. Wired and wireless interfaces like Wi-Fi, Bluetooth, LoRa, GSM, etc. are used to achieve connectivity between these modules.

The connectivity block is considered the backbone of any IoT system. Protocols like Bluetooth, Wi-Fi, Z-Wave, ZigBee, etc. satisfy the wireless connectivity criteria and they are used to interface with any application or module. The modern communication

systems used for connectivity are more about compactness and mobility, cost-effectiveness, and supporting multiple applications while simultaneously supporting high-speed data streaming. An antenna is an obligatory component of any radio communication module and microstrip patch antennas can very well satisfy many of the demands put up by modern communication systems.

An IoT connectivity system is highly application-specific. It is based on different factors like the place where it is to be deployed along with the sensors or devices, the number of devices deployed, the range of connectivity required, the power constraints of the system, the accuracy of data, the cost-effectiveness required, and many more. In this modern age of miniaturization and mobility, microstrip patch antennas that can cover a wider area and those that can be easily integrable with IoT-enabling devices like the ESP8266 modules while they can simultaneously support more than one application are yet to be optimized.

Patch antennas are known for their features like low profile, low cost, and small size. The challenges faced while designing patch antennas are their narrow bandwidth and performance deterioration at higher frequencies. This thesis is about designing and fabricating microstrip patch antennas that can overcome the disadvantages of patch antennas and meet the standards required for IoT system connectivity through IoT-enabling modules like ESP8266.

The research work was done by giving emphasis on the fact that most of the IoT-enabling communication protocols are in the sub-6 GHz frequency spectrum and IoT applications require low-cost, compact antennas which work on sub-6 GHz communication protocols. After a thorough literature analysis, MIMO antennas with DGS were designed to attain antennas working on the desired range of frequencies with good performance and compact size. Wide-band and multi-band sub-6 GHz antennas are designed along with an antenna working at the most versatile 2.4 GHz frequency. Isolation between the component antennas is also enhanced using the DGS technique for better communication system performance. The antenna structures proposed in this thesis are designed and simulated using the High-Frequency Structure Simulator (HFSS) tool by Ansys and are later fabricated using Computer Numeric Control (CNC). The antennae are fabricated on the popular, low-cost, effortlessly available FR4 substrate, and are then tested using a Vector Network Analyzer.

Four antenna designs are discussed in this thesis to cater to any sub-6 GHz communication protocols employed for different IoT applications including narrowband applications, wideband applications, and multi-band required applications, with short and long-range coverage. The first and second antenna structures are like Log-Periodic structures. The first antenna discussed is a single, narrow-band, monopole antenna, with a co-planar feed, working at 2.46 GHz. The second structure discussed is a MIMO antenna system with DGS covering a range of operational frequencies (wideband) of almost 2 GHz between 2 GHz to 4 GHz with medium and long-range covering protocol support. The next antenna structure studied works in the sub-GHz range where LoRa modules are used. This antenna is specially proposed for medium-range IoT applications using LoRa or ESP8266 modules and can support LPWAN technology. A tri-band MIMO antenna is finally proposed to work at 2.4 GHz, 5.2 GHz, and 5.8 GHz IoT applications systems. Parameters such as the reflection coefficient, radiation characteristics and gain, and MIMO parameters (in the case of MIMO antennas) are studied for all the designed antenna structures.

ACKNOWLEDGEMENT

First, I would like to pay my thanks to Almighty God who gave me life and power, without which the work would not have seen the light of the day.

I feel privileged to express my sincere thanks to my guide **Dr Praveen Kumar Malik** who led me to this point. His passion, discipline, and guidance have been the stepping stones to my growth as a scientist and as a human being over the last four years. I express my special thanks to his dedication to delivering valuable education to his students.

It is a great privilege to express my deepest and most sincere gratitude to my mentor and colleague Dr Sandeep Sharma for the valuable suggestions and guidance during the thesis. His integrated and dynamic personality can never go unacknowledged.

I wish to acknowledge the infrastructure and facilities provided by the School of Electronics and Electrical Engineering, Lovely Professional University, and the Research Department to guide me on a timely basis regarding the norms and guidelines.

I am very thankful to **Prof Payal Pahwa**, and **Dr Niranjan Bhattacharya,** and my friends: **Ms Maansi Gulati**, **Ms Usha Sharma, Mr Risheek Kumar, Dr Shikha Gupta, Dr Ritesh Vyas, Mr Pradeep Kumar, Dr Dilip Diwedi, Mr Jatin Gaur, Ms Sneha, Dr Abdul Rahim,** and **Mr Raja Ram** who has been constant pillars of support throughout this work.

Finally, I would like to thank my family members. I am grateful to my mother who is encouraging and supporting me constantly and without her support, every step in life seems impossible. I owe all my achievements to my father, who is not only my father but also a teacher who taught me the lessons of life. I pay my thanks to my sister and her family for giving me never-lasting support and to my son who has been an inspiration to me ever since he came into my life.

21st October 2023

Table Of Contents

List of Tables

List of Figures

List of Appendices

CHAPTER 1

INTRODUCTION

Today, we experience a digital world around us with high-end technology influencing every walk of human life. Over the last few decades, digital technology has evolved tirelessly, and now it is nearly impossible to even think about day-to-day activities without it. Till around the 1950s, the whole focus of the technical world was on mechanical systems and the development of new machines and devices that could replace the mechanical efforts of human beings. With the invention of transistors in the late 1940s, the electronic industry started progressing. It did not take much time for the electronic industry to start exploiting the advantages of digital systems. Within no time, processors and computers conquered the whole focus of the technological industry. By the 1970s, the first computer, ENIAC ("Electronic Numerical Integrator and Computer"), was ready. Further, the silicon wafer technology advanced exponentially, inventing more and more consumer electronic devices with enhanced features and controls. Today, we stand at the doorstep of its latest state with the Internet of Things (IoT), Deep Learning (DL), Machine Learning (ML) and Artificial Intelligence (AI).

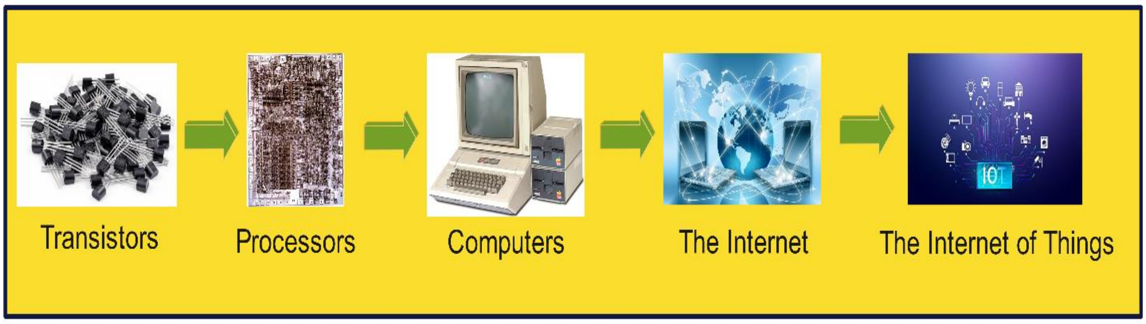

Figure 1.1: Stepwise Evolution of the IoT Technology

Technological evolution never has had any setbacks since the invention of the transistors. This is pictorially represented in Figure 1.1. Microprocessors containing multiple transistors were developed after the invention of transistors and their miniaturization, resulting in more electronic devices, and better-performing computers. Then came the Internet, in the 1990s, with the development of the World Wide Web and this revolutionized electronic communication. Now, we stand at a point where all devices and equipment connected to the Internet are linked to one another. Since the first men went to the moon, even more competent processors have been made, and at present, a normal Motor Car, irrespective of the company, holds more computational power compared to the entire intelligence that was possessed by the space vehicle of the early century. Currently, increasingly powerful, and cheaper computers and technologies are available as the "information revolution" unfolds around us. Consequently, these technologies are now widely used in all aspects of our day-to-day life. It has invaded all fields including finance, trade, healthcare, the entertainment industry, education, terrestrial exploration, defense industry, communication technology, the digital market, and the government and its institutions. To summarise, at the beginning of the Industrial Revolution, it was human mechanical power that was incorporated into machines for comfort and convenience, but now computers are being built with human cognition and intelligence [1].

1.1 INTERNET OF THINGS (IOT)

With no ambiguity, the "Internet of Things" is one of the most exquisite and attractive technologies of the current digital era. Following the two phenomenal revolutions of the personal computer and the world wide web, IoT is the third evolution which is set to contribute yet another huge dive in the arena of digital information technology. Everything and anything can be connected to the internet through this platform. There are several fields where IoT has the potential to be applied, including day-to-day life and well-being of people, military and satellite communication systems, various industries, environment and agriculture monitoring systems, public safety, traffic and transportation, and a multitude of other components as well. [2]. Up until this point, we had a wide variety of smart devices. IoT is all about establishing connections between the billions of physical devices that are currently connected to the web of the internet and developing a platform for the sharing of their data to further improve and facilitate human existence. Having a wired or wireless communication component facilitates the collection of information and its exchange [3]. As an illustration, consider a modern smartphone that has features like voice recognition, facial recognition, mobile accelerometer, adaptive brightness, GPS tracking, and more. On the other hand, the gadget can be considered smarter if the smartphone can adjust its brightness based just on data received from the GPS receiver or the orientation in which the device is being held. Each component is assigned to carry out various functions. Therefore, a more attractive system can be created if the attributes can communicate with one another or if they are able to share a database.

The Internet of Things acts as a connecting platform for electronic, software, and sensor embedded-objects to the internet, where data can be collected and exchanged [4]. In any case, far-off frameworks inside a house, like, the locking system, the Air Conditioner, the lighting in the house, the cooler, and many more gadgets can be connected to a solitary stage forming a smart style of living. Likewise, various components in a vehicle can be linked to interact and share data with one another, and in a more advanced stage, a smart vehicle can even be linked to a smart home for greater efficiency. The representation in Figure 1.2 is a straight-forward look at IoT which shows its true potential.

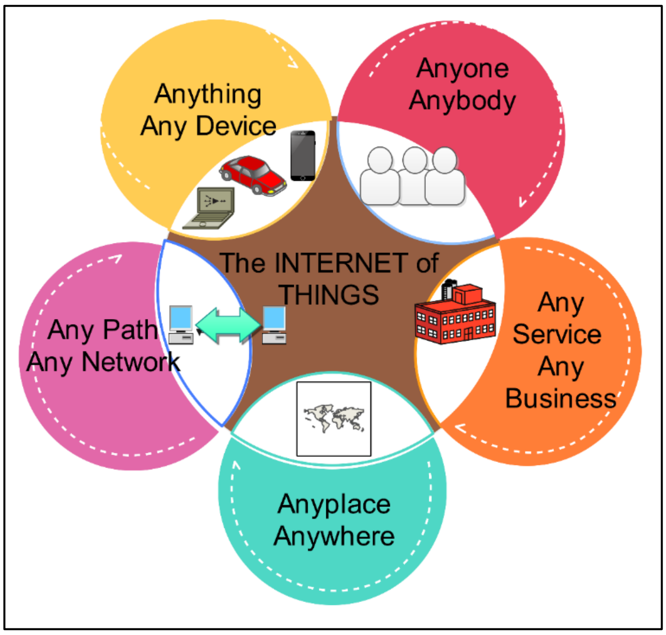

Figure 1.2: A representation of the actual implication of IoT

In the year 1999, when both "Radio Frequency Identification Technology" and the Internet were very novel to the market, Kevin Ashton, (also known as the Father of IoT), first proposed the idea of implementing IoT in the P&G products supply chain. Kevin anticipated that this scheme could possibly enable PCs to totally construct a framework including data collection, interpretation, and exchange setting up smarter systems with more functions [5].

Up until this point, we had numerous gadgets, every one of them being smart and jam-packed with technologies to simplify day-to-day life. IoT is about associating billions of such gadgets all over the planet, that are connected to the internet, to make a common stage for their information where it can be exchanged, analyzed, and shared to enhance of human life. IoT has in it a communication module, for physical or remote correspondence of the gathered information, and a sensor system, in order to detect, gather, and send information [6]. The gadgets that we use, have rebuilt themselves into articles with the assistance of the internet and a few upcoming technologies that incorporate advanced communication modules, and smart sensor nodes. According to the description of the Internet of Things in [7], it can be characterized in three specific sections, the 'Things" or fundamental parts of this framework, “connectivity" and “information collected and processed” which are being used for various purposes. An IoT framework is effectively executed when every one of the specified three standards is performing at its best possible levels. The entire IoT framework is tied in with detecting, and imparting the information collected to an IoT stage of high-end processing and the client or customer interest and its retransmission to the client who is at the beneficiary end. An IoT framework comprises three significant parts which are shown in Figure 1.3

i) Sensors or gadgets

ii) Connectivity framework

iii) People and Purposes

IoT, in short, is a blend of technologies. The progress and expansion of RFID technology, empowering the tracking and detecting of devices, individuals, and creatures, played a significant impact on the foundation of IoT. There can be two sorts of RFID organizations, simple individual RFID tags and more complicated networks of RFID [8]. RFID innovation has a restraint of being intended for pre-tagged items.

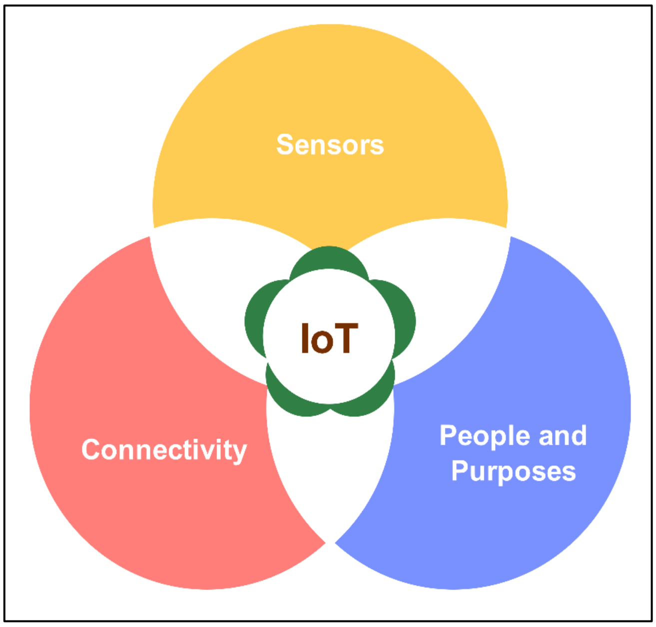

Figure 1.3: The major components of Internet of Things

The innovative IoT technology will upsurge its operating areas to the telecom industry, information technology and informatics, modern electronic gadgets, and sociology completely. It will take advantage of the worldwide connection through the internet which is omnipresent today, by incorporating RFID labels in eatables and drinks, records, household equipment, and so on. The sensors or actuators are installed to sense, collect, and exchange the data required for the application and this data is then available with a web of data exchange platform which is a lot bigger than the internet. Full-scale interoperability will be available for the devices connected without exception if they are connected to the internet. This makes "things" independent, free, and versatile. The threats existing are in terms of data security, and privacy as shown in Figure 1.4.

Extensive research and studies have been carried out in the areas of smart sensors, high-end computers and processors, and good, efficient, and compact communication technology for more than a decade now in order to exploit the features and promises of IoT technology to its maximum. Major application areas of IoT are summarized in Figure 1.5

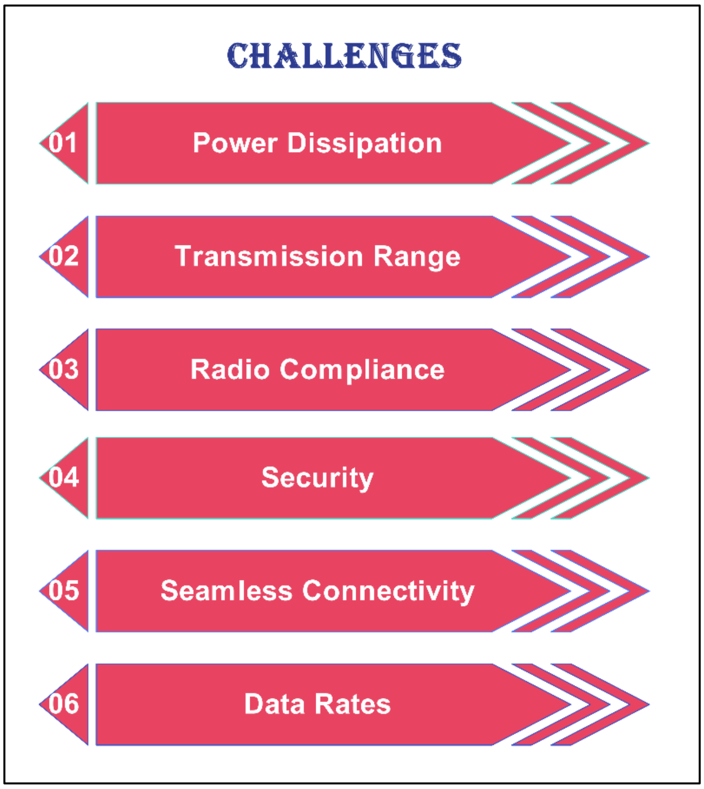

Figure 1.4: The challenges faced by an IoT system

Some common applications of IoT include:

- *"Smart Interactive home"*

It is one of the most prevalent and alluring applications of IoT. Its popularity has pulled around 256 companies and startups to its Analytics database. More and more companies are still stepping foot into this area to provide better services at cheaper rates.

- *"Smart City"*

Smart homes were further expanded to smart cities by adding water distribution management systems, traffic control systems, environmental monitoring systems, waste management systems, and many more. The IoT solutions in all these aspects helped with traffic and time management, reduced pollution and noise, and provided cleaner and safer cities.

- *"Smart grids"*

Smart grids are a special application in a smart city. A future smart grid can ensure the utilization of the characteristic behaviours of electricity suppliers and consumers from the past to improve the efficiency and reliability of power supply systems and ensure their utilization economically.

- *"Smart Health"*

The digital healthcare system and telemedicine bring forward the idea of smart medical devices and equipment with a lot of additional facilities compared to the traditional medical systems. This can highly enhance the medical care and attention given to patients, especially in pediatrics and old age.

- *"Smart supply chain"*

IoT can help in tracking the commodities and sharing the inventory information of goods on road with the suppliers for its smart management.

- *"Smart farming"*

The concept underlying in smart farming or precision agriculture is about enabling the agrarian sector to utilize all available setup it needs including the weather reports and soil quality and to use high-end technologies, such as "Big Data," the cloud, and the "Internet of Things" (IoT), for mechanizing, tracking, and supervising activities.

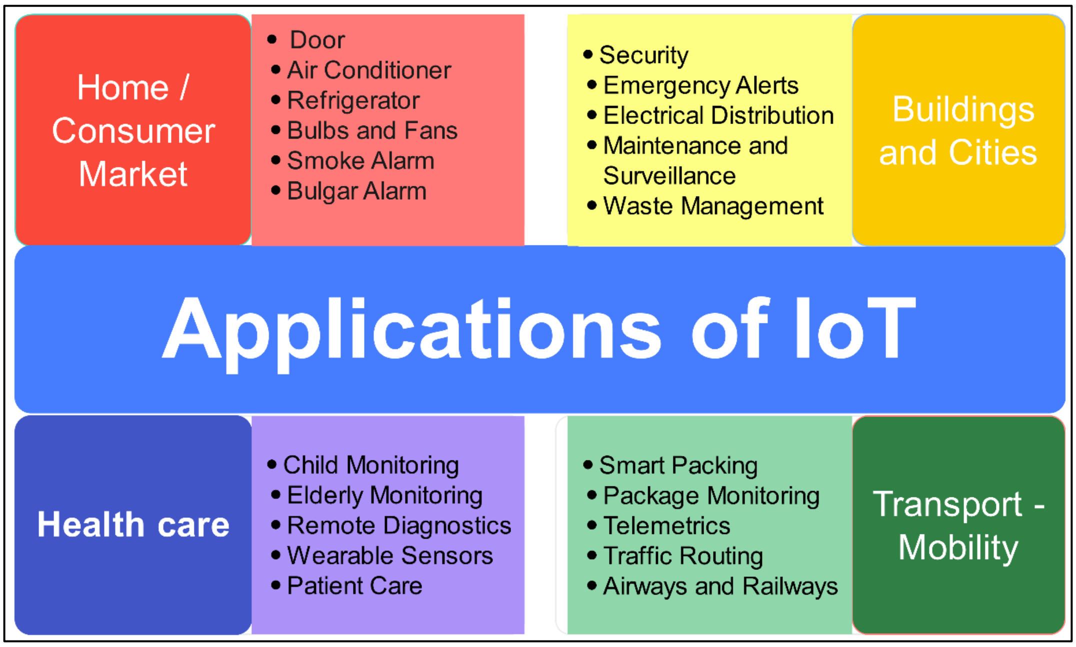

Figure 1.5: Major application areas of the Internet of Things

Network of Things called IoT, will offer a platform for linking the advanced and high-end machines or components to a platform or network where data is collected, processed, and made accessible in order to enable a much more powerful, competent system. Human interaction with things and equipment around would be more efficient and effective with the implementation of IoT. It creates a more intelligent, time-saving, and secure environment for human life. IoT will be the finishing touch to connect, assess, and integrate the existing technologies to unlock their full potential. To make the necessary data easily accessible, IoT needs to be integrated with advanced and effective wireless communication technology

1.2 THE MICROSTRIP PATCH ANTENNAS

Antennas are metallic devices, capable of radiating or collecting radio energies. When information is to be transmitted by a wireless channel, it is first converted into electrical signals and then they are fed to an antenna through a guided medium. The antenna radiates the electrical signal, containing the information, as electromagnetic waves, into the free space. At the receiver end, the antenna can detect and receive the electromagnetic waves in the atmosphere or vicinity and gather the transmitted information from them. The antennas are available in a variety of sizes and shapes, as per the demands of the application. As in the case of a dipole, which generates and propagates EM waves by the movement of both positive and negative charges, the antenna is also so arranged to attain oscillations of positive and negative charges, which in turn results in the generation of EM waves and their propagation through free space.

At the application of alternating potential to a conductor, oppositely charged particles will start accumulating at both ends of the conductor (antenna in this case). As the polarity of the potential shifts, the accumulated charges also interchange sides. These shifting sides of the charged particles can be considered as oscillations of the charged particles. The charge concentrations meet at $t=T/4$ while interchanging their position and at this point of intersection, an electromagnetic wave separates from the conductor and starts to propagate forward. This is the electromagnetic wave that will propagate through free space, to the receiver. At the receiver antenna/conductor, it senses the presence of electromagnetic waves in space and these waves cause an accumulation of charges at both ends of the conductor. The oscillations of these accumulated charges according to the received EM wave cause voltage fluctuations corresponding to the transmitted message.

A class of planar antennas that have been extensively researched and developed in the past three or four decades is the Microstrip Patch Antennas (MPA). Microstrip patch antennas are a type of smart antenna, and the world today would indeed be impossible to imagine without them. The features of microstrip antennas like the low cost, low-profile, planar, robustness (as per the surface on which it is mounted), etc. along with easily designable operational parameters, have attracted communication engineers and in today's world, MPAs have completely monopolized the wireless communication industry. Even though MPAs have drawbacks like reduced gain, limited bandwidth, and polarization impurity, they still find a wide range of fields where they fit in well [9]. MPAs were initially used in military and defence as they were the best candidate that could be easily integrated into fast-moving spacecraft and rockets. With time, the studies, and research on MPAs were able to improve their performance parameters by various techniques and this enabled in extension of the application fields of MPAs. The other industries, wireless gadgets, mobiles and wireless communication systems, GPS, and navigation systems, and many more fields started utilizing the advantageous features of patch antennas. Due to their compact size and planar nature, these antennas are extremely versatile.

The history of patch antennas pulls back to the 1950s but they gained attention when the VLSI and IC industry kicked off their era around the 1970s. The launch of VLSI technology and extensive research in the field of semiconductor physics resulted in large-scale miniaturization of electronic systems. This further marked the start of the age of consumer electronics. With time, these gadgets gained more and more popularity and became an inevitable part of daily life. Since then, patch antennas have also been studied extensively to overcome their drawbacks and to be utilized in and with modern electronics. Communication engineering, especially wireless communication also advanced simultaneously and today we are in the digital era where technology can hardly be detached from day-to-day life.

The idea of a printed antenna was happily welcomed as its applications were innumerable. This field still faces never-ending demands for improvement as the related technology saw no looking back. Wireless communication standards keep improving day by day and antenna designs have to keep up with the growing demand now, at the doorsteps of 5G, miniature and efficient microstrip antennas to support the upcoming technology are just inevitable.

The microstrip patch antennas have seen a steady graph of development since the growth in integrated circuits and VLSI. Microstrip antenna consists of very of a conducting patch and ground plane on either plane of a dielectric substrate material, as shown in Figure 1.6.

The radiating patch on the Microstrip antenna was rectangular at the beginning and as researchers went on with their studies the patch used changed to different geometrical patch shapes and different shapes provided different properties like some of them helped in the miniaturization of the size of the antenna where some others provided higher gain and directivity and some else gave better bandwidth and so on.

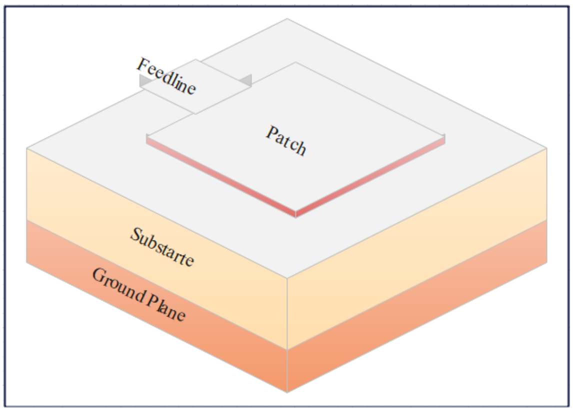

Figure 1.6: Structural organization of basic MPA depicting its layers

1.3 MOTIVATION

Today, digital technology is in high gear because it has proven to be indispensable to human life and has unbelievably stamped itself into our everyday day. A new technique usually goes through a series of steps while being optimized and that includes the process of discovery of the idea, the engineering of this idea, and finally the implantation and transformation of this idea into a reality. A true transformation of any idea into a useful technology is indeed the result of the contribution of more than one related technology. Likewise, the digital age has also advanced through these stages to usher in the era we know today as the digital age.

Since the advent of computers, technology has never had to look back. The industrial revolution was all about relaxing the mechanical strain on humans by implementing heavy machinery and now the digital revolution, at this stage, is all about embedding human intellect into machines [10].

The “Internet of Things,” is watched upon as the most significant phenomena of the twenty-first century. Following the gigantic transformations in the digital information industry, computers, and the world of the Internet, the next technology that will contribute another significant milestone in this field is the Internet of Things. The IoT creates a large platform for connecting every device that is connected to the internet. The Internet of Things might very well enhance every field of human walk, from people's daily lives and health care systems to armed services, satellite navigation, enterprises, surveillance systems, public health, security, and so on.

Nowadays, we have a plethora of gadgets, which are intelligent by themselves. Implementation of IoT will ensure the networking of millions and billions of such intelligent devices, which are connected to the internet, to be interlinked to each other, capable of sharing each other’s data and making much smarter decisions for themselves. Thus, IoT is expected to simplify human life much more. For this process to happen, a communication module should be installed, wired or wireless, to facilitate the data-sharing process. The efficiency of this communication module will directly monitor the efficiency of the system.

IoT is a recent revolutionary technology that is yet to be exploited to its maximum potential. The planar antennas and their efficiency are a vital part of a node to be activated for IoT. The better performance of the device is the result of its entire component’s performance. Microstrip antenna is proposed to be designed and fabricated which would help in the better performance of IoT-enabled devices. It will add to the quality of IoT applications in terms of coverage area and signal strength as our aim is to design an optimized antenna for IoT applications that will cover a larger area and be compatible with the other device systems. With advancements in IoT devices for wireless communication, many Industrial issues will be well tackled where different machines (manufacturing individual parts) of a single modal, communicate with each other and perform assembling and designing as per requirement without any human interference.

Energy consumption and device size have always remained major areas of concern with IoT technology. Large-scale data collection, its manipulation, and decision making followed by transmitting the results of these calculations when and where required has further amplified the intricacy of the system we are dealing with. So, to sum up, in order to enhance the performance of the communication module of IoT systems, antennas in the module also need to be optimized in terms of size, cost, performance, and power consumption.

1.4 STATEMENT OF PROBLEM

From the detailed survey of currently available literature on IoT antennas, it is well evident that IoT systems need good-performance radiating systems to augment the performance of the communication module of the IoT systems. The communication module of the IoT system is greatly oriented according to the application for which it is designed but in this modern world, which holds miniaturization, portability, and ease of use as its logo, communication systems with antennas which are i) compact, ii) having good performance parameters, iii) supporting multiple communication protocols, and iv) having good range of coverage are highly desirable.

1.5 SCOPE OF THE PROPOSED WORK

This work emphasizes on designing and fabricating microstrip patch antennae for emergent IoT applications. Antenna parameters like the frequency of resonance, the bandwidth for operation, VSWR (Voltage Standing Wave Ratio), the gain and directivity, along with the MIMO performance parameters like ECC ("Envelope Correlation Co-efficient"), DG ("Diversity Gain"), Isolation, MEG ("Mean Effective Gain"), and TARC ("Total Active Reflection Co-efficient") are to be optimized for the good performance of the antenna in the IoT system. The HFSS ("High-Frequency Structure Simulator") Software tool is used in the designing, simulation, and optimization process of the antenna and the following are the steps in the process.

i. An extensive literature review and analysis of already existing antennas and their parameters.

ii. Designing, analyzing, and optimizing a compact antenna for IoT applications in terms of operating frequency, gain, and range of coverage.
iii. Simulation of the proposed structure in HFSS software, along with fabrication and testing of the design for validation of the simulated results with experimental results.
iv. A comparative study of the designed compact IoT antenna with other similar antennas in the literature.

1.6 RESEARCH OBJECTIVES

Following are the research objectives set for this work.

i. To study, review, and design a Microstrip patch (Array/MIMO) antenna which could be utilized in the IoT enabled modules like ESP8266 module to meet the incipient demands.
ii. Optimize the antenna performance parameters like Gain, Radiation pattern, etc for the better performance of the system.
iii. To design a Microstrip antenna that covers a wider radiation area as compared to the present system.
iv. Real-time implementation of designed and fabricated Microstrip antenna with enough isolation to simultaneously support various IoT applications.

The research objectives are fulfilled in this study through the design of 4 different antennas meeting the required parameter specifications for various IoT applications. The designed antennas are explained in detail in Chapters 5, 6, and 7 in order to fulfill the formulated research objectives. These designed antennas cater to all operating frequencies of various IoT applications in the sub-6 GHz spectrum.

Antenna 1 referred to in Chapter 5 is a compact monopole antenna with high gain, designed for various 2.4 GHz IoT applications. 2.4 GHz frequency is highly versatile as it supports various wireless protocols such as Bluetooth, Wi-Fi, ZigBee, etc. This antenna can be integrated with the ESP8266 module and other IoT-enabling devices as an external antenna to facilitate various IoT short and medium-range applications like smart homes. **This design and study fulfill objective 1 of the research objectives**.

Antenna 2 discussed in Chapter 5 is a miniaturized MIMO antenna system with good radiation properties and radiation efficiency with a wide bandwidth of 2 GHz. The operational frequency range of this antenna, (2.01 to 4.04 GHz), includes WiMAX (supporting an operational range of up to 50 KM) and WLAN frequency bands and enables medium and long-range IoT applications. The compactness of this antenna along with good performance enhances their use with small sensor nodes deployed for various surveillance applications. The MIMO diversity parameters of this antenna is optimized by employing the DGS technique. **The proposed compact MIMO antenna system fulfills objectives 1, 2, and 3.**

Antenna 3 in this study, discussed in Chapter 6 is a LoRa range supporting monopole antenna. LoRa is an emerging and proposed protocol for various long-range, low-bandwidth IoT applications and is highly power efficient. IoT applications like geographic studies, war field deployments, etc. can employ the proposed antenna as these applications are required to transmit small amounts of data for surveillance and cannot be frequently attended to, in order to replace the power module. The use of 'Chirp Spread Spectrum' in LoRa enables it to support a range as long as 15 KM. **Antenna 3 fulfills objectives 2 and 3 of this study.**

Antenna 4, as discussed in Chapter 7, is a 2-element compact multiband MIMO antenna to fulfill objectives 1,2 and 4. This antenna has good isolation and is designed to resonate at three WLAN frequencies to support different IoT applications simultaneously. Multiband antennas can help in supporting various applications simultaneously and are highly desired in modern wireless applications as multi-tasking is considered an additional advantage to save space while not compromising performance. The antenna has also been tested for operation at 2.4 GHz with the help of an ESP8266 module. **This study helps to fulfill objectives 1, 2, and 4 of the formulated objectives.**

1.7 ORGANIZATION OF THIS THESIS

This thesis provides an insight into microstrip patch antennas, its working principle, the major parameters of concern, different techniques used in the literature to enhance their performance including the use of slots, defected ground, and MIMO antenna systems which could be used in the emerging IoT applications. It also includes the analysis, design, optimization, fabrication, and testing of various antennas that could be used in various IoT applications. The whole study is systematically organized into the following chapters.

Chapter 1: Introduction It contains an introduction to the upcoming IoT technology and explains the deep-rooted role of microstrip antennas in IoT systems. This chapter also comprehends the problem statement, the motivation that led to this study, and the application scope of this thesis.

Chapter 2: Antenna System Overview The chapter explains the microstrip patch antennas, the various performance parameters of microstrip patch antennas, MIMO antenna systems, and their advantages along with the various MIMO performance parameter metrics. The chapter also gives an overview of the DGS ("Defected Ground Structure") technique which is widely utilized to improve various performance parameters of planar microstrip-fed patch antennas.

Chapter 3: State of Art An extensive literature survey on the microstrip antennas designed for IoT applications is studied in this chapter. The antenna specifications desired for IoT applications and the communication protocols employed for specific applications are discussed in detail. The various MIMO and multiple-band antennas employed in IoT systems are also discussed in this chapter.

Chapter 4: Microstrip Patch Antennas: Design and Simulation Tools All the tools and software used for the design, simulation, and testing of microstrip patch antennas are reviewed in this chapter.

Chapter 5: Log-Periodic Antennas for IoT Applications This chapter studies a compact IoT antenna that is intended to function at 2.46 GHz and a miniaturized dual-port MIMO system with an operational frequency range of 2 GHz from 2 to 4 GHz. It explains the co-planar feed and the effect of rectangular slots on the co-planar feed. The MIMO system design and the parametric study with the result discussion are elaborated here in the chapter. The software simulated and the experimentally measured values are verified further. Antenna 1 of this chapter fulfils the defined objective 1 and the Antenna 2 fulfils objectives 1, 2, and 3.

Chapter 6: Wideband LoRa Antenna for IoT Applications. The LPWAN technology and other major communication protocols used in various IoT systems are discussed in this chapter. The chapter also gives a detailed study of a wideband antenna with DGS to work on the LoRa sub-GHz frequency. This antenna design and its results fulfill objectives 2 and 3.

Chapter 7: Compact Tri-Band MIMO for IoT Applications A multiband dual-element MIMO antenna system is studied and analyzed in this chapter. The study includes the antenna system exploiting the advantages of CSRR as DGS. The simulated and the measured results are verified and validated. This design and its results fulfill objectives 2, 3, and 4.

Chapter 8: Conclusion and Future Scope This section explains the conclusions drawn from this study. It also puts forward the future scope in this field of research.

1.8 CONCLUSION

This chapter commences by unmasking the status of the present digital era and its various phases of development. A brief introduction is given to the trending IoT technology. The role of microstrip patch antennas in the advancement of this technology is discussed which formed the motivation to proceed with research work. This chapter also summarises the organization of this study.

CHAPTER 2

ANTENNA SYSTEMS FOR IoT-AN OVERVIEW

2.1 INTRODUCTION

The first major breakthrough in the evolution history of human race is the mankind communicating with one another. It might be one of the very first technique man tried to master. The process of communication, the ways in which communication can be done, the reach of communication, all evolved well with time. Long range communication started from smoke signal and using birds and messengers to deliver the messages has been the very being stages. Over the period, communication systems have evolved to a huge extend and now we stand at the doorsteps of ultra-modern age where devices can communicate with each other. The modern era of communication is marked with the high-end technologies like IoT, AI, ML and DL.

Communication systems are basically classified as wired and wireless communications. When wired systems has a physical connection between the transmitter and the receiver, wireless system depends on radio waves for the transmission of messages from the transmitter to the receiver and vice versa. Antennas are inevitable part of a wireless communication system to transmit information. The electrical energy from the transmitter is transmitted as electromagnetic waves, through free space or water, to the receiver. A basic wireless communication system is shown in Figure 2.1.

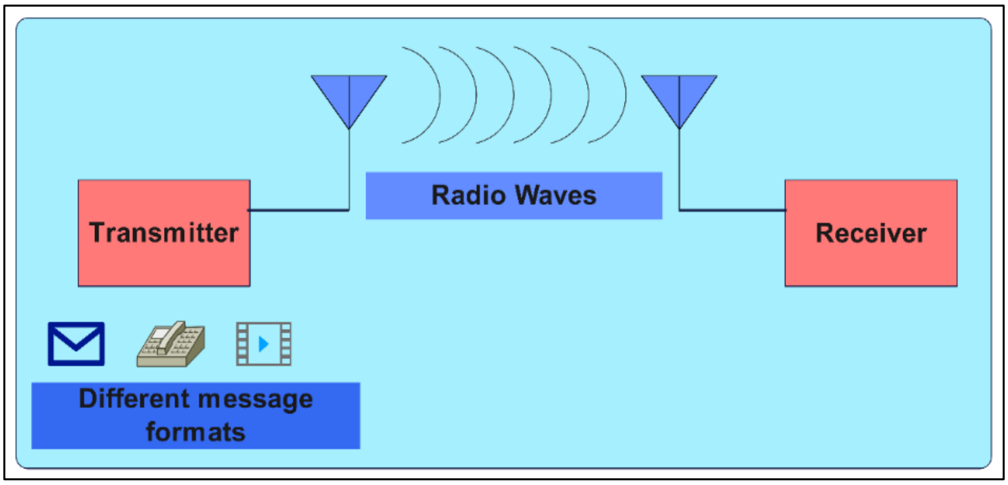

Figure 2.1: A pictorial representation of a basic wireless communication system

After digitization, modern-day wireless communication demands coverage around the world, support innumerable message formats, low latency, reliability, ultra-high speed, low power, etc. Never ending studies and research is going in the field of communication systems and antennas to meet with the demands of modern-day communication systems.

2.2 BASICS OF ANTENNAS

An antenna is anything that can receive or radiate EM waves. It is an inevitable part of a radio communication structure. In the present day, antennas are available in all shapes and sizes. They can be as small as the ones added to the mobile phones and very huge as the antennas used for the reception of satellite signals.

Wireless communication is basically done using radio waves. Radio waves are like water waves which propagates through several successive peaks and valleys. Wavelength and frequency are two important parameters used to characterize a radio wave. The radio spectrum for communication ranges from 3 KHz to 300 GHz.

During the process of wireless communication, the electronic circuitry at the transmitter side generates radio waves, which are then made to radiate into free space through an antenna. The energy radiated into the space by the transmitter antenna propagates through space and some other antennas can sense and capture these energy waves. They are the receiver antennas and they can then decode the energy back to the original message format with the help of advanced electronic systems. So, antenna plays a vital role in transmitting and receiving radio waves. The antennas used for various applications will be designed and optimized to operate over a particular range of frequencies.

2.2.1 Types of Antennas

Antennas are classified according to their structure and application as shown in Figure 2.2.

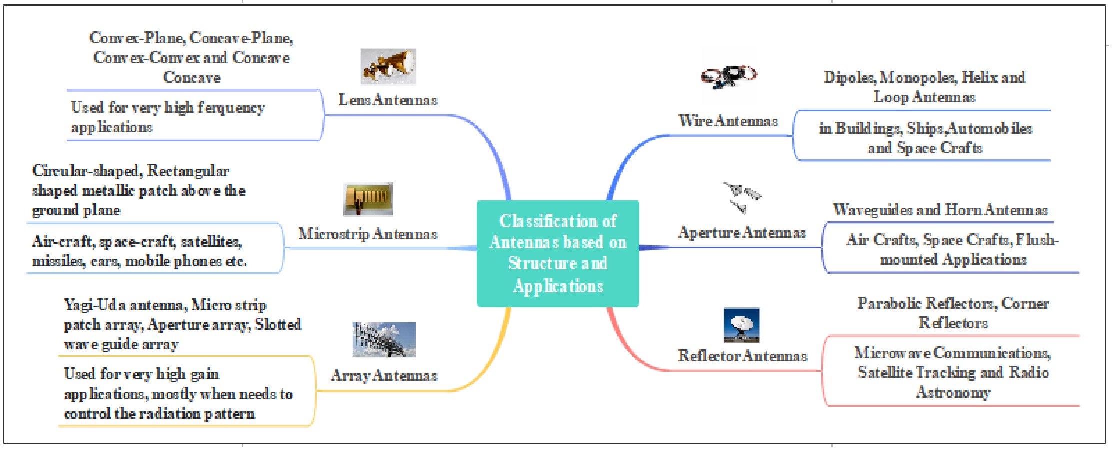

Figure 2.2 Summarises the board classification of antennas based on their structure and applications

Antennas are also characterised based on their radiation pattern. According to the radiation pattern, antennas are classified as

- **Omnidirectional Antennas**: They are also known as isotropic antennas and they radiate in all directions. These antennas are often used as reference antennas while analyzing other antennas.
- **Directional Antennas**: They are also known as bean antennas and has the major power channeled to a particular direction.

2.2.2 Fundamental Antenna Parameters

The following are the fundamental antenna parameters studied to determine how effective the antenna works. These parameters include

- **The Radiation Pattern:** The Radiationpattern is the graphical representation of field dispersion of the antenna w.r.t the directions.
- **Directivity and Gain:** Antenna directivity refers to the measure of the amount of energy in the direction where the antenna is radiating its most. In other terms, directivity is the ratio of maximum power to the average power radiated by the antenna.
- **Radiation Efficiency:** As in all efficiencies, the radiation efficiency is the ratio of useful power to the input power. Efficiency will not be 100% as the antennas are made of conductive materials with ohmic losses.

- **Bandwidth:** The variance between the highest and lowest frequencies between which an antenna's performance is maintained to a specific level is referred to as its bandwidth.

2.3 MICROSTRIP PATCH ANTENNAS

Microstrip patch antennas were developed around 1950s by Deschamps but it was during 1970s, when the electronic circuit miniaturization revolution and the up trout of VLSI industry happened, these antennas came into limelight. It is a simple antenna which is built on a substrate material. It has a metallic patch on its one side and ground plane on the other. The basic elements present in a patch antenna are

- Radiating patch
- Ground surface
- Dielectric substrate and
- Feedline

Microstrip antennas has been extensively studied and researched for the last few decades. They have found wide range of applications in the military and commercial sector wireless communication modules. Owing to its size and low and planar profile has made it the researcher's favourite antenna.

2.3.1 Working Principle

The feedline couples excitation energy to the patch structure as shown in Figure 2.3 and the patch radiates electromagnetic energy through its width side as visualised in Figure 2.4.

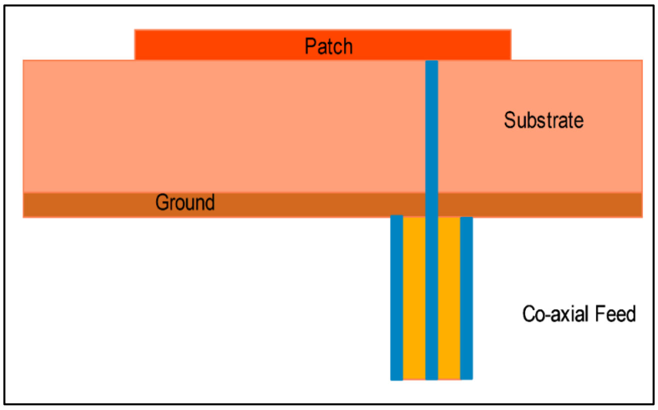

Figure 2.3: Microstrip patch with a co-axial feed

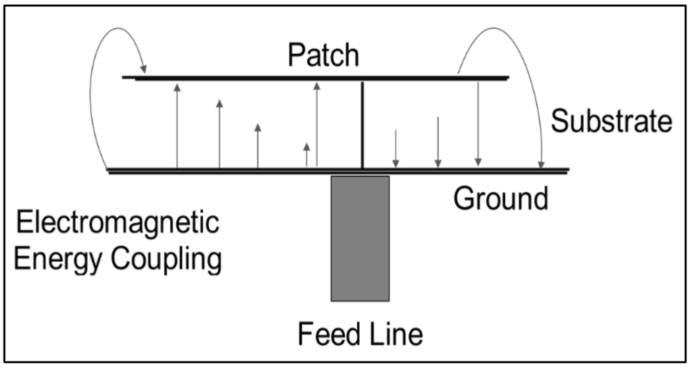

Figure 2.4: The electromagnetic radiations from the microstrip patch

2.3.2 Feeding Techniques

There are basically 4 ways in which a microstrip patch antenna is fed with EM energy. The characteristics, advantages, and disadvantages of the four feeding techniques for patch antennas are (i)co-axial feeding, (ii) microstrip line feeding, (iii) aperture coupled feeding and proximity coupled feeding.

2.3.3 Merits and Demerits

The major merits and demerits of microstrip patch antennas are briefed in Table 2.2.

Table 2.1: Microstrip Patch Antennas: Merits and De-merits

Advantages	Disadvantages
❑ Light weight and low volume. ❑ Low profile planar configuration which can be easily made conformal to host surface. ❑ Can be produced by the PCB technology. ❑ Low fabrication cost, hence can be manufactured in large quantities. ❑ Supports both, linear as well as circular polarization.	❑ Extraneous radiation from feeds and junctions ❑ Poor end fire radiator except tapered slot antennas ❑ Low power handling capacity. ❑ Surface wave excitation.

❑ Can be easily integrated with microwave integrated circuits (MICs). ❑ Capable of dual and triple frequency operations. ❑ Mechanically robust when mounted on rigid surfaces.	

2.3.4 Applications of MPA

The low profile, planar nature and compact size of MPA found applications in the field of defence industry, space vehicles and aircrafts. But today, MPA found its way into every field of technology and life. Some major applications of MPA are listed in Figure 2.5.

2.4 DGS TECHNIQUE IN MICROSTRIP PATCH ANTENNAS

"Defected Ground Structure" (DGS) refers to the small slots and slits of any geometrical shape, inserted into the ground plane of microstrip antenna. It may be a single defect (unit cell) or a there may be several periodic and aperiodic imperfections to form the DGS.

Planar microstrip lines, coplanar waveguides, and conductor-backed coplanar wave guides, have been integrated with DGS [11–22]. Addition of a defect to the ground plane alters the equivalent line parameters. The additional element embedded, (be it of any shape), alters the current distribution of the ground plane and introduces additional resistances, capacitances, and inductances, to the original line parameters. So, in short, the defect engraved into the ground plane alters the actual line parameters to give some unexpected variations in the operational parameters of the antenna.

DGS has a wide variety of applications as listed below.

- DGS enhances the performance of filter systems, co-planar waveguides, microwave amplifiers, and antennas

- DGS is used to lowering mutual coupling between two networks
- DGS can be utilized to boost the range of operation and gain attained by the system
- DGS suppresses the higher order harmonics
- DGS is employed for suppression of undesirable cross-polarization
- providing notched bands to prevent interference with any band
- to reduce component size etc. are some applications of DGS.

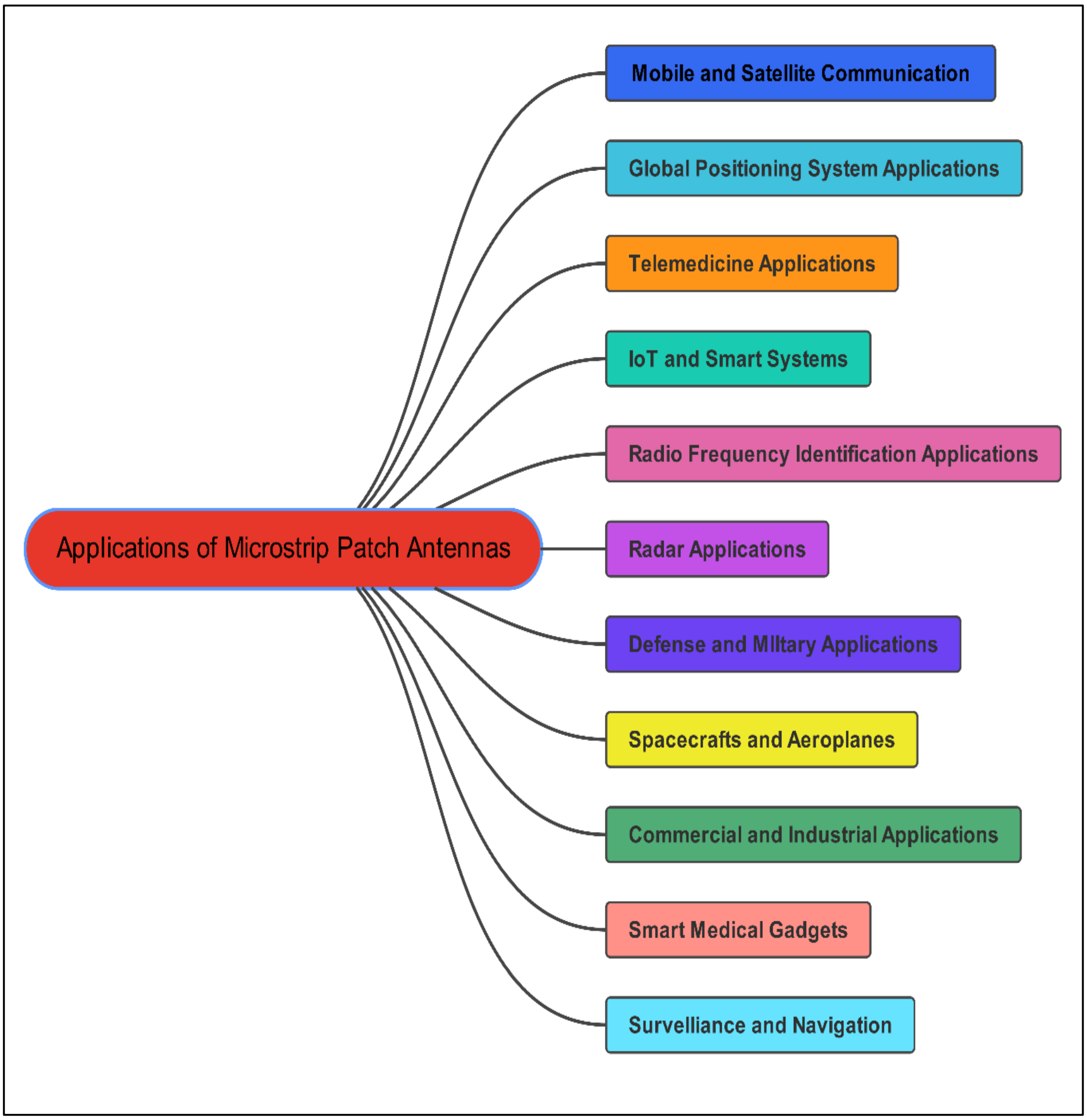

Figure 2.5: Application Areas of Microstrip Patch Antennas

2.5 MIMO SYSTEMS IN ANTENNAS

The antenna system has been undergoing constant evolution to keep up with the field's increasing demands and growing market. Modern wireless networks require increased data rate and throughput in addition to better security and speed [23]. After the introduction and assessment of numerous technologies, massive MIMO with high beamforming capability is being considered in order to meet modern demands. As with every fundamental communication system, MIMO's advanced wireless technology contains many transmitters and receivers, and a wireless communication channel. The area between the source antenna and the destination antenna, including atmosphere, buildings, people and animals, vehicles and cargos, trees, air, and so forth, is referred to as the channel. As the “Channel Capacity Theorem,” states, the capacity for transmission of any channel will depend on the bandwidth accessible for the transmission and governs the data transmission rate in a wireless channel as shown mathematically in Equation 2.1. Figure 2.6 depict a 3×3 MIMO antenna system's structural layout.

$$C = B \log2(1 + S/N) \text{ bps}, \quad \text{------------------------------}(2.1)$$

where "B" represents the operational bandwidth and "S/N" denotes the signal-to-noise ratio, as per to the Shannon-Huffman theorem.

Higher data rates are required for the enhanced multimedia experience which is the demand of the current communication systems. This can be accomplished either by expanding bandwidth or the transmitted power to amplify the SNR. The transmission bandwidth cannot be expanded because to the extremely congested spectrum allotment, and an intensification of power transmitted is not permitted above specific limit [24]. Here MIMO system can help by providing more than one antenna at the source and destination side to improve both the data rate and throughput. Multiple antennas will be strategically arranged and operational at the same time in a MIMO system. We gain a slight advantage in SNR by using numerous antennae. With the increment in the antenna count, channel fading can be controlled and more data inputs are received through multipath propagation. This enhances the SNR of the system. Figure 2.7 shows the possible antenna formats which can be employed in communication system.

SISO employs single antenna for both transmission and reception and it is the simplest form of antenna system. Following are the merits and demerits of a SISO system.

Advantages

- Simple
- No diversity
- No additional processing required.

Disadvantages

- Limited performance
- Interference and fading
- Limited channel bandwidth
- Limited throughput
- Limited SNR

SIMO, also known as receiver diversity, employs multiple antennas at the receiver. It is specially used to combat the effect of fading and are present in two forms as (i) switched diversity SIMO and (ii) maximum ratio combining SIMO.

Advantages

- Relatively easy to implement

Disadvantages

- Requires data procession additionally.

MISO or transmit diversity uses multiple antennas at the transmitter and a single antenna at the receiver end. Same data is transmitted redundantly from transmitter antennas.

Advantages

- Processing is moved to the transmitter side which brings a positive impact on size cost and battery life of the system.

Disadvantages

- Data needs to be processed.

MIMO is the use of multiple antennas both at the transmitter and the receiver end. Spatial Multiplexing is a major feature in MIMO in which the multipath are utilized as additional channels to carry data.

Advantages

- Better channel robustness
- Better throughput
- Coding can be employed to separate data from different paths.

Disadvantages

- Additional processing required
- Additional number of antennas is employed.

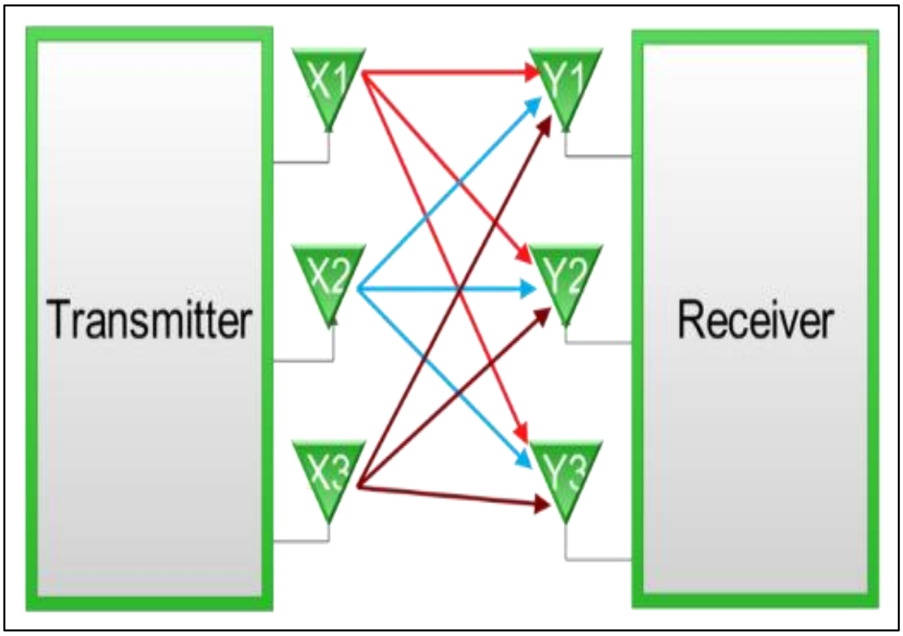

Figure 2.6: A simple 3×3 MIMO antenna system

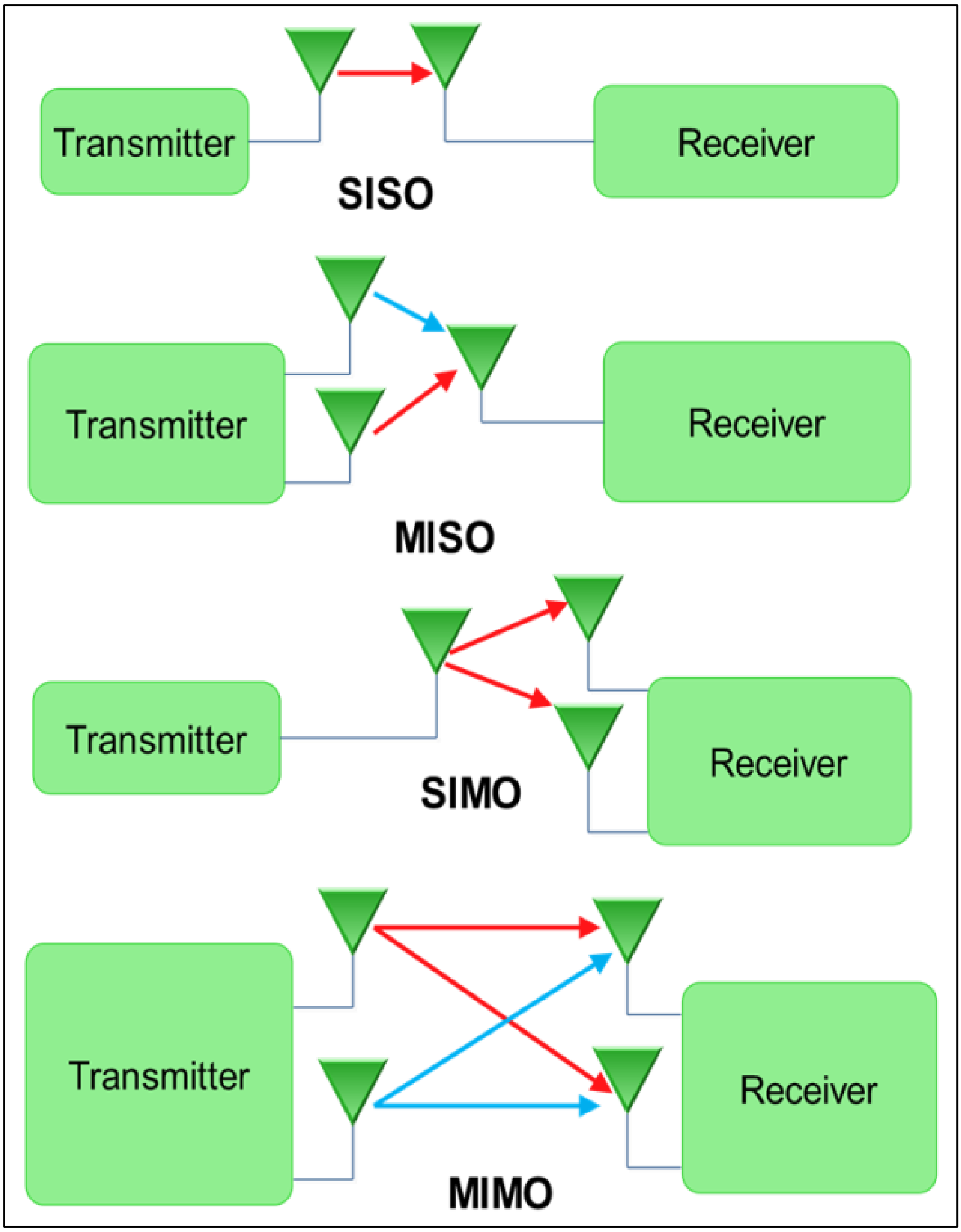

Figure 2.7: Different antenna formats used in communication systems

2.6 CONCLUSION

The chapter studies the basics of antennas and the relevant classification and parameters. The working principle of microstrip antennas, their advantages, disadvantages, and applications and two versatile techniques which can be employed in microstrip antennas for its performance enhancement as Defected Ground Structure (DGS) and Multiple Input Multiple Output (MIMO) as discussed along with their advantages. Antennas designed for the upcoming technologies like IoT, will use these techniques extensively to enhance the performance and meet the requirement of the modern communication technologies.

CHAPTER 3

STATE OF THE ART

3.1 INTRODUCTION

Latest advancements of digital technology have pushed the limits of its supporting technologies and wireless communication systems has become an inevitable part of advanced digital world. The communication technology has witnessed steep progress in the last decade to keep up with increasing challenges of the modern world. The “Internet of Things” has taken world to a new era of digitization where the things connected to the internet are enabled to talk to each other. Communication between the IoT sensor nodes/devices/things has elevated the need to have a good communication system at each sensor node/device. The things network further enabled smart cities, smart grids, smart traffic systems, smart agriculture and so on. This further forced the evolution of modern patch antennas to meet various needs of IoT applications. IoT communication systems are highly application specific as IoT has now spread to a vast diversity of all fields not excluding daily life, medical systems, military, industry, vehicles, and transport. There are IoT applications where the communication systems are expected to support low data rates, low latency whereas some other applications demand high data rate, fast and unswerving communication module. Power constrains and size constrains also play a substantial role in the IoT communication modules as applications may require sensor nodes to be deployed to remotely accessible areas and the size of the sensor nodes may also be limited. In short, IoT applications are impossible without an efficient communication system and the communication module of an IoT system is highly application specific. Antenna being the main component of a wireless communication module, will also have to meet with the demands of these applications.

3.2 LITERATURE SURVEY

The literature survey on IoT antennas is organised in two sections in this chapter

- Monopole IoT Antennas

- MIMO antennas for IoT

3.2.1 Monopole IoT Antennas

Vikram and Kashwan [25] proposed a circularly polarized RFID reader antenna, to work at 2.45 GHz for RFID, IoT and various ISM band applications. The structure is mapped out on a compact Roger material. The antenna offers an 81% efficiency and a directivity of 7.44 dBi. the gain of the antenna was measured to be 6.5 dBi.

Labade et al., [26] suggested a dual band antenna with ACS feed to function at 2.45 GHz and 1.8 GHz. The antenna has a semi-circular shape and is built on FR4 substrate of size 24×10×0.144 mm^3. The bandwidth includes 1.7 to 2.02 GHz and 2.25 to 2.65 GHz. The design also offers a radiation efficiency of 94% and can be used for GSM, Bluetooth, Wi-Fi, and IoT Applications.

Jha et al., [27] designed a multiband antenna in truncated octagonal shape. The antenna is fed by a co-planar feed and is linearly polarised. This antenna resonates at 4 different frequencies including 848 MHz, 2.42 GHz, 3.26 GHz, and 5.78 GHz including the frequencies of (697 MHz-991 MHz), (2.38 GHz-2.5 GHz), (3.07 GHz-3.35 GHz) and (5.61 GHz-5.92 GHz). The gain of the bands is claimed to be 2.76 dBi, 3.29 dBi, 5.96 dBi and 5.5 dBi respectively. The antenna is proposed for TV broadcasting, automated RFID Applications of IoT, other 5G applications and LTE-4G. The designed antenna is built on the Polyguide material which has a dielectric constant 2.32 and size 130×90×6.35 mm^3.

Hasan et al., [28] discussed an antenna with dual notch band for WiMAX and WLAN IoT applications. The radiating surface of the antenna included a planar circular ring structure. The antenna was built on low cosy, lossy substrate FR4, which has ε_r of 4.4. The dual notch bands were seen at 3.6 GHz and 5.8 GHz in the Ultra-Wideband frequency spectrum ranging from 3.1 GHz to 10.6 GHz. The gain of the antenna was observed as 5.1 dBi or 11.5 dBi. The total size of the proposed structure was 24×26×1.6 mm^3.

Masius et al., [29] designed an antenna of size 18×17×9.3 mm^3 on soda lime glass of dielectric constant ε_r, 3, for IoT RF energy harvesting applications. The Dielectric Resonator Antenna (DRA) is made of 6 to 7 layers which can aid in RF energy harvesting for IoT supportive systems. The designed radiating element has a high 6.69 dB gain and resonates over 5.85 GHz. The antenna is also coupled with slots to augment its performance. The dimensions of the proposed energy harvester is 18×17×9.3 mm^3. The bandwidths observed for this antenna were ranging between (5.57-6.3) GHz and (5-6.04) GHz resonating at 5.85 GHz.

Naidu et al., [30] discussed an Asymmetric Co-planar Strip (ACS) fed antenna of size 12×16×1.6mm^3 built on FR4 substrate. The antenna has an alphabet e like geometry which is designed using meandered rectangular strips. The antenna offers dual band of 100MHz (2.4GHz-2.5GHz) and 1200MHz (4GHz-6.1GHz) each with a gain of 3.7 dBi. The two resonant frequencies are 2.45GHz and 5.5GHz which could be employed by communication protocols like Bluetooth, WLAN, WiMAX and other IoT applications.

Saha et al., [31], studied and proposed a flexible wideband UWB antenna for various wearable and IoT applications. The size of the proposed design is 3.1×32.7×0.254 mm^3 and the antenna is printed on Kodak photo paper of ε_r, 2.85 with a peak gain of 4.87 dB. The radiating patch included a circular structure which is printed in the substrate with inkjet printer and a double steeped ground plane. As the antenna is designed on photo paper, it is flexible and ultra-thin.

Arun and Karl, in [32], proposed a reconfigurable antenna for energy harvesting. The patch is ring shaped as it is simpler than other patch shapes and as it can offer better multi-banding. The antenna is also incorporated with PIN diodes to facilitate switching action and the PIN diodes are controlled by Node MCU. The size of this antenna is 50×50mm^2. The antenna can be tuned to multiple frequencies of operation as 1.8 GHz, 2.4 GHz, 3.5 GHz, and 4.5 GHz with gain of 1.6 dB, 1.9 dB, 2.7 dB and 2.5 dB respectively. The intended applications of the antenna include to work in GSM1800 band, DCS1900, Bluetooth, Wi-Fi, ISM Band, WiMAX, WLAN, and satellite communication.

Mao et al., [33], designed and studied a compact antenna of size 14×14 mm^2 offering dual bands of operation between (3.4-3.6) GHz and (5.725-5.825) GHz. The authors propose to use designed antenna to connect the IoT nodes using Wi-Fi and 5G networks. The antenna is also seen to have an omni-directional radiation pattern. The antenna is designed in two steps where an L-shaped patch is further bend to a U-shaped radiating patch for reduction in the size. The antenna resonated at 3.5 GHz and 5.8 GHz and offered gain of 1.76 dBi and 3.32 dBi respectively.

Shafiqie et al., [34], in their study, proposes an energy harvester using a rect-antenna to facilitate the IoT nodes deployed in power constrain areas. The system is designed to gather RF power at versatile 2.4 GHz frequency. The antenna structure includes a patch antenna, in rectangular shape, which can act as lumped components and rectifier to perform energy gathering. The gain of the system is 5.6 dBi with a size of 57.5×54×1.6 $mm^{3,}$ on FR4 substrate.

Sanil et al., [35] analysed the performance of a microstrip antenna with multiband operations for IoT applications through satellite communication. The radiating structure includes a basic antenna, rectangular shaped, with two rectangular stubs popping to either side from the top and bottom. The designed antenna resonates at 5.8 GHz, 6.76 GHz and 8.4 GHz and attains circular polarization. As the frequencies of operation lies in the C and X bands, the antenna can be used to perform in C, Ku, and Ka bands. The simulation gains of the antenna are 3.95 dB, 5.05 dB and 11.17 dB respectively.

Kumar et al., [36] proposed a wideband antenna resonating at 7.5 GHz. The proposed design is polygon shaped and additional stubs are attached to enhanced the working parameters of the antenna. The frequency range of operation of the optimized antenna is between 2.8 GHz to 9.4 GHz and it offered a gain of 3.0393 dBi. The antenna is of 23×18×1.6 mm^3 built on low-cost FR4 substrate.

Park et al., [37] discusses a compact antenna with two inverted V dipoles. The suggested cross-inverted V antenna is reconfigurable in terms of polarization to avoid interference. The antenna can operate with vertical, horizontal, right hand circular and left-hand circular polarization. The antenna is built on Taconic TLX-9 which has a dielectric constant of 2.5. the 80×80×15 mm^3 sized antenna resonated at 5.8 GHz. the gain of the antenna is 5.2 dBi (vertical polarization), 4.61 dBi (horizontal polarization), 5.25 dBi (right hand circular polarization) and 5.51 dBi (left hand circular polarization). The antenna , specially is designed for reducing interference in 5G IoT applications.

Islam et al., [38] designed and analysed a modified meander line antenna in the inverted S-shape. The antenna is connected to a rectangular box like structure. A parasitic patch is also added to the antenna design which greatly augmented the antenna's performance. Optimization of the rectangular block along with the addition of parasitic element improved gain and efficiency of the system. The $40 \times 10 mm^2$ structure is built on FR4 and works at 2.4 GHz.

Vamseekrishna et al., [39] proposed an omega-shaped slotted antenna with PIN diodes for remote sensing applications, extra-terrestrial communication systems and various IoT applications. A Node MCU is used to control the PIN diode to attain the alterations in the current directions and attain the desired frequency of operation. The reconfigurable frequency band of the antenna includes (1.57 -2.15) GHz, (2.13 -3.0) GHz, (3.17 -3.43) GHz, (5.2 -5.8)GHz, (6.3 -6.78) GHz, (8.31 -8.90) GHz, (9.04 -9.58) GHz and (12.03 -13.14) GHz.

Khalili et al., [40] discusses patch antenna using bio-degradable substrate of dielectric constant 1.34. the suggested antenna is eco-friendly and can be used for smart floors in smart houses. The antenna has two operational bands of (863-873) MHz and (2.4-2.5) GHz. The simulated gain observed for these impedance bandwidths are 5.8 dBi and 2 dBi respectively.

Piao et al., [41] studies a dual band antenna, compact in nature, for various applications in sub-6 GHz frequency band. The antenna consists of two resonance loops which are energized by two other feeding loops. There are metal frames added to the ground of the antenna system to enhance lower operational band. Two resonant frequencies are 0.92 GHz and 2.45 GHz and the antenna size is $50 \times 30\ mm^2$.

Gomez et al., [42] designed and fabricated an ultra-thin slot monopole antenna with Co-planar Waveguide feed. The ENrG's thin E-strate of ε_r 22 is used for the fabrication. The CPW fed antenna is fabricated by electro-textile technique and inkjet printing technique. The $66 \times 62 \times 0.04\ mm^3$ ultra-thin, flexible antenna resonates at 2.75 GHz and 5.8 GHz with gain of 4.52 dB and 5.19 dB respectively.

Burtowy et al., [43] proposed and analysed a low-profile antenna which has an electronically steerable parasitic array radiator. The set-up can estimate the DoA

(Direction of Arrival) of signal from sensor nodes. The circular shaped patch has a radius of 80 mm and height of 10 mm. its built on FR4 and resonates at 2.45 GHz. The gain of this system ranges between 7.3 dBi to 7.5 dBi.

Ramesh and Mohan in [44] discusses an antenna for smart health system. The transmission module for signals from an ECG monitoring system is designed and implemented using rectangular Zig fractal antenna. It supports triple band of operation namely 2.4 GHz, 3.5 GHz, and 5.8 GHz. The system helped in contactless heartbeat monitoring system. The antenna has a modified ground and four folded arms and is of a compact size of $12\times18mm^2$.

Elijah and Mokayef, [45], suggests a rectangular inset fed radiating patch embedded with dual U-shaped slots. The compact structure is of size 24.7×20.8 mm^2 and is built on FR4 substrate. The antenna is designed to resonate at 5.755 GHz with a gain of 2.54 dB and bandwidth of 167.6 MHz.

Olan-Nunez et al., [46] designed and studies a dual-slot antenna array system on a thin substrate and thick substrate. The variations in gain and bandwidth were studied for both the cases. The antenna is of size 50×54 mm^2 and resonates at 5.8 GHz. When built on a thin substrate, it has a bandwidth of 617 MHz and gain of 6.7dBi with efficiency of 94%. The same antenna structure on thick substrate showed a bandwidth of 455 MHz with a gain of 7.23 dBi and efficiency of 92%.

Singh et al., [47], proposes a penta-band frequency reconfigurable, square shaped antenna with fractal stripping and slotting geometry with DGS. The DGS of the antenna included a U-Slot and two ring shaped slots. The equivalent inductance and capacitance will be varied by a PIN diode connected to the U-slot in the DGS. There are two parasitic strips added to either side of the radiating patch and two PIN diodes are connected between them. The 25×25 mm^2 antenna on FR4 substrate resonates at 5 different frequencies, 3.85 GHz, 4.14 GHz, 4.43 GHz, 4.91 GHz and 6.01 GHz with gain 2 dB, 2.90 dB, 2.50 dB, 4.42 dB and 3.01 dB respectively. This antenna offers to work for WLAN, WiMAX, C-Band and IoT applications.

Kirtarva et al., [48], designed a flexible antenna on PET (polyethylene terephthalate) substrate with ε_r =3.2. The antenna designed is a circular monopole of size

47×25×0.135 mm^3 with CPW feed. The operational frequency range of the antenna is the UWB range of frequency ranging from 3.04 GHz to 10.70 GHz and an addition band of 15.18 GHz to 18 GHz. The system attains a good gain of 3.94 dBi and efficiency of 95.7%. the antenna is proposed for flexible IoT applications and free space applications.

Rashid et al., [49], discussed a rectangular patch antenna with a slot in the shape of alphabet 'L' and truncated edges on low cost FR4 substrate. The antenna size is 25.83×21.7×1.524 mm^3 and has three resonant frequencies as 2.4 GHz, 3.9 GHz and 5.7 GHz with a maximum gain of 3.14 dBi. The antenna is also tested for SAR (Specific Absorption Rate) and average SAR for 10g tissue is 0.09. The antenna is suggested to find application in the IoT field, Medical filed and in wearable applications.

Abdulkawi et al., [50] suggested a square microstrip antenna embedded with 4 slots and analysed with two different substrates. The antenna system is also examined while feeding with microstrip line and co-axial cable to attain single and dual bands of operation respectively. The antenna could provide gain with the second substrate (RT Duroid 5880). The size of the antenna is 36.4×36.4 mm^2. the working frequencies included 2.4 GHz (with microstrip line feed) and 2.4 GHz and 2.8 GHz (with co-axial probe feed. With RT Duroid substrate, the gain attained is 3.95 dB and 3.45 dB. The antenna is proposed for IoT applications.

Albert Sabban, [51], designed and analysed a circular antenna with and without stacking and with and without CSRR. Embedding CSRR improved the gain and reduced the antenna size. The structure, in circular shape, has a diameter equal to 35.5 mm and is built on metamaterial. The system offers an operational bandwidth from 2.4 GHz to 2.9 GHz when stacked and embedded with CSRR, 1.8 GHz to 3.2 GHz while simulated as a circularly polarized antenna and 2.4 GHz to 2.9 GHz when added with CSRR. The gain in all three cases is 7.6-8.3 dBi, 10-14 dBi and 7.5-8.2 dBi respectively. The antenna is suggested for 5G devices, IoT applications, Bio-Medical systems, and energy harvesting.

Patnaik and Kartikeyan, [52], proposed a dual band and triple band antenna. The dual band antenna is designed using a dipole and a monopole and adding an extra monopole and DGS to this system attained triple bands for operation. The monopoles are placed in optimized angles to attain 3 resonant frequencies. The three resonant frequencies included 3.5 GHz, 5.8 GHz and 28 GHz which are ideal for 5G, RFID and mobile IoT applications.

Sreelakshmi and Sankar, [53], designed an antenna for IoT nodes energy harvesting in ISM and WiMAX communication bands. The radiating patch consist of a closed square ring along with a square shaped split ring resonator. The substrate, Rogers RT 5880 (ε_r =2.2) is of size 24.8×24.8 mm^2. The antenna offers two operational bands, (2.3-2.5) GHz and (3.4-3.6) GHz with a gain of 2.7 dB (2.4 GHz) and 2.35 dB (3.6 GHz).

Moutaouakil et al., [54] explains a simple rectangular patch antenna which is modified by embedding five circular slots. The size of the antenna is 72.44×56.02×1.6 mm^3. The antenna offers three resonant frequencies (3.921 GHz, 4.86 GHz, and 5.16 GHz) with gain 4.1 dB, 3.2 dB and 3.9 dB respectively. The application fields suggested for this antenna are IoT and UWB applications.

3.2.2 MIMO Antennas for IoT

MIMO stands for "Multiple Input Multiple Output". MIMO is a method which is widely applied to communication systems to improve their performance and upgrade them to meet the demands of present-day wireless systems. In simple words, MIMO is a technique in which more than one antenna is employed at both the transmitter/source and receiver/destination side of a communication system.

MIMO antenna systems can provide

- Better spectral efficiency compared to alternative systems at lower cost.
- Improved channel capacity
- Support to modern-day high-speed communication by allowing a wide range of application without utilizing additional bandwidth or signal power.

- The check on the limit of power than can be transmitted by one antenna

MIMO antennas are designed and proposed for IoT applications. An extensive literature survey of MIMO antenna designs proposed for IoT applications is summarised in the following section.

Kim and Nam in [55] designed a bilateral symmetric bug-shaped antenna for the use in symmetric platforms. The antenna is systematically designed and analysed using characteristic mode of analysis. The proposed antenna has 3-ports which can work in Mode 1, Mode 2, and Mode 3.

Yu et al., [56] designed a two-element patch array and used a 3D structure using metamaterial to attain isolation. Two-port rectangular MIMO antenna is designed and M-shaped 3D structure is embedded in DGS to achieve an additional isolation of up to 18 dB. The system is tuned to work at 2.4 GHz. The ECC for the MIMO system is almost 0 and the gain is 5 dBi at the centre of the operational band.

Kiem and Chien, [57], proposed an effective decoupling network using transmission line, for MIMO antennas. The paper implements double, dual -band radiators, one for WLAN at 2.45 GHz and 5.25 GHz and the second for LTE (1.8 GHz) and WiMAX(3.5 GHz) using the "transmission line decoupling technique (TLDL)". The system observes highest gain of 4.5 dBi (2.45 GHz) and 5.3 dBi (5.25 GHz) after implanting TLDT and radiation efficiency of 85% and 64% respectively. Similarly, the LTE WiMAX antenna radiates with an efficiency of 88% at 1.8 GHz and 65% at 3.5 GHz.

Jha et al., [58] proposes a 5-element MIMO for IoT systems. MIMO system is designed of size $65\times120\times1.56$ mm^3 on FR4 substrate. The MIMO structure includes 2, 2 element MIMO systems. The first 2 element MIMO are folded meander line which covers the 687 MHz-813 MHz LTE band and 2.4 GHz RFID band and the second set contains another two element MIMO covering four more bands as (754 -971) MHz, (1.65 -1.83) GHz, (2 -3.66) GHz, and (5.1 -5.6) GHz. A spectrum sensing antenna is also added to this system of MIMO antennas to cover the radio ranges of (668 -1.94) GHz and (3 - 4.6) GHz.

Chouhan et al., [59] designed a quadport MIMO antenna in octagonal shape for S-band frequency purposes and human interface device. Isolation in the MIMO is achieved by the addition of parasitic lines and a T-shaped structure in DGS. The bandwidth of operation for this antenna is (2.1 to 4) GHz and a 2.83 dBi gain at versatile 2.4 GHz. ECC for the antenna is as low as 0.026. The measure of interaction between the elements is achieved well below 15 dB. The 54.98×76×1.6 mm^3 sized antenna offers a performance efficiency of 82%.

Moradi et al., [60] proposes a CPW fed 4-port MIMO antenna with operateing frequency band of (2.25 to 2.75) GHz covering Wi-Fi (2.4 GHz) and LTE (2.6 GHz) bands. The coupling between the elements is controlled using parasitic element and the value is below 14 dB. ECC for the system is below 0.2 and the gain ranges between 5.33 dBi and 6.97 dBi. The designed MIMO structure can be used for indoor and outdoor WAP (Wireless Access Points).

Rezapour et al., [61] designed a two "E-coupled rectangular dielectric resonator antennas" and used a negative permittivity substrate as a 1^{st} and 2^{nd} layer to enhance isolation. The bandwidth ranges between1.97 GHz to 3.317 GHz with a circular CSRR embedded in the ground plane. One layer contains 2×3 circular CSRR. For the single layer operation, mutual coupling is below 11 dB and its below 20 dB for double layer operation. The frequency band of operation for the two-layer antenna is (2.60 to 2.64) GHz.

Hu et al., [62] proposes the use of 2 "composite right-left-handed (CRLH)" structures such as meander-line in order to design a miniaturized two-band MIMO working at (0.66-1.06) GHz and (1.68-2.88) GHz. The gain of the structure ranges between -0.2 dBi to 3.5 dBi and has an efficiency above 38%. DGS and grounded branching are employed to attain isolation above 13.5 dB and the antenna is proposed for various wireless terminal applications.

Sanad and Hassan, [63], proposes a 34×34 mm^2 sized 2-port MIMO antenna to operate within the frequency range of (0.7-3.8) GHz and (3.3-7) GHz. The MIMO antenna can operate with an efficiency of above 75% and isolation above 20 dB. The

MIMO system is planned to implement in Mobile handsets along with other IoT applications.

Chauhan et al., [64] designed and analyzed a four port MIMO antenna which can be employed for Wi-Fi applications. The radiation efficiency of the antenna is above 79% and the gain attained is 2 dB. The operating band of the radiator is (2.34-2.56) GHz with a size of 140×120 mm^2.

Kumar et al., [65] proposes a 4-port MIMO for IoT applications. Radiating elements are sickle shaped and uses tapered CPW feed. The reduction in interaction (isolation) between antenna elements is achieved after arranging them orthogonally. A complementary slot added to the ground plane hugely enhanced the bandwidth. The operating frequency range for this antenna is 3.1 GHz to 40 GHz. Further, notch bands are achieved at 2.4 GHz. 5.5 GHz. and 7.5 GHz by implementing a slit in L-shaped, and CSRR in the radiating structure with an isolation of more than 20 dB and ECC is reduced below 0.03.

Kumar and Khanna in [66] designed and studied a 4-port MIMO for 4G, 5G and IoT applications. The "theory of characteristic modes" is expended to design the "planar inverted F antenna (PIFA)" in L-shape. The resonant frequencies are 17 GHz, 12.5 GHz and 3.5 GHz. By using complementary metamaterial structure in the ground surface, the MIMO system could achieve an reduced coupling of 21 dB and above.

Maurya and Bhattacharya,[67], designed and proposed a 33×57.5 mm^2, dual element MIMO working for UWB bandwidth, and NB-IoT along with WLAN applications. Antenna elements is comprised of a rectangle patch as to provide the UWB operational bandwidth. An inverter L-shaped metallic slot is added to the patch, to achieve a second band for NB-IoT applications. Addition of a shorter L-shaped strip to the ground plane included the third band of 2.4 GHz. The isolation between the elements is achieved by careful orientation of the component radiators. Coupling between the elements is reduced to less than 14 dB and maximum ECC is 0.0471.

Dkiouak et al., [68] proposed a compact MIMO antenna with two operational bands and high isolation. The antenna geometry included two "nine-shaped" elements placed orthogonally on FR4 substrate of size 27×21×1.6 mm^3. An additional slot is added to the radiating patch for the second operational band, (5.19 to 5.41) GHz and the addition of two slots in the DGS improved the isolation between the elements. Isolation achieved is more than 22.5 dB and the two operational bandwidths are (5.19-5.41) GHz and (7.30-7.66) GHz making it suitable for various WLAN and X-Band applications.

Palanisamy and Subramani in [69], suggested a compact UWB MIMO antenna for IoT applications. The antenna contains 8 ports. The size of the 8-port MIMO is 54×54 mm^2. Three “metallic via holes” are integrated to the square shaped radiating patch, to achieve UWB bandwidth. Isolation between the elements is improved by ring shaped structure and Koch fractal is embedded to the ground to attain better electrical characteristics. The efficiency of the system is in the range of 70% to 90% and gain fluctuates between 2 to 7.6 dB.

Thiruvenkadam et al., [70] uses “asymmetric meandered radiator” and DGS to scheme a quad-band MIMO which can be employed in modern IoT applications. Isolation between the two elements is achieved by arranging them in a “chiral” pattern. The frequency bands covering GSM, WiMAX, WLAN and 5G with an isolation of more than 18 dB and gain of 3.6 dBi are the highlights of this antenna system. The antenna is proposed for smart homes and other IoT applications owing to its compactness, and low profile.

Chattha et al.,[71] discussed a 4-element and octa port MIMO for different 5G applications. Ground dimensions of the antenna are 60 ×120 mm^2 and antennas occupy the crooks of the ground portion. Slots engraved on to the ground, aids in the reduction of mutual coupling. Operational bandwidth for this antenna is 2.4 GHz – 3.8 GHz and covers all the 5G frequencies below 6 GHz. The gain ranges from 3.2 to 5 dB over the operational bandwidth.

Mathur and Dwari in [72] proposed a MIMO antenna with reconfigurable frequency and port. The 4-element MIMO is made of orthogonally orientated annular rings with PIN diodes to switch between narrow band and wide band operations. The MIMO can be configured to work in 4 different states as “UWB, mid-band, 5G and WLAN”. The same antenna is also capable of operating as 2-port and 4-port MIMO system.

Wani and Kumar, in [73], designed and investigated a 4-element UWB MIMO of size 35mmx35mm. The stubs included in the ground plane along with the orthogonal orientation of the antenna elements are employed to achieve an isolation of above 15 dB between radiating elements. This antenna is proposed for UWB MIMO applications. All diversity parameters are observed to be within the desired range.

Sharma et al., [74] proposed a 6 element MIMO system, WLAN, and sub 6GHz applications and X-band applications. Out of 6 element, 1^{st} two identical elements, covers the frequencies for IoT applications (727-1066) MHz and WLAN and Wi-Fi applications (5.28-6.2) GHz. In the second set of antennas, the NB-IoT band, the (5.5-5.8) GHz Wi-Fi and the (7.2-8.9) GHz X-bands are covered. The final set covers the (3.1-3.8) GHz band which can be used for sub 6 GHz modern wireless applications. Isolation between the radiating elements is achieving using stubs and decoupling networks.

Khurshid et al., [75] designed a low-profile MIMO antenna of super wideband, (2.3-23) GHz, for IoT applications. The quad-element antenna is of size $60 \times 55 \times 1.2$ mm^3. The elements are orthogonally arranged to attain an isolation of over 20 dB

Nagendra and Swarnalatha, in [76], designed and fabricated a four-port MIMO antenna for multiband IoT applications. The three operational resonant frequencies are 1.44 GHz, 2.3 GHz, and 4.2 GHz. The meandered design of radiating element claims to achieve good gain and the SRR provides good isolation.

3.2.3 Base Papers Referred for Designed Antennas

The log-periodic structured antennas, antennas mentioned in Chapter 5 of this study are based on the following publications.

Nashuha et al [80], proposed a trapezoidal antenna which is log-periodic structured. The antenna offers a wide bandwidth of 34.8 GHz from 5.2 GHz to 40 GHz with a maximum gain of 17.8 dBi. An elliptical dielectric lens was used in this antenna system to enhance the radiation characteristics. The antenna was built on RO4003 and was proposed for various broadband applications in the modern communication systems.

Modasiya et al suggested a slotted log-periodic antenna for various navigational purposes in [81]. This antenna was built on FR4 substrate of size 42×42×1.6 mm^3 to offer wideband characteristics. The antenna gain was observed to be 4.5 dBi.

The wideband antenna proposed in Chapter 6, for LoRa protocol is based on the following work.

Kumar et al, [65], proposed a super wideband qual element MIMO antenna for frequencies from 1.3 GHz to 40 GHz, rejecting 2.4 GHz, 5.5 GHz, and 7.5 GHz, for IoT applications. Antenna is built on 22×34 mm^2 RO4003C substrate with L-shaped and CSRR slits to achieve band notch at the three desired frequencies. The structure offered an attractive wideband property.

The multiband antenna proposed in Chapter 7, is attained through the design of a combination of modified rectangles with slot and modified DGS.

Biswas et al, [115], suggested a UWB MIMO antenna with two modified rectangles. The ground plane of this antenna is added with DGS to enhance isolation of the system. A stub between the two antennas aided in attaining a expansive notch band from 4.98 GHz to 5.96 GHz.

3.3 CONCLUSION

An extensive survey of IoT antennas available in the literature is studied in this chapter along with its structure. The monopole antennas and the MIMO antenna systems are studies with all the relevant parameters.

CHAPTER 4

ANTENNA DESIGN AND SIMULATION TOOLS

4.1 INTRODUCTION

The process of antenna design involves multiple iterative steps. Designing a desired antenna, according to the desired frequency of operation, gain, bandwidth and radiiation characteristics, is a hard-won process and it involves various steps as design and simulation and optimization of the antenna in software, hardware fabrication of antenna and concluding with the real testing of designed antenna in a lab. These processes are carried out orderly and carefully to achieve the final antenna proposed for a particular application or frequency of operation.

The antenna types and designs have evolved over time. Present day antennas, specially microstrip patch antennas involves complex structures, minute detailing and careful design. Therefore, the analysis process and the current distribution in the structure is highly complicated to analyse manually. Now a days, antennas are so designed and simulated in software first and once the design is finalized after many effortful iterations, antenna is fabricated and tested to verify the simulation results. Three major techniques used in antenna simulation tools are

- "Finite Element Method" (FEM)
- "Methods of Moments" (MoM) and
- "Finite Difference Time Domain" (FDTD) Method

4.2 SIMULATION TOOL- HFSS

HFSS, High Frequency Structure Simulator, is a very popular simulation software widely used in antenna design. It is a design and simulation software, specially intended for high frequency electronic products like

- Antennas and antenna arrays
- Microwave and RF components
- Interconnects with high switching speed

- Filters and connectors and
- High performance ICs and PCBs.

This software is very popular in the field of RF, microwave and antenna design, high speed electronic systems, emerging and growing technologies like IoT and satellite implementations etc

HFSS uses an “electromagnetically aware adaptive meshing technology” and the “targeted meshing technology” is applied to the specific geometry of the design. By doing this, a “fully coupled electromagnetic matrix” is calculated and solved for each point specified in the frequency sweep applied to the design [77].

It is also user friendly and provides “Graphical User Interface,” and are used for modelling high frequency 3D designs. It was initially developed by Prof. Zoltan Cendes, with his students in 1990. It works on the Finite Element Method (FEM) with options to simulate, visualize, automate, and model electronic designs of very high frequencies.

4.2.1: Antenna Design in HFSS

The general procedure followed for antenna designing using HFSS is graphically represented in Figure 4.1. After launching the simulation tool, HFSS, the antenna design is drawn in the design window. Other handy windows are Status Bar, the Message Manager, the Project Manager, and the Progress Window. Once the design is successfully drawn, the materials are assigned to the patch, ground, and the substrate. The radiating and the ground surface are generally “Perfect E” material. The substrate can be taken according to the properties, cost, and availability. FR4 and Rogers RT Duroid 5880 are some commonly used substrate materials. In the next stage, ports are assigned excitation and boundary conditions are set and before running the simulation, the solution set up is set. Far field set up is also added to evaluate antenna parameters as gain and other radiation characteristics including radiation.

In HFSS, result is easily and graphically made visible to the user. This helps in easy analysis. The design process is continued till the required outputs are attained. In HFSS, redesigning and making modifications in the design are made easy. The modified design can be run again by the following steps. The basic parameters under study includes S-Parameters, VSWR, Gain, Radiation patterns (both 2-D and 3-D) and directivity. Graphical results are also available in Excel file for further documentation.

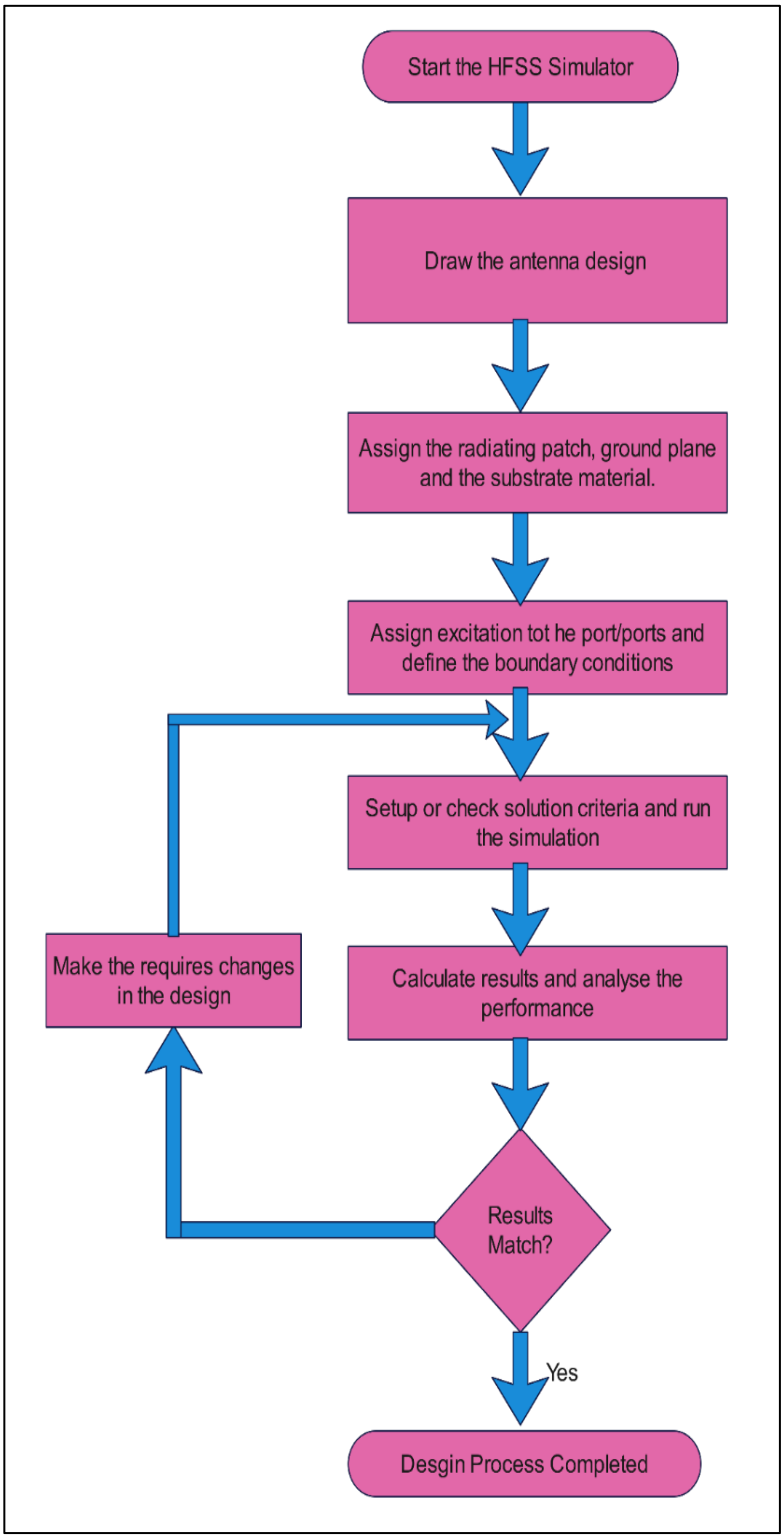

Figure 4.1: The simulation procedure for an antenna design in HFSS software.

4.2.2 Design Steps for Antenna

The following can be the design steps adapted for the process but it is not mandatory that these steps should be in the given order.

1. Draw the ground as per the calculated dimensions
2. Place a box, to be the substrate, over the ground and assign the thickness for the substrate from the available thicknesses.
3. Assign the dielectric material for the substrate.
4. The patch is carefully designed and modified according to the operational frequency required for the application.
5. The feedline to the patch is also designed mathematically and then drawn in the software.
6. The patch and feed line are then united to simulate the feeding operation of the patch with electromagnetic energy.
7. Patch and the ground surface are assigned with pure conducting material or copper.
8. Assign the port through which the patch can be excited by coupling electromagnetic energy.
9. Finally create the radiation box and assign its boundaries.

4.2.3 Simulation and Results analysis of the antenna

1. Before the simulation process, the analysis setup is set to the desired frequency of operation. The frequency sweep is also then added to the range of frequencies to be investigated.
2. Simulate the design
3. To plot the results, right click on results and click on create the data report. From here, any parameter can be analysed graphically.

4.3 GRAPHICAL REPRESENTATION OF RESULTS FOR DOCUMENTATION-ORIGIN PRO

Origin Pro is an interactive computer program used for “Scientific graphing and data analysis”. It runs on Microsoft Windows and is produced by Origin Lab Cooperations.

It has spreadsheet at its front end. It is available in four languages, namely, English, Chinese, German, and Japanese. The latest release of Origin is Origin 2022b.

4.4 MEASUREMENT TOOLS

After the simulation and fabrication, the antenna is then tested for it performance. There are various measurement devices and setup for this process. The major measurements discussed here are

- Vector Network Analyzer (VNA)
- Spectrum Analyser
- Anechoic Chamber

4.4.1 Vector Network Analyser

A VectorNetwork Analyzer, commonly abbreviated as the VNA, is a laboratory instrument to measure and analyse networks operating in RF and microwave frequencies. The network performance is measured as a vector. The range of measurable frequencies includes from KHz to hundreds of GHz depending on the device specifications. VNA measures the phase and amplitude of the signal frequency along each point of sweep inputted. A VNA generates a signal and analyses the performance of the given network to this signal. VNA can analyse different devices and circuits or complete systems with source and receiver and has a good measurement accuracy. A VNA is very useful to measure the S-Parameters, i.e., the scattering parameters.

4.4.2 Spectrum Analyser

Spectrum analysers are like VNA in many ways but they are different too. A spectrum analyser is basically meant to analyse the signals that are fed to this instrument. It measures the signal attributes like the its signal level or the carrier signal, the phase disturbances or sidebands. It has a varied range of analysable bandwidth in comparison with the VNA as a spectrum analyser is expected to analyse the whole spectrum around the signal. Usually, spectrum analysers are used for testing of scalar components in which only magnitude of the wave, w.r.t its frequency, can be determined.

4.4.3 Anechoic Chamber

An anechoic chamber is a defined space specially designed, at which the EM waves cannot reflect from any waves or surfaces. A reflection free space. It is also closed completely to avoid any other form of energy entering this space. It is widely used to test some parameters of the antenna where other interferences are ruled out. The following are some parameters of an antenna system measured in an anechoic chamber.

- 3D spherical plots
- Gain
- Polarization
- Radiation pattern and
- Radiation efficiency of antenna.

Figure 4.2 shows the look of an anechoic chamber.

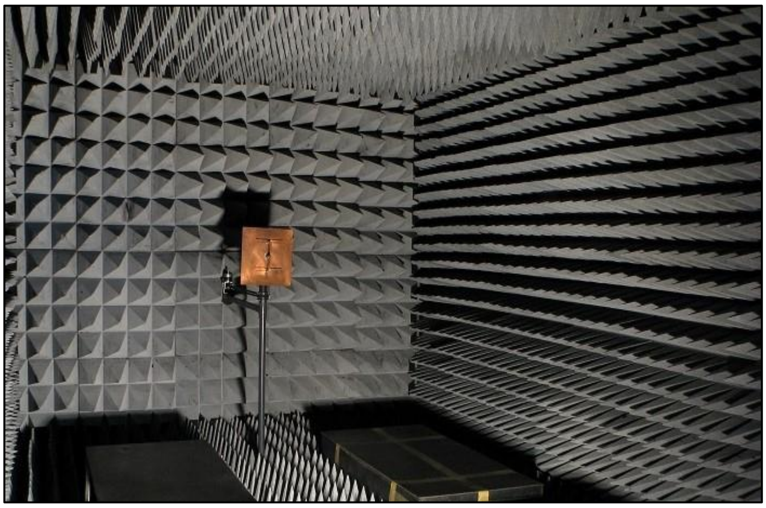

Figure 4.2: An anechoic chamber

4.5 CONCLUSION

This chapter studies the various software and tools required for antenna design, simulation, and testing. The High Frequency Structure Simulator (HFSS), for designing and simulation, the OriginPro, for publication of results, the various testing and measurement tools including the Vector Network Analyser (VNA), the Spectrum Analyser and the Anechoic Chamber are briefly explained.

CHAPTER 5

COMPACT LOG-PERIODIC STRUCTURED ANTENNAS FOR IOT APPLICATIONS

5.1 INTRODUCTION

IoT has set its footprints on every field of life and it is still extending its popularity into wider extends. IoT is a blend of various high-end technologies designed to sync in support each other to extend a different dimension of applications and utilities. IoT is based on an inter-connected chain of high performing sensors and the communication between these sensor nodes are relied on various modern communication technologies as per the application. IoT modules mostly uses wireless mode of communication and antenna element is an inevitable component of wireless technology. Communication modules of IoT system mostly demands them to be

- Miniaturized in size
- Low-energy consuming
- Low cost and
- Reliable.

In the present scenario, a particular communication standard or protocol, is still to be finalised for the IoT systems and therefore a multitude of existing communication protocols has been widely utilized in IoT systems as per application [78]. As the application areas of IoT are innumerable, a single wireless standard could hardly meet the demands of all IoT systems. IoT is widely employed for surveillance purposes, and making smart systems which may be within a few meters to large KMs of coverage. They include applications which includes a few sensor nodes to thousands of sensor nodes. Likewise, the size of the system, replacement options of the nodes, cost and reliability constrains, everything varies with application for IoT systems.

The communication protocol employed for a particular application is selected as per the above said requirements and constrains. The communication protocols can be divided roughly into three categories as per their range of operation. This is shown in Figure 5.1.

- Short-Range Protocols
    - (i) "Near Field Communication" (NFC)
    - (ii) "Bluetooth"
    - (iii) "Zigbee"
    - (iv) "Z-Wave"
    - (v) "Bluetooth Low Energy" (BLE) etc
- Medium-Range Protocols
    - (i) "Wireless Fidelity" (Wi-Fi)
    - (ii) "Wireless Local Area Network" (WLAN)
    - (iii) "Narrow Band IoT" (NB-IoT)
    - (iv) "Long Range" (LoRa)
- Long-Range Protocols
    - (i) "Low Power Wide Area Networks" (LPWAN)
    - (ii) Cellular Systems
    - (iii) "Global Systems for Mobile Communications" (GSM)
    - (iv) Sigfox etc.

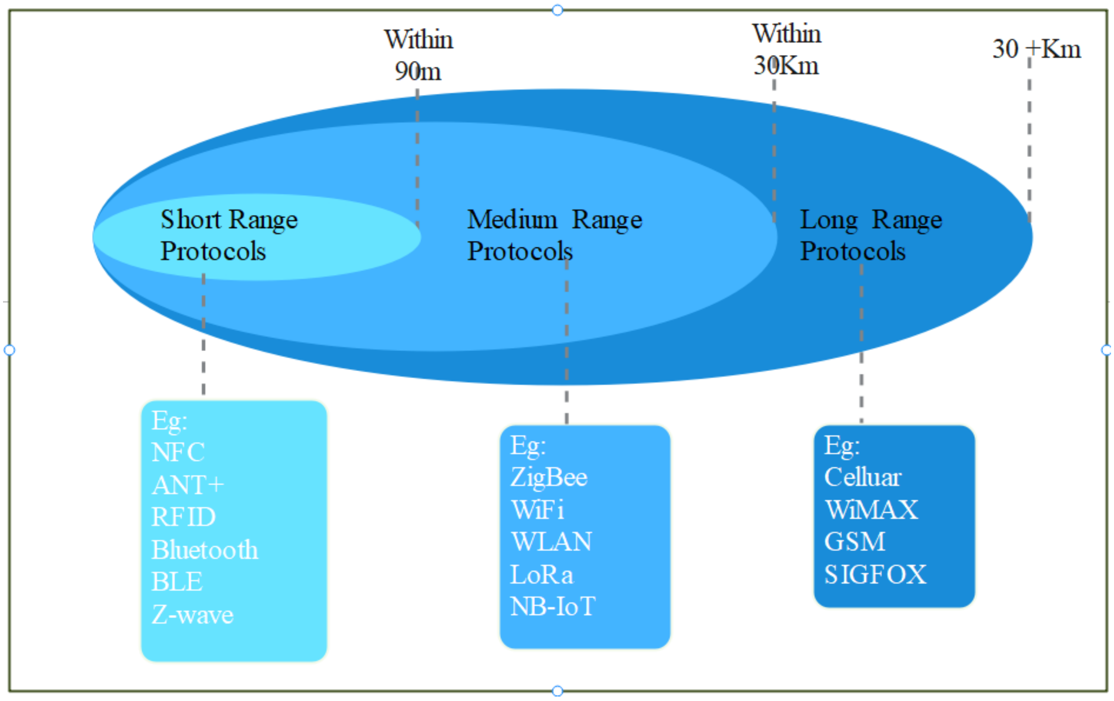

Figure 5.1 Communication Protocols employed in different IoT systems as per the requirement of range of connectivity required.

IoT has seen to be employing antennas tuned to a single frequency and multiple frequencies. Sub-6 GHz frequencies are widely employed in IoT applications. Some applications prefer to employ the most versatile 2.4 GHz frequency to connect the component nodes due to its already existing infrastructure and ease of operation. Various short range communication protocols are also centred around this frequency. There are also wideband antennas designed, which could support multiple communication protocols as per application requirements. Modern wireless systems demand antennas with simple design and multiband operational capabilities [79].

5.2 THE HISTORY AND THEORY OF LOG-PERIODIC ANTENNAS

The history of Log-Periodic antennas pulls down to 1952, when John Dunlavy invented it for United States Air Force. But he was not given credit for his invention due to "secret" classification. There have been lawsuits filed regarding the patent ship of Log-Periodic antennas between Urbana-Campaign and Channel-Master and Blonder-Tongue Labs. Log-Periodic antennas are a modified version of Yagi-Uda antennas.

The LP (Log-Periodic) antenna or LP aerial is also known as Log-Periodic Dipole Array (LPDA), and it consist of many radiating elements with gradually increasing length. The elements are connected to a common feedline from the centre. This special structure and multiple radiating elements provide wideband directional characteristics with good gain. These antennas were initially developed to enhance the UHF (Ultra High Frequency) and VHF (Very High Frequency) band usage. The LP arrays can be

- Zig-Zag Log Periodic arrays
- Trapezoidal shaped Log-Periodic systems
- V-Log Periodic Systems
- Slotted Log-Periodic Systems or
- Dipole Log-Periodic array system.

Some relevant Log-Periodic structured antennas in the literature are summarized in the following Table 5.1 given below.

The potential of Log-Periodic structures can be exploited for upcoming IoT applications. The size and characteristics can be tuned using different techniques like embedding slots, applying DGS (Defected Ground Structure), and implementing high end techniques like MIMO systems.

Table 5.1: Literature review on existing Log-Periodic Structured antennas

[80]	An ultra-wide-band trapezoidal Log-periodic antenna is proposed for operation in the frequency range of 5.2 GHz to 40 GHz on RO4003 substrate. The gain of this antenna is 17.8 dBi. This antenna is proposed for emerging broadband applications in communication systems.	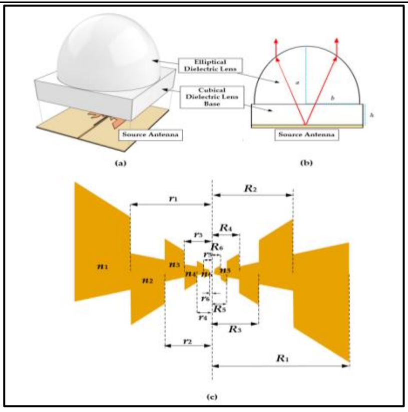
[81]	A Log-periodic antenna with wideband characteristics is designed with a slot. The antenna is designed using FR4 and the antenna size is 42 mm×42 mm×1.6 mm. The observed antenna gain is 4.5 dBi. It is designed to operate in the Low L, High L and S band for navigational applications.	
[82]	A butterfly shaped antenna is proposed for X-band civil and military applications. The antenna is designed using both FR4 and metamaterial and the antenna size is 380 mm×138 mm×1.6 mm. The patch length of the antenna is varied logarithmically and the dimension of each strip is according to the log-periodic structure design. The operational frequency range for this antenna is from 8 GHz to 12 GHz and observes a gain of 4.52 dB with metamaterial substrate. This antenna is proposed for X-Band applications.	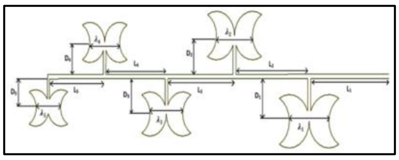

A miniaturized antenna design upholds a challenge to antenna designers as the utilization of a compact base (ground plane) will greatly restrict the bandwidth, gain and other radiation characteristic parameters of the antenna. The design and the design dimensions will greatly influence the performance of the miniaturized antennas. This chapter discusses two highly miniaturized antennas which are log-periodic structured and designed and developed on FR4 substrate. The designed antenna offers radiation characteristics which would make it a good choice for small sensor node IoT system applications.

5.3 A MONOPOLE CO-PLANAR FED LOG-PERIODIC ANTENNA FOR IoT APPLICATIONS

5.3.1 Introduction

The communication systems these days need to be compact and energy efficient systems supporting various technologies, increased coverage, higher speed, ultra-low latency, and massive connections. The antennas being a vital part of these systems has also greatly evolved during these times incorporating various new techniques and technologies. The WLAN system connections and operations are a bare minimum expectation from every mobile device in today’s world and the support to other systems simultaneously. The 2.4 GHz frequency has remained as the most popular frequency for over a couple of decades as it was the first frequency to be brought into the consumer market of wireless networking and microwaves. When FCC declared the unlicensed spectrum, the already licensed frequencies were steer cleared and considered from other popular available frequencies. The 2.4 GHz has larger unobstructed range and requires smaller antenna in addition to relatively effective dielectric heating. 2.4 GHz has remained the admired frequency ever since the emergence of wireless technology.

5.3.2 Antenna Design Evolution and Dimensions

A novel CPW (Co-Planar Waveguide) fed miniaturized monopole antenna is devised and proposed for IoT systems. Radiating patch of the antenna is Log-Periodic shaped and is built on low-priced FR4substrate having thickness 1.6mm. FR4 material is easily available and cheap. The dimensions of FR4substate material are calculatedly assumed as a multiple of desired resonant frequency of 2.4 GHz and it is 0.16 λ_r. The trapezoid shaped arms of the radiating log-periodic structure to both sides from the centre is chosen according to the geometric-ratio equation for log-periodic structured antennas as in Equation (5.1).

$$\tau = \frac{R_n}{R_n - 1} \qquad \text{---------------------(5.1)}$$

A grounded co-planar feed is used in the design in which there are two additional ground plane patches to either side of the feedline. The co-planar ground is so called because the ground plane, radiating patch and feedline are on same. Structure of such a feed is shown in Figure 5.2. this feeding technique helps in the erasure of alignment issues which usually arises due to etching on either side of the substrate. The dimensions of this co-planar system are calculated using the design equations given in Equation (5.2).

$$q = \frac{1K\,(k_2)\,K'(k_1)}{2K\,(k_1)\,K'(k_2)} \qquad \text{-------------------(5.2)}$$

where

$$k_1 = \frac{a}{b} \text{ and}$$

$$k_2 = \frac{\sinh\left(\frac{\pi a}{2h}\right)}{\sinh\left(\frac{\pi b}{2h}\right)}$$

The so designed CPW feed is fixed at 2mm from the feedline on either side.

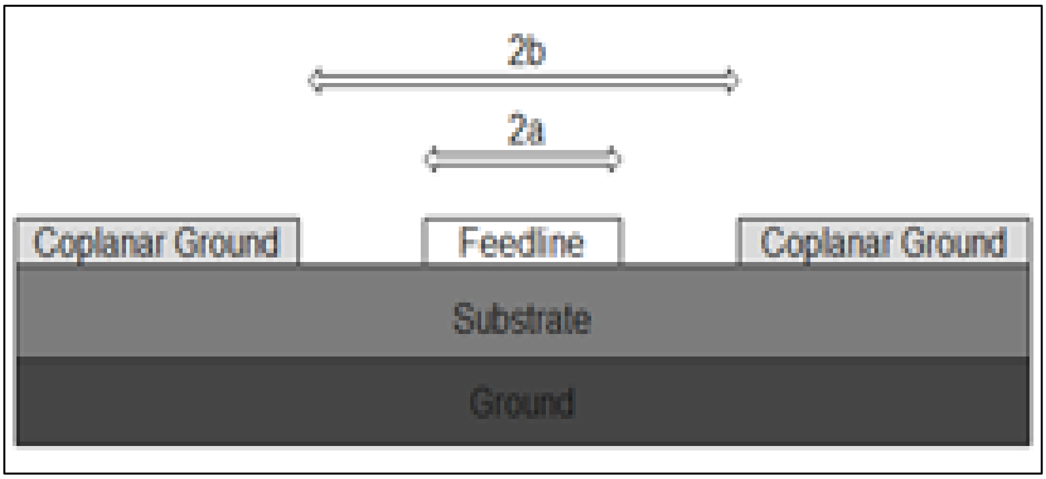

Figure 5.2 Structure and design of a CPW feeding technique

The log-periodic structured radiating element with so designed CPW feed is the first design stage and is named as Ant 1. The schematic of Ant 1 is shown in Figure 5.3. The simulated values for the return loss and voltage standing wave ratio (VSWR) for Ant 1 is as shown in Figure 5.4 and Figure 5.5. Ant 1 resonates around 3.6GHz with a return loss of -15.24 dB. Ant 1 has a bandwidth of 170 MHz ranging between 3.5 GHz and 3.67 GHz. the VSWR for Ant 1 remains below 2 and the maximum value for the same is 1.814 over the operating frequency range.

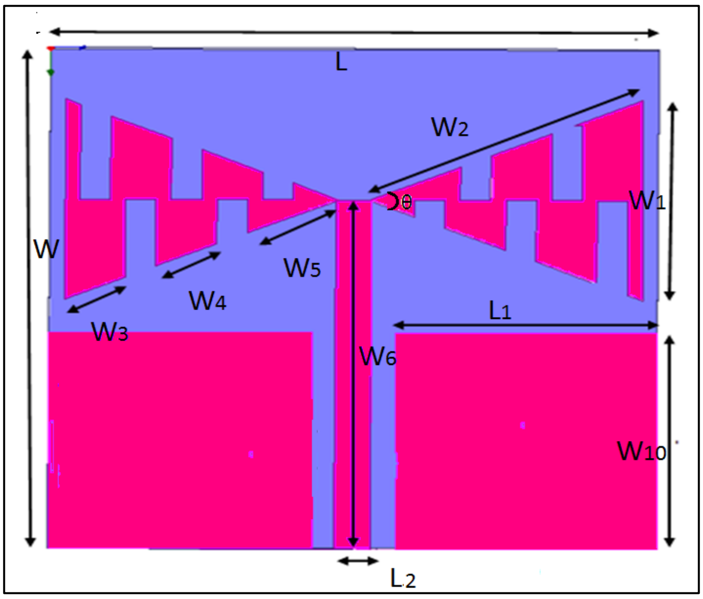

Figure 5.3: Schematic of Ant 1.

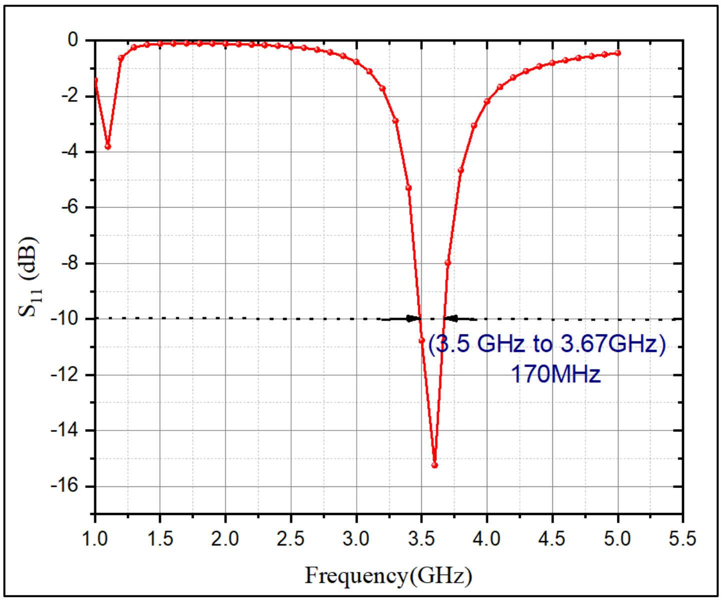

Figure 5.4: Simulated S_{11} of Ant 1

The wireless protocol and the operating frequency of an IoT module is picked out based on many factors like the speed and reliability of communication, the area of coverage required, the nodes connected, cost of the system, amount of data to be transmitted etc. The IoT systems widely employs 2.4 GHz for the communication between nodes and furthermore a lot of communication protocols like Bluetooth, Wi-Fi, LoRa, Zigbee etc operates at 2.4 GHz. So, it will be greatly beneficial to tune the designed compact antenna to 2.4 GHz.

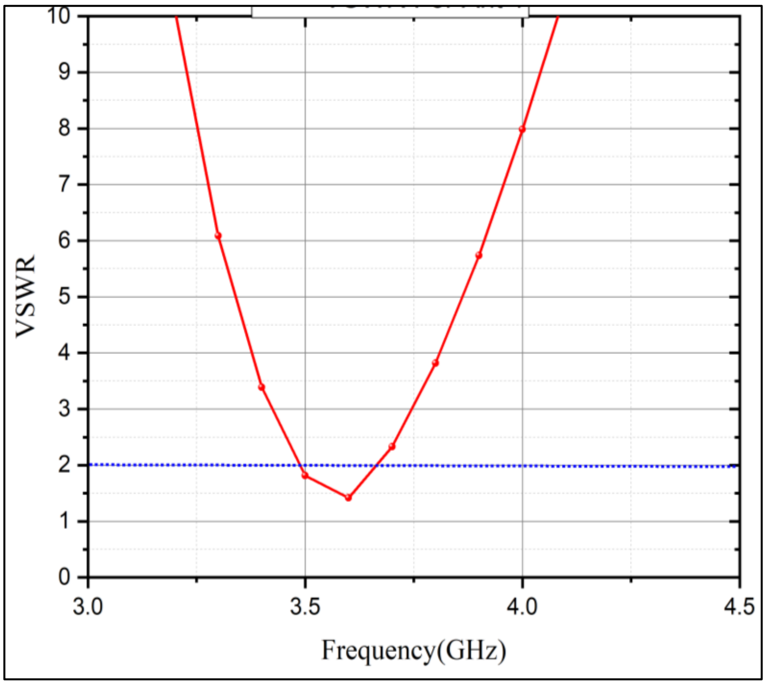

Figure 5.5: Simulated VSWR Curve for Ant 1 with respect to different frequencies.

Ant 1 is further modified to Ant 2 by the addition of two rectangular slots of dimension $7.4\ mm \times 3\ mm$ in the co-planar ground plane. The slot is fixed at a height of $3mm$ from the port of the antenna. The schematic representation of Ant 2 is shown in Figure 5.6. The design dimensions for the proposed antenna are given in Table 5.2.

Table 5.2 Final Proposed Antenna Structure Dimensions

Parameter	**Dimension**	**Parameter**	**Dimension**
L	$20\ mm$	W_3	$2.18\ mm$
L_1	$7.5\ mm$	W_4	$2.18\ mm$
L_2	$1\ mm$	W_5	$3.17\ mm$

L_3	7.4 mm	W_6	13.95 mm
θ	48°	W_7	4 mm
W	20 mm	W_8	2 mm
W_1	8 mm	W_9	3 mm

The use of these rectangular slots to the co-planar ground plane shifted the resonant frequency from 3.6 GHz to 2.46 GHz with a return loss of 29.56 dB. The graph implying the return loss for Ant 2 is shown in Figure 5.7.

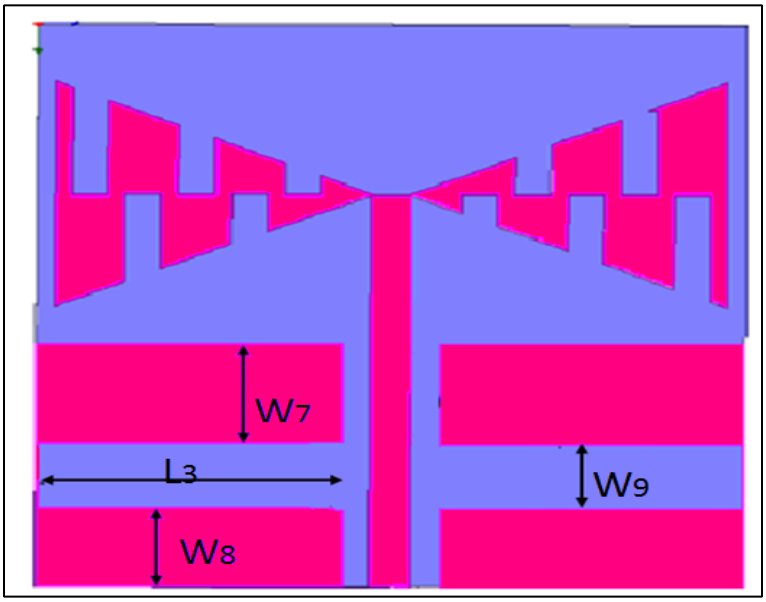

Figure 5.6: Schematic of Ant 2 showing the slot in the co-planar ground

The prototype of the designed antenna after fabrication is shown in Figure 5.8.

5.3.3 Parametric Study on slot size

A couple of parametric studies are done to optimize the antenna design and to achieve 2.46 GHz resonance. The shift in the frequency of resonance is achieved by the addition of a co-planar ground slot. The dimensions and position of the slot-structure embedded is finalized by the parametric study. Figure 5.9 shows the slot dimensions set under parametric study.

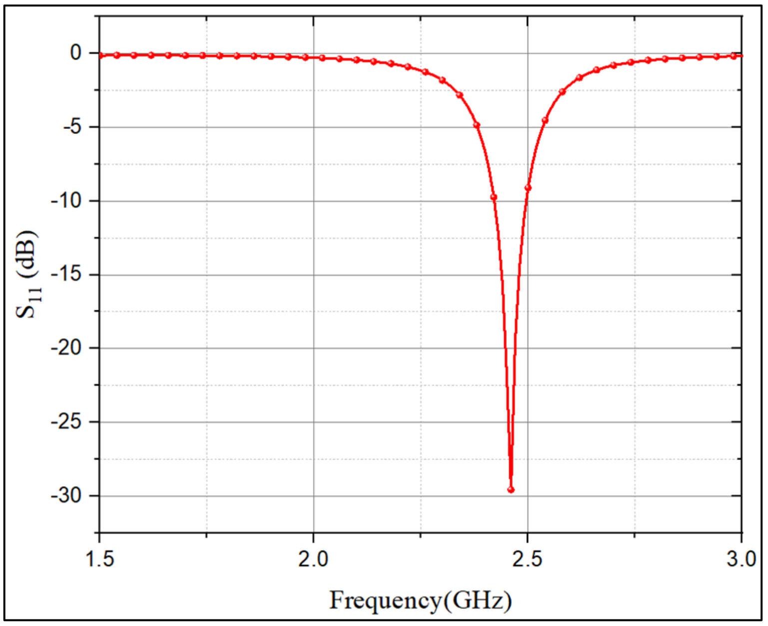

Figure 5.7: Return Loss for Ant 2

Figure 5.8: Fabricated prototype for the proposed antenna (Ant 2)

Parametric Study on Width of the Slot

The width of the slot, W_9 is investigated parametrically. The resonant frequency shifted according to the variation in the width of the slot. The parametric examination result performed on the W_9 dimension (width of slot) is as shown in Figure 5.10. The results shows that a return loss of 30.35 dB is attained at 2.29 GHz.

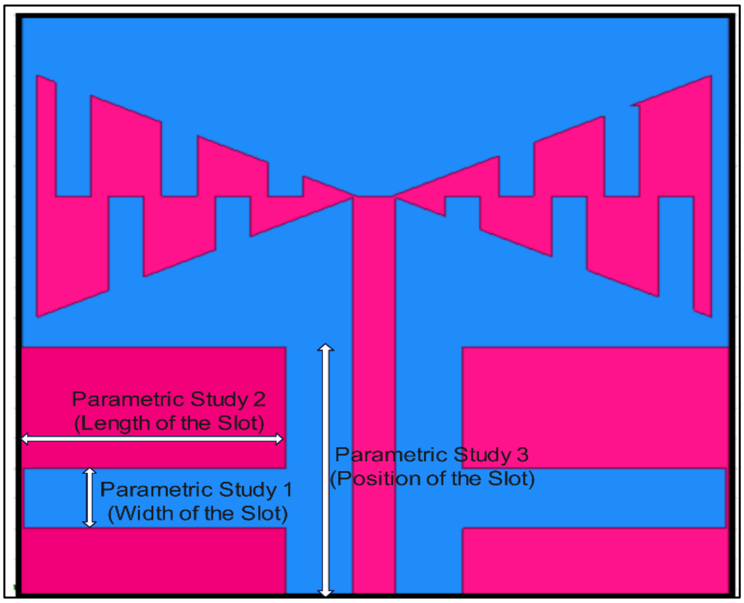

Figure 5.9: Ant 2 schematic showing the dimension under parametric study.

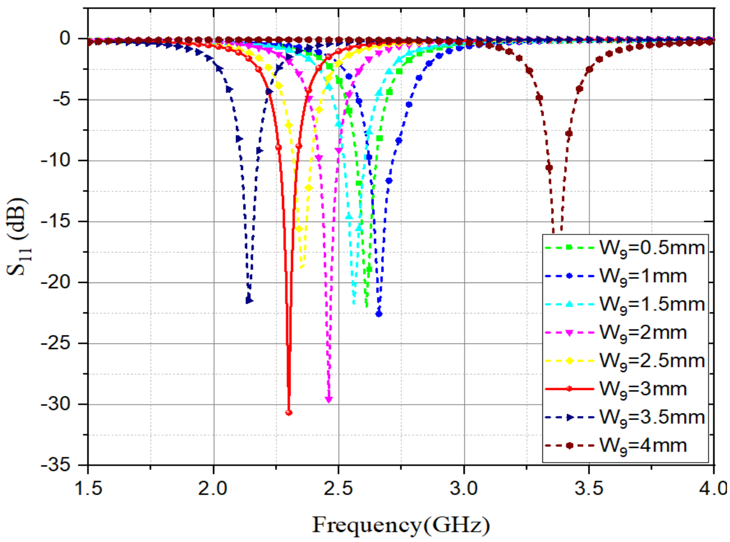

Figure 5.10: Parametric study results on width of the slot on co-planar ground

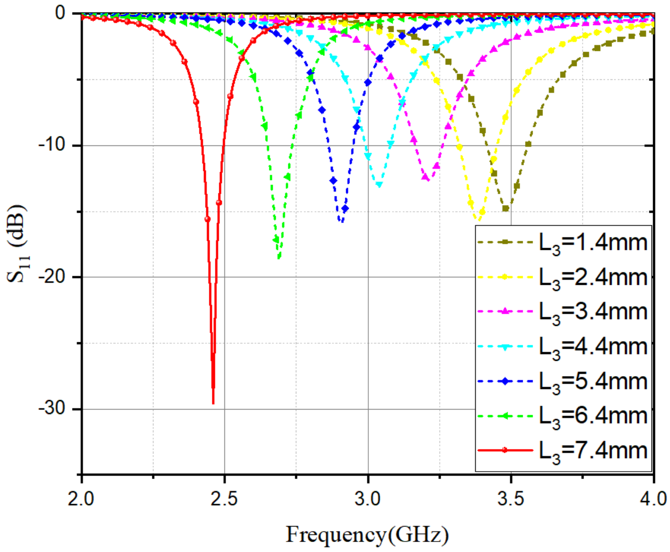

Figure 5.11. Parametric study results on L_3 varying from 1.4 mm to 7.4 mm

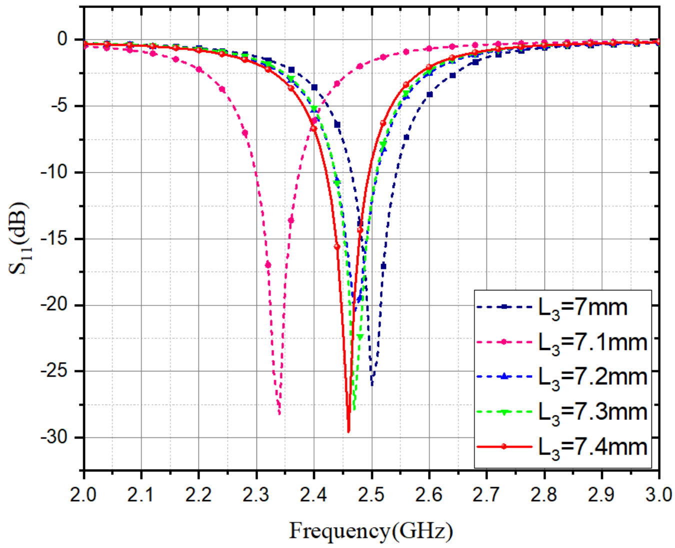

Figure 5.12: Minute Parametric study results on L_3 varying from 7 mm to 7.4 mm

Parametric Study on Length of embedded Slot

Length of slot embedded in co-planar ground also influences resonating frequency and the S_{11} as shown in Figure 5.11 and 5.12. It is seen that as length of the slot is reduced, the resonant frequency shifts to the right. The best return loss is obtained at $L_3 = 7.4$ *mm* at 2.46 GHz.

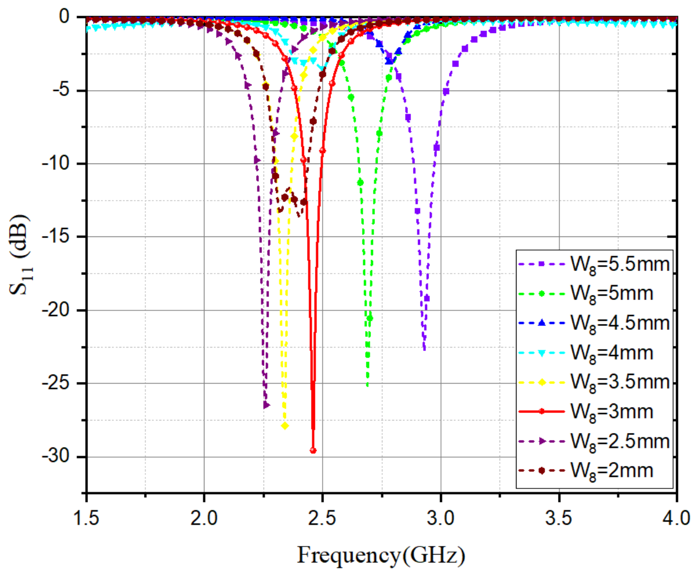

Figure 5.13: Parametric Analysis study done on the position of the slot on the co-planar ground.

Parametric Study on the position of the Slot

Parametric study was also conducted on the position of the $L_3 \times W_9$ structure on the ground. The slot was positioned from a distance of $2mm$ to $5.5mm$ from the feed point. At $3mm$ from the feed point, the structure resonated at 2.46 GHz marking an S_{11} of 29.56 dB. Figure 5.13 depicts the outcome of parametric study done in positioning the slot.

5.3.4 Results and Discussions

A compact microstrip antenna is designed, fabricated and tested for IoT applications. The proposed antenna is tuned to 2.46 GHz with a return loss of 29.56 dB. The bandwidth for the proposed antenna ranges between 2.43 GHz to 2.5 GHz effectively giving a working bandwidth of 70 MHz. The final antenna, Ant 2, is designed by incorporating an optimized slot structure on co-planar ground. Return loss measures the amount of energy that is released by antenna system and for good performance the return loss is preferred to be lesser than -10 dB. The S_{11} and frequency of resonance for the antenna with and without slot on the ground plane is given in Figure 5.14.

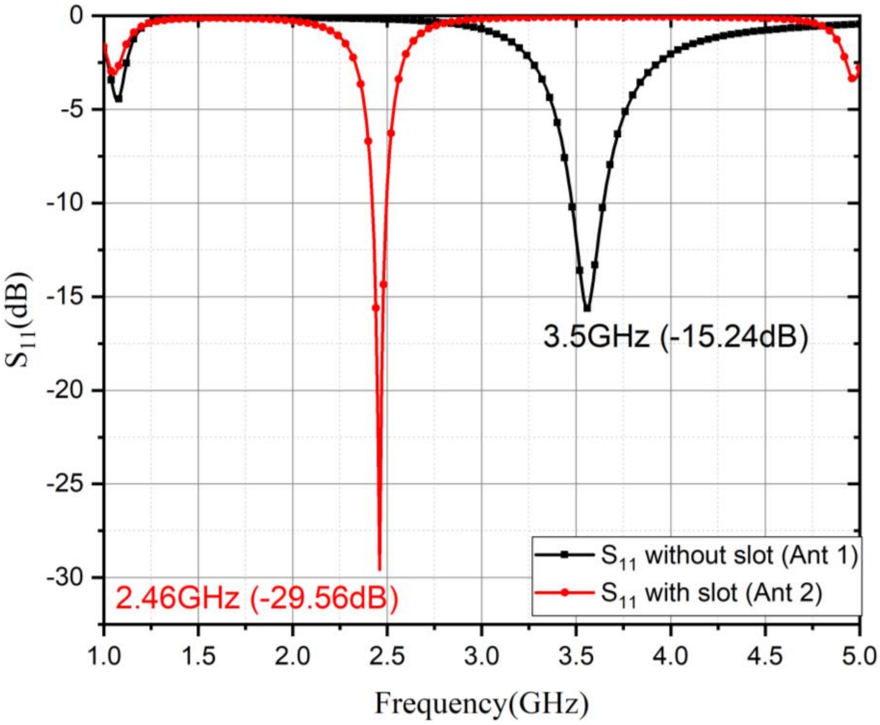

Figure 5.14: Return Loss for Ant 1 and Ant 2

The Voltage Standing Wave Ratio (VSWR) is measuring the efficiency of the antenna to transfer power from the source to the load. The acceptable range of VSWR for a well performing antenna needs to be between 0 and 2. The VSWR plot for both Ant 1 and Ant 2 is given below in Figure 5.15.

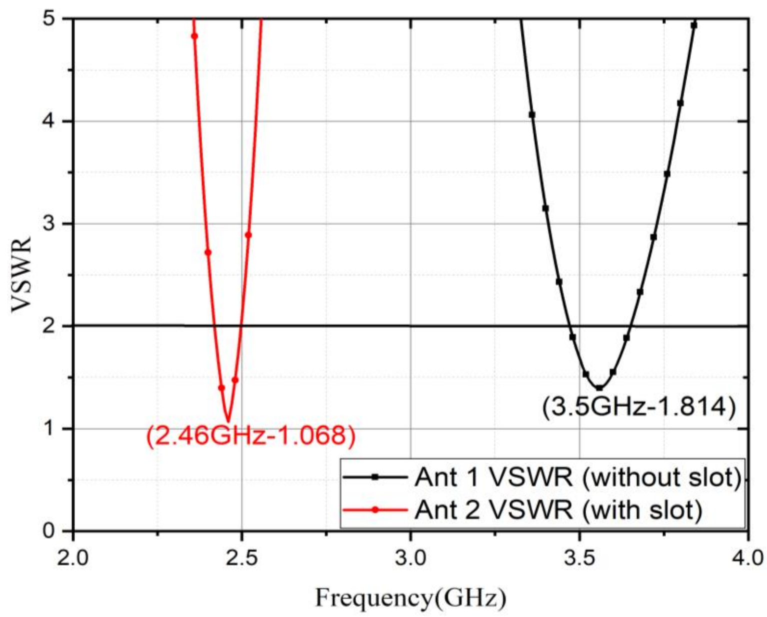

Figure 5.15: Voltage Standing Wave Ratio (VSWR) for Ant 1 and Ant 2

Gain describes an antenna's directionality, and microstrip antennas usually have low gain. Having a high gain is always desirable for an efficient antenna. Figure 5.16 demonstrations that the Ant 2 attains 9.34 dBi gain at 2.46 GHz.

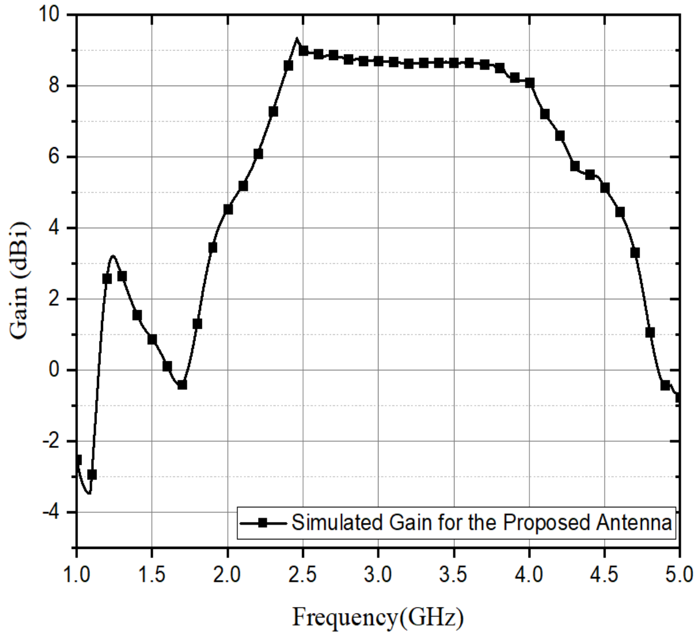

Figure 5.16: Gain and Frequency plot for the proposed antenna (Ant 2)

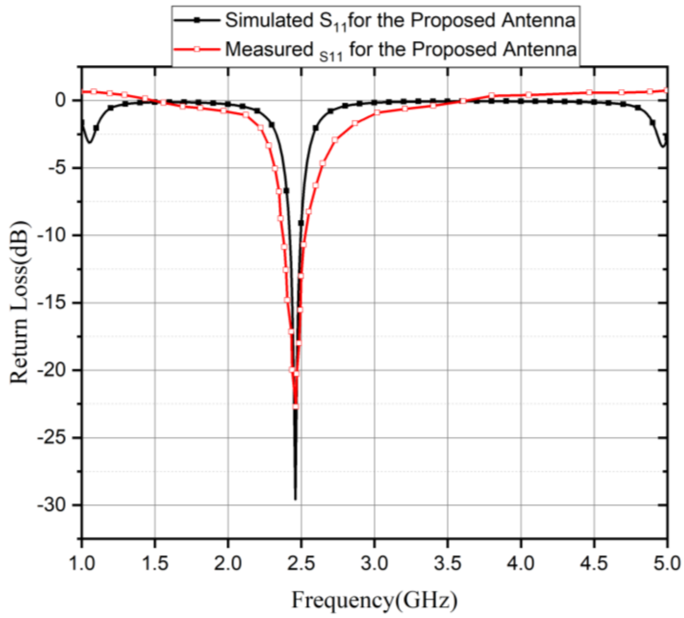

Figure 5.17: Simulated and Measured S_{11} for Ant 2

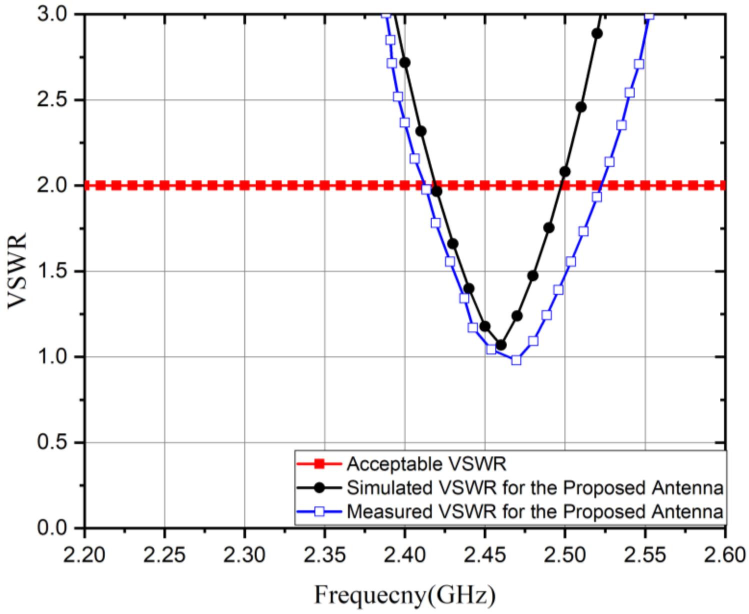

Figure 5.18: Simulated and Measured VSWR for Ant 2

After fabrication on the most used, low-cost, FR4 substrate, experimental analysis of proposed design was done with spectrum-analyser along with network analyser. Measured outcomes were, to a good extend, similar to simulated results unless for the reduction in gain from 9.34 dBi to 5 dBi. This might be due to slight losses during process of fabrication and difference in fine tuning of instruments during practical measurement. The simulated and measured return loss (Figure 5.17), VSWR (Figure 5.18) and Gain (Figure 5.19) are as given below.

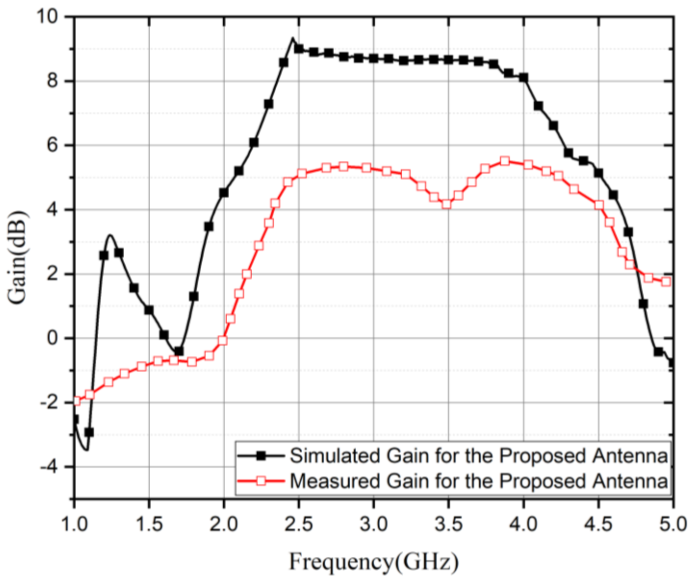

Figure 5.19: Measured and simulated gain for Ant 2

Table 5.3: Current State of Art on similar antennas

Ref. No	Type of Feed	Size	Bandwidth	Gain	Substrate Used
[26]	ACS	$24\times10\times0.144mm^3$	(1.7-2.02) GHz and (2.25-2.65) GHz	2.5dB	FR4
[27]	CPW	$130\times90\times6.35mm^3$	(697-991) MHz / (2.38-2.5) GHz / (3.07-3.35) GHz / (5.61-5.92) GHz.	2.76dBi/ 3.29dBi/ 5.96dBi/ 5.5dBi.	Poly-guide
[30]	ACS	$12\times16.5\times1.6mm^3$	(2.4-2.5) GHz / (4.0-6.1) GHz	3.7dBi	FR4
[31]	CPW	$3.1\times32.7\times0.254mm^3$	(3.2-30) GHz	4.87dB	Kodak Paper
[32]	Microstrip Line	$24\times26\times 1.6mm^3$	8.9GHz (3.1-12GHz)	5.1dBi/ 11.5dBi	FR4
[33]	Microstrip Line	$14\times14mm^2$	(3.4-3.6) GHz/ (5.1-6.1GHz)	1.76dBi/ 3.32dBi	Rogers RO4003
[83]	Microstrip Line	$40\times5\times5.35mm^3$	915MHz/ 868MHz	---------	Rogers RO4003
[84]	Co-axial Feed	$56\times56\times35.3mm^3$	2GHz-6GHz	>1.5dBi-5.18dBi	FR4
[85]	CPW	$20\times25\times 1.6mm^3$	(4.8-6.8) GHz	------	FR4
[86]	CPW	$20\times37\times 0.508mm^3$	(2.085-2.72) GHz (2.89-4.35) GHz (4.59-7.055) GHz	(-2.4- 0.08) dBi (-1.27-2.62) dBi (1.05-4.39) dBi	Rogers 4350

Proposed Work	**CPW**	**20×20× 1.6mm^3**	**(2.43-2.5) GHz**	**9.36dB**	**FR4**

5.4 A 2-ELEMENT LOG-PERIODIC STRUCTURED MIMO ANTENNA FOR IoT APPLICATIONS

5.4.1 Introduction

The modern-day communication systems are expected to support very high data rates application like unhindered and low latency video streaming and also low data rate and unswerving communication between adjacent nodes [58]. MIMO antenna systems, which uses multiple antennas at the transmitter and receiver side, ensures higher data rates and better channel capacity at no extra cost of bandwidth [59]. A wideband MIMO system which can support more than one communication protocol is highly desired for IoT applications and WiMAX technology, which was so far in the shadow of LTE, also has the potential to be an alternative communication technology for IoT applications [68]. WiMAX systems are characterised by provisions to cover above 30 KM with no complicated installations required. Table 5.4 summarises the significant features of WLAN and WiMAX technologies.

Table 5.4: Features of WiMAX and WLAN communication protocols

Specification	WiMAX	WLAN
Standard	IEEE 802.16 d/e	IEEE 802.11b
Data Rate	70 Mbps	1–54 Mbps
Coverage distance	50 km	Around 100 m
Operating Frequency	2.3 GHz, 2.5 GHz, and 3.5 GHz	2.4 GHz and 5.8 GHz
Channel Bandwidth	1.25 to 20 MHz	25 MHz
Applications	Broadband Connectivity, USB Dongles, Metropolitan Area Networks	Automation of substations, Control and Monitoring of sensor nodes

MIMO uses multiple antennas at the transmitter and receiver. This technique has proved to be useful to accomplish higher throughput and better data rates. Limitations in channel capacity and the amount of transmitted power can also be overcome by MIMO technique [65]. MIMO systems can offer spatial multiplexing (different signals transmitted simultaneously through different antennas) and diversity gain (same signal received through diverse paths). The major challenge faced in designing a MIMO antenna system is reducing the interaction between the radiating elements and attaining a minimum isolation of 15 dB between them.

A miniaturised two element MIMO system with size *15mm×17mm* is discussed in the sections below. It has a wide range of coverage of above 2 GHz and can be utilized for intermediate (medium) and long-range communication between IoT operational points (nodes) using WLAN and WiMAX communication technologies. The defected ground method is a technique used to augment and shift the bandwidth and to suppress the interaction between the component elements in the MIMO structure.

5.4.2 Antenna Design Evolution and Dimensions

The radiating element geometry is like a trapezoidal toothed log-periodic structure as shown in Figure 5.20. As the structure tends to form a cone towards the apex, the conductor fields attenuate with distance from the feed point.

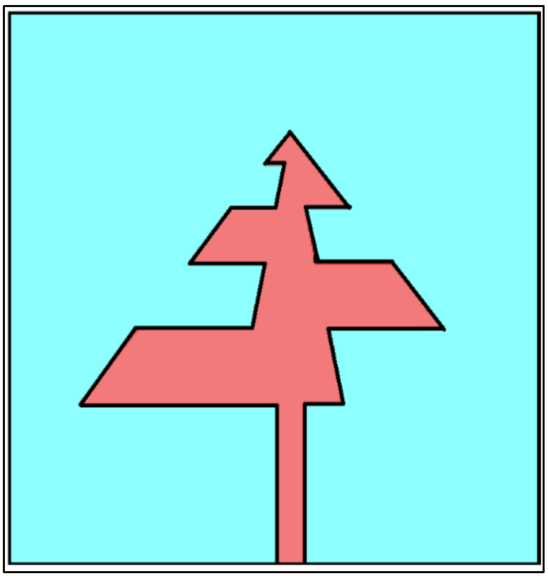

Figure 5.20: Structure of single radiating element

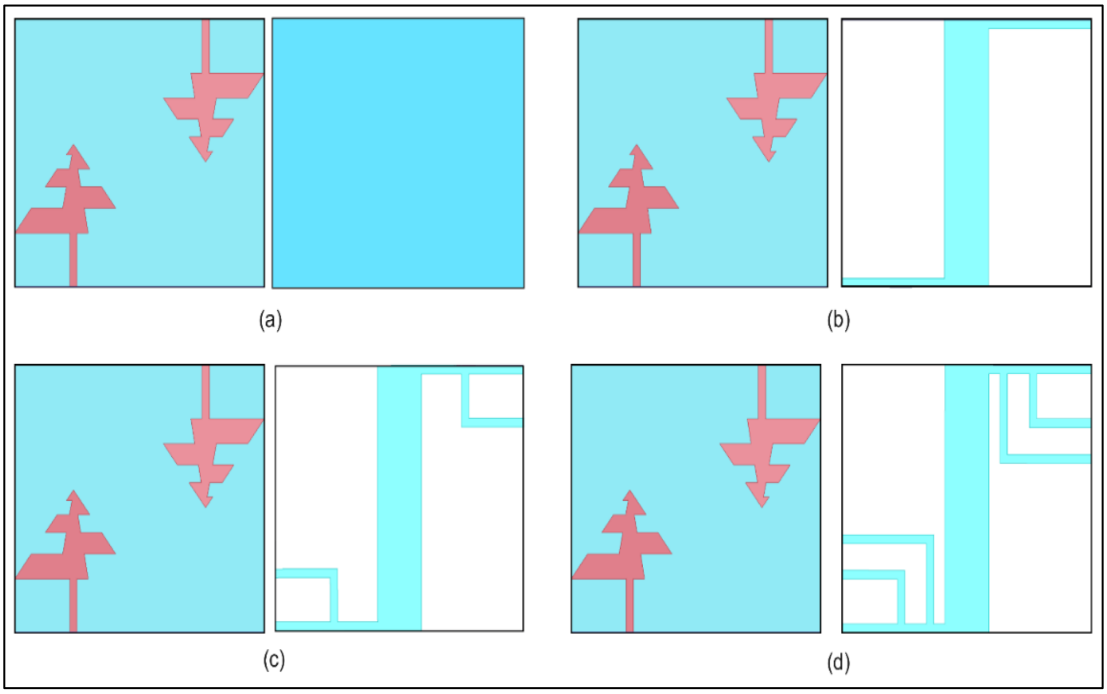

Figure 5.21 Evolutionary stages of antenna. (a) Stage 1 with two element MIMO and no DGS named as **Ant I**. (b) Stage 2, two element MIMO with two slots in ground plane-**Ant II**. (c) Stage 3, Two element MIMO with one L-shaped rectangular slit in DGS-**Ant III**. (d) Two element MIMO with two L-Shaped rectangular slits in the DGS-**Ant IV**.

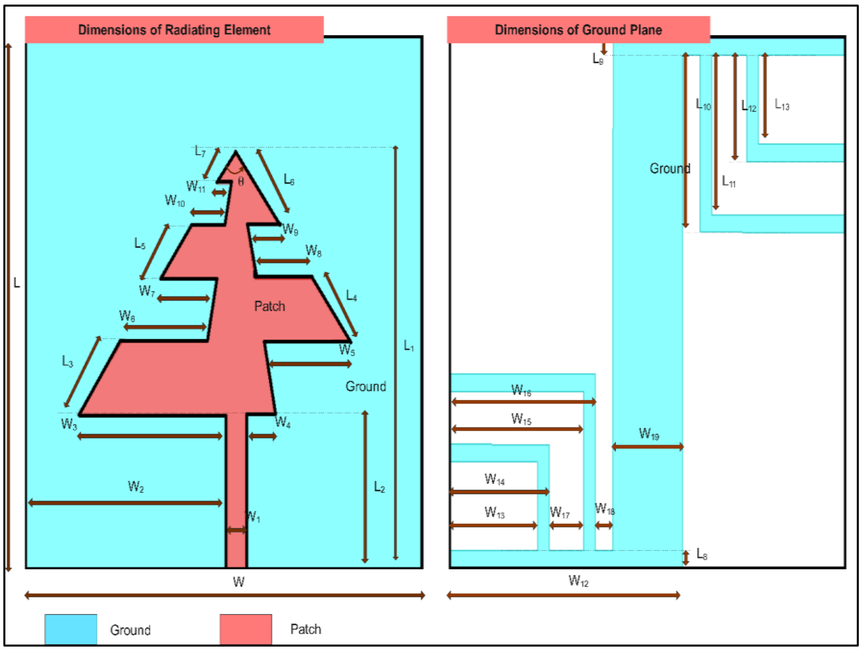

Figure 5.22: Dimensions of radiating element and ground

Table 5.5: The antenna design dimensions

Dimensions of the Patch				**Dimensions of the Ground Plane**			
W	17mm	L	15mm	W_{12}	10.0mm	L_8	0.50mm
W_1	0.5mm	L_1	7.5mm	W_{13}	3.75mm	L_9	0.50mm
W_2	3.75mm	L_2	2.5mm	W_{14}	4.0mm	L_{10}	5.0mm
W_3	3.75mm	L_3	1.792mm	W_{15}	5.75mm	L_{11}	4.50mm
W_4	0.75mm	L_4	1.536mm	W_{16}	6.25mm	L_{12}	3.0mm
W_5	2.14mm	L_5	1.280mm	W_{17}	1.70mm	L_{13}	2.75mm
W_6	2.15mm	L_6	1.792mm	W_{18}	0.75mm		
W_7	1.44mm	L_7	0.768mm	W_{19}	3.0mm		
W_{10}	0.84mm						
W_{11}	0.38mm						

Microstrip line feed is used for the antenna. The evolutionary stages of the antenna are shown in Figure 5.21. Ant I is a two element MIMO system with radiating element structured similar to trapezoidal toothed log-periodic structured. Ant II is Ant I with a modified ground plane. Two rectangular slots are added to the ground side to alter current distribution of the ground plane. Ant III is the structure with an addition of an L-shaped slit to the ground surface and Ant IV added one more L-shaped slit to Ant III to minimize mutual interaction between the radiating elements. Figure 5.22 and Table 5.5 shows the dimensions of the radiating patch and the ground. The stage wise S-parameters for all the antennas is given in Figure 5.23 (a) -5.23 (d)

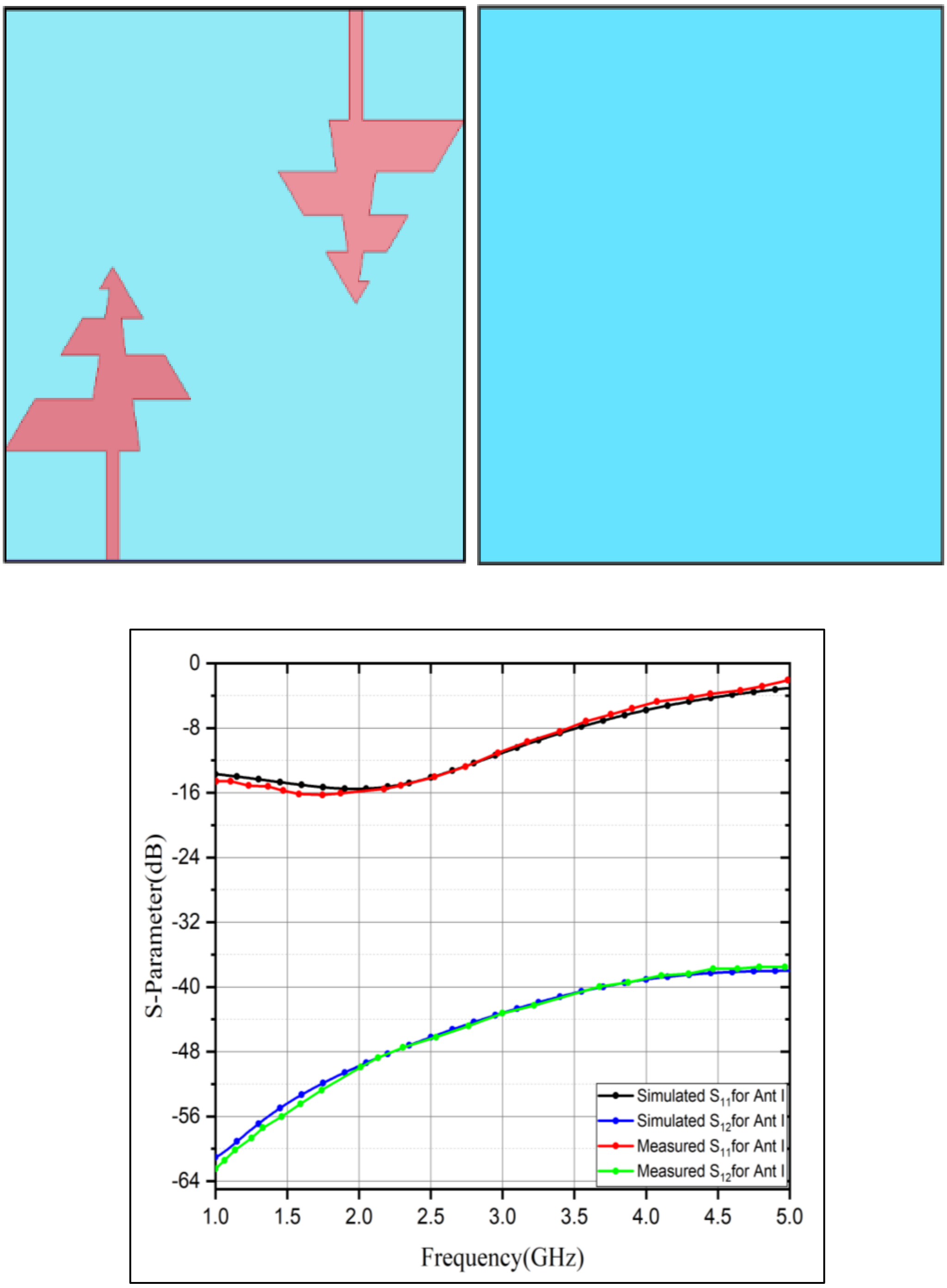

5.23 (a): The patch and the ground plane of Ant I with corresponding S-parameters

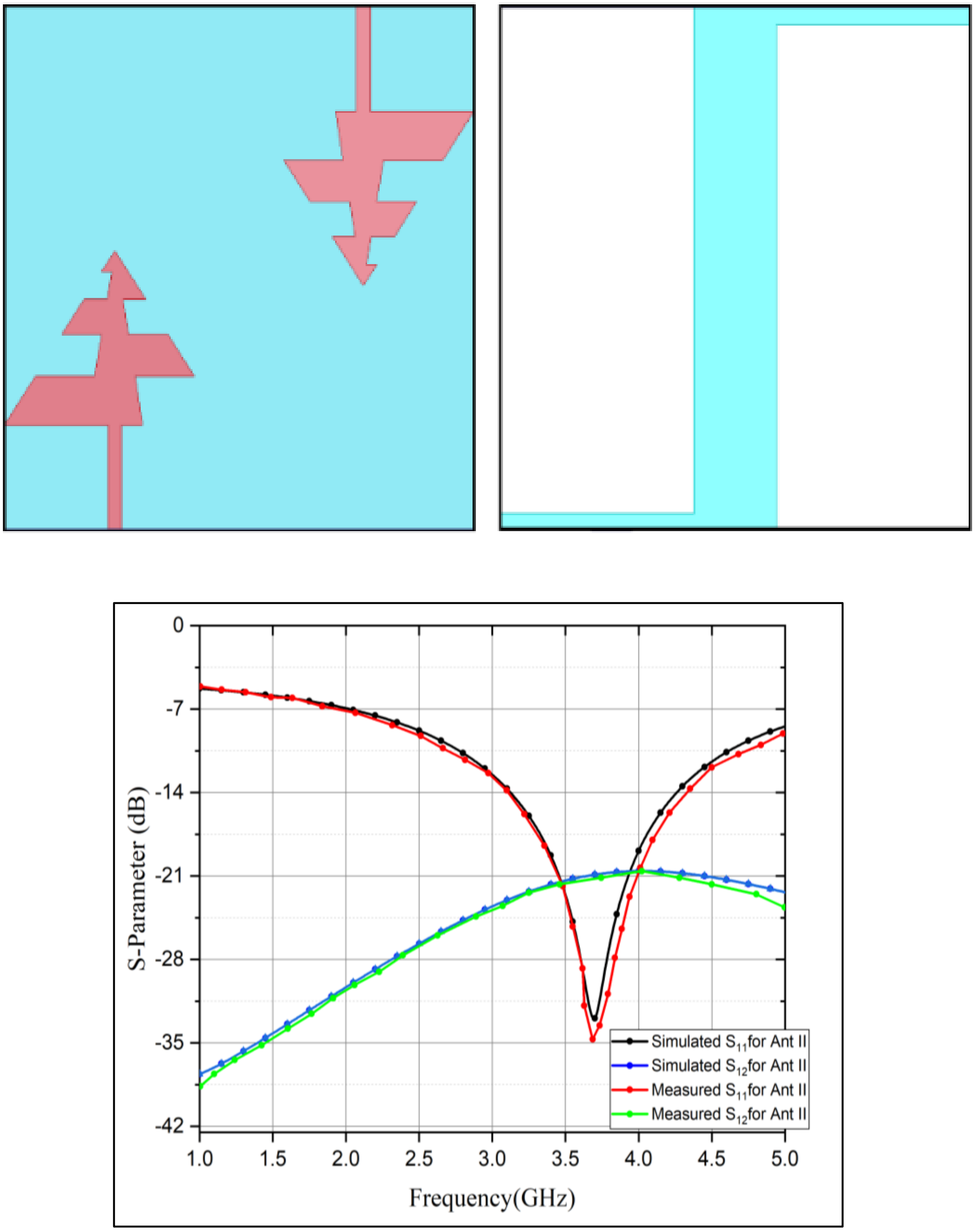

Figure 5.23 (b): The patch and the ground of Ant II with corresponding S-parameters.

Ant I, as seen in Figure 5.23 (a), gives an operational bandwidth of 2.94 GHz. This is without implanting any defect on the ground plane. A defect in the ground surface of the design is supposed to modify current distribution and thereby control the radiation characteristics of the antenna. Ant II, as shown in Figure 5.23 (b), is Ant I with a modified ground plane. Ant II ground is cut with two slots of *14.5mm×7mm* as indicated in Figure 5.23 (b) and Ant II provides an operational bandwidth from (2.69

to 4.69)GHz. The mutual interaction between the radiating elements of Ant II is below 20 dB

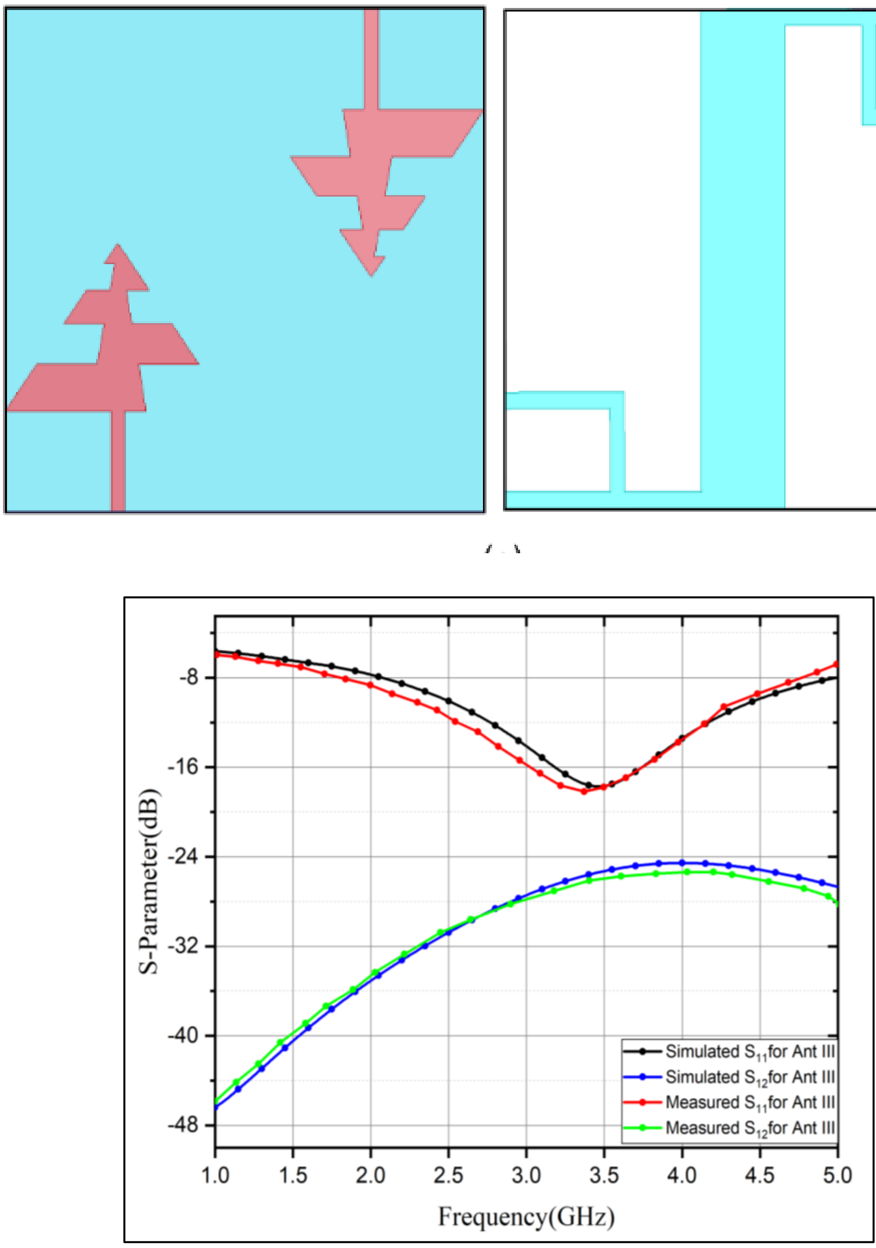

Figure 5.23 (c): The patch and the ground of Ant III with the corresponding S-parameters.

Addition of a rectangular L-shaped slit of size $L_{12}\times W_{14}$ to Ant II, further shifted the impedance bandwidth to the left to be between 2.48 GHz to 4.47 GHz and reduced the mutual coupling further to below -24 dB. Ant III and its corresponding S-parameters are indicated in Figure 5.23 (c).

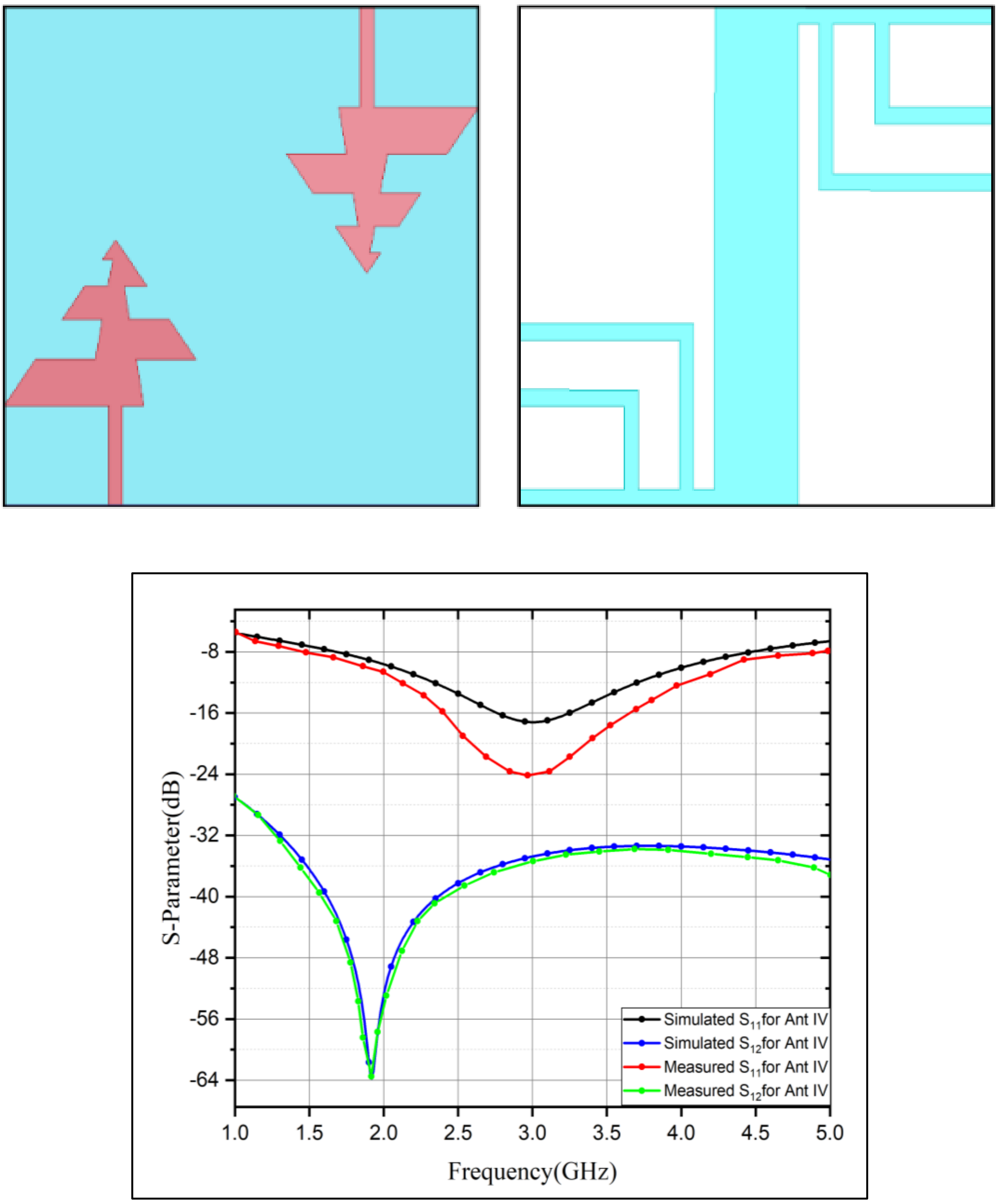

Figure 5.23 (d): The patch and the ground plane of Ant IV with the corresponding S-Parameters.

Further, a second L-shaped slit was added again as shown in Figure 5.23 (d). This slit is of 0.5mm width and $L_{10}\times W_{16}$. Ant IV offered a bandwidth of 2 GHz between (2.06 to 4.04)GHz with an isolation of more than 30 dB.

5.4.3 Parametric Study

The DGS of the ground plane was optimized using a bunch of parametric study. In stage 2, Ant II has a rectangular slot embedded in the ground plane. The length and width of this slot is *14.5mm×7mm*. Both these dimensions were put under parametric study as shown in Figure 5.24 and Figure 5.25. A return loss of 31.6 dB was observed for the length *l=14.5mm* as in Figure 5.21 and a width of 7mm improved the return loss to 35.5dB. The bandwidth of the system remained unaffected by the changes in the width of the slot as shown in Figure 5.25. So, the rectangular slot of stage 2, Ant II has an optimized slot cut in its ground plane of size *14.5mm×7mm.*

The DGS of Ant II is added with a slit of dimension $L_{12}\times W_{14}$ and 0.3mm width. The addition of this L-shaped slit has seen to shift the bandwidth to the left of the frequency spectrum and slightly improve the isolation from 20 dB to 24 dB. Figure 5.26 shows the parametric investigation done on the width of this slit to optimize it at 0.3mm.

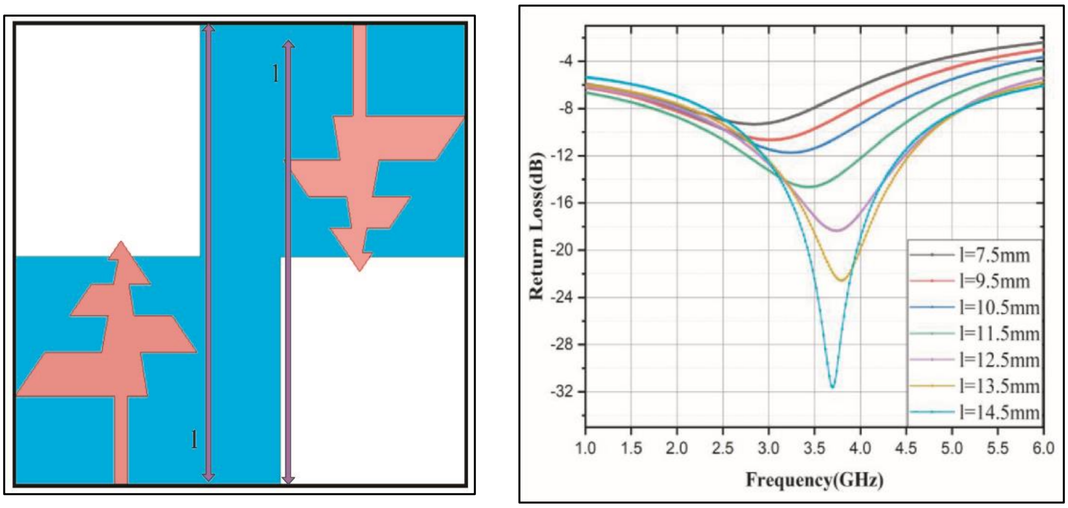

Figure 5.24: Parametric analysis results on the length of the rectangular slot added in the ground plane. Length variations of the slot between 7.5mm to 14.5mm.

A bigger L-shaped slit is added to the DGS of Ant III to design the ground plane for Ant IV. The width of the second slit is optimized to 0.5mm after parametric study as shown in Figure 5.27. the slit of $L_{10}\times W_{16}$ dimension and 0.5mm width shifted the bandwidth further to the left to include the most popular frequency bands for IoT applications and improved the isolation between the antenna elements to 30 dB.

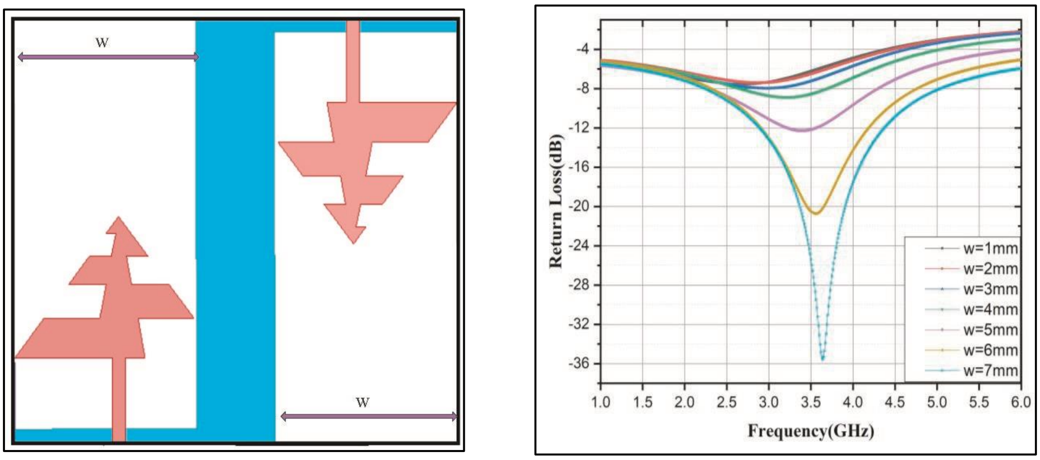

Figure 5.25: Parametric study results of the study done on the width of the rectangular slot embedded in the ground plane. Width variations of the slot varied between 1mm to 7mm.

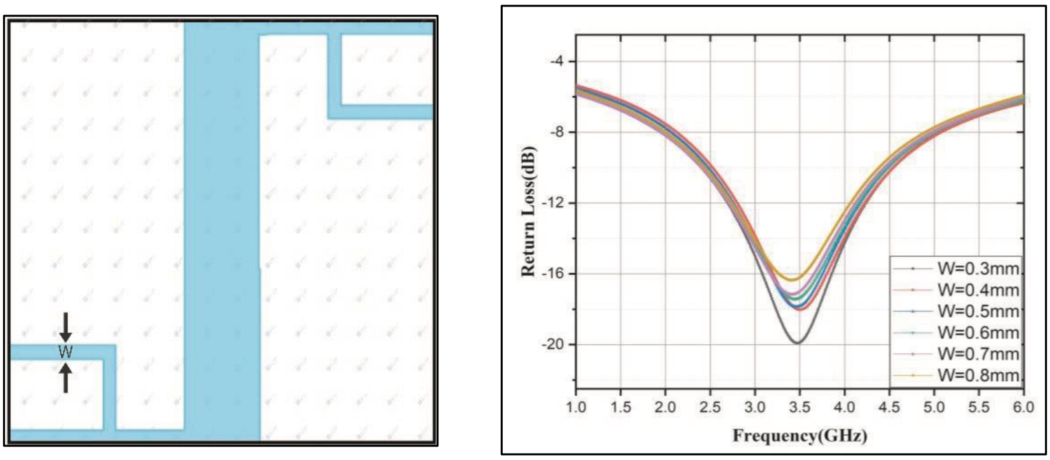

Figure 5.26: Parametric study outcome on different widths varying from 0.3mm to 0.8mm showing maximum return loss when *w* = 0.3mm.

5.4.4. Results and Discussions

A two port MIMO antenna is designed, simulated, and experimentally analysed after fabrication. The simulated results of antenna parameters and the experimentally measured results are found to be in good agreement with each other. The popular PCB substrate, FR4 of thickness 1.6mm is used to fabricate the antenna owing to its advantageous properties of brittleness, minimizing interference and maintaining signal integrity apart from being cheap and easily available. The picture of the both planes of the fabricated antenna is shown in Figure 5.28.

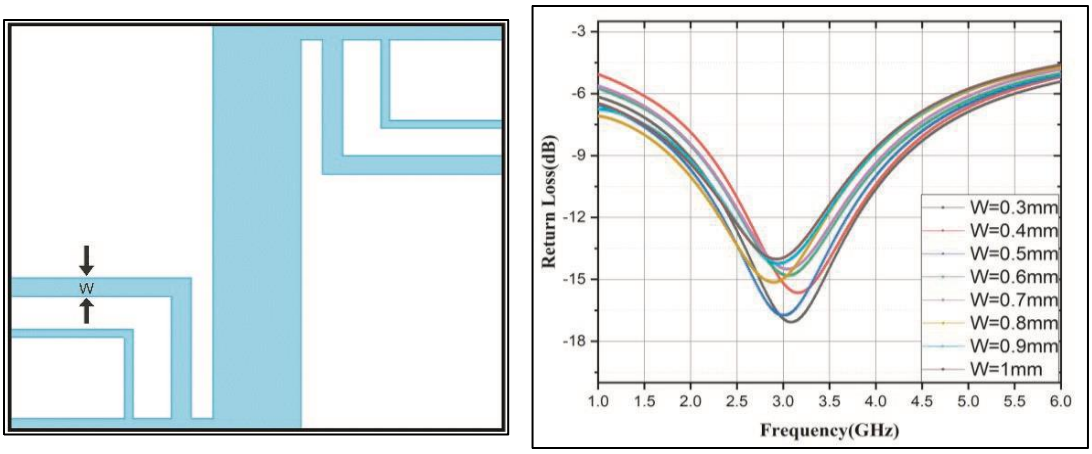

Figure 5.27: Parametric study outcome on numerous widths changeable from 0.3mm to 1mm showing maximum return loss when *w* = 0.5mm.

Figure 5.28: The image of the radiating patch and ground plane for the fabricated Ant IV (final proposed design) antenna compared with the size of a standard 1Re coin.

Figure 5.29 sows the experimental setup for the measurement of S parameters and radiation characteristics. An anechoic chamber, network analyser and spectrum analyser are used for the same. The ports relate to SMA connector which are used as co-axial RF cables in order to link the ports of the antenna to the analyser.

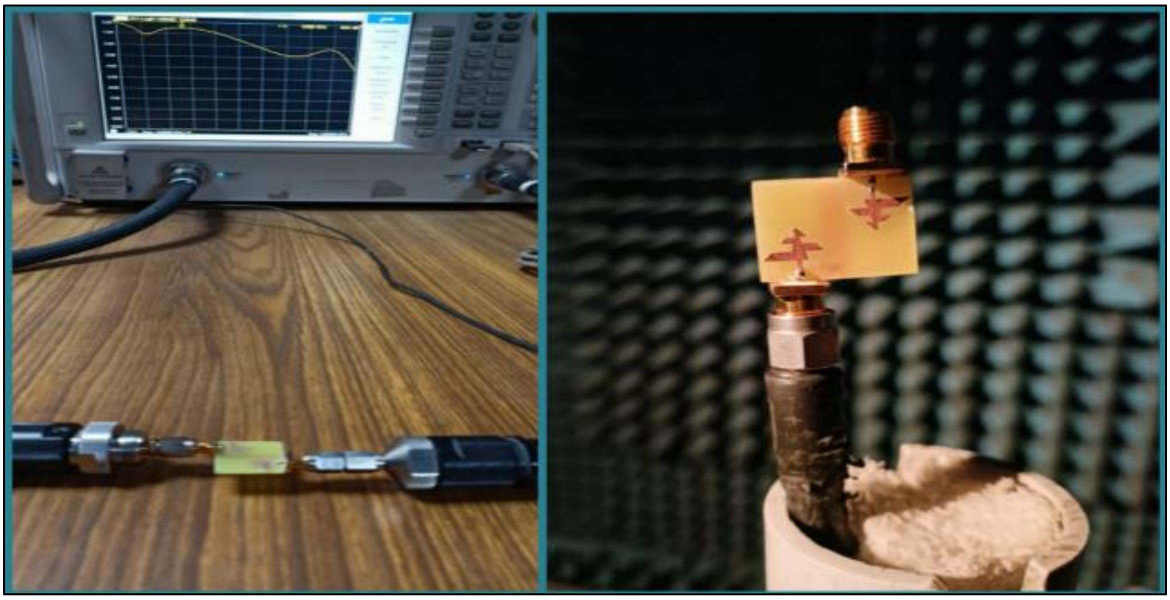

Figure 5.29: The testing set up for the designed antenna to study the antenna parameters and radiation characteristics.

S-Parameters

The summary of all simulated and measured S-Parameters for the design is given in Figure 5.30.

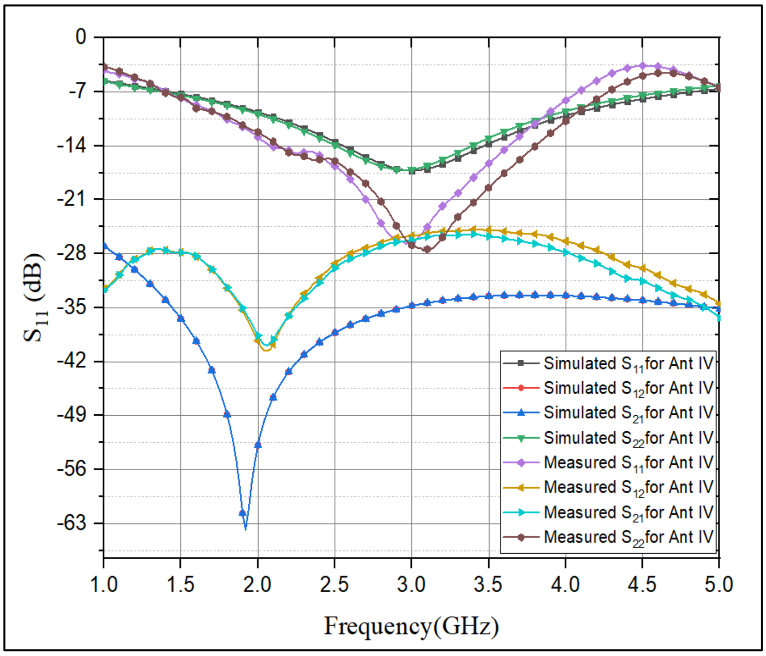

Figure 5.30: The simulated and measured S-parameters for all the stages of design.

Gain

Gain measures the power communicated and accepted in a particular direction. The power that an antenna radiates in a specific direction is compared to the topmost radiation of an isotropic source. The addition of DGS to the current distribution creates an opportunity to increase gain. Figure 5.31 depicts the measured and simulated gain in relation to frequency variations. Gain varies from 0.96 dBi to 2.9 dBi across the operating frequency range. At 2.56 GHz, the maximum gain is 2.9 dBi

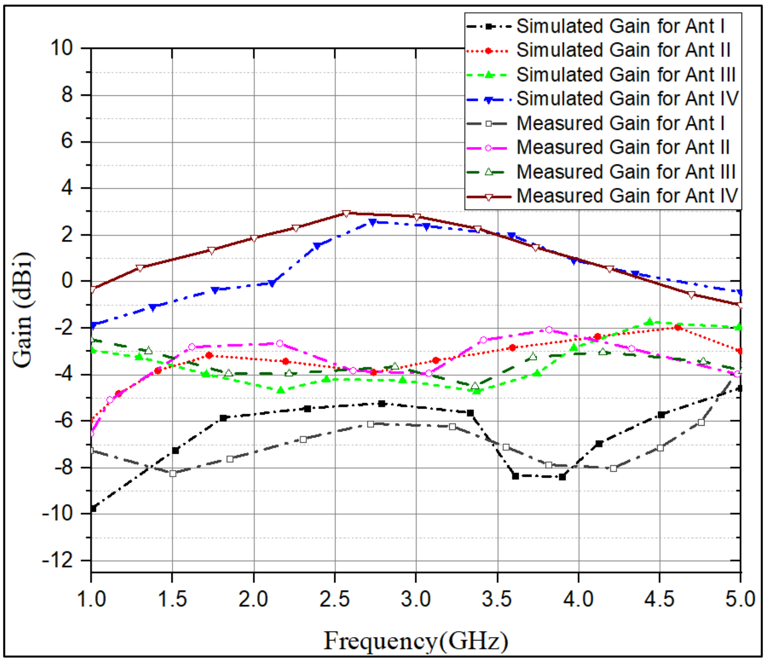

Figure 5.31: Simulated and measured gain variations for stages with respect to frequency variations.

Radiation Efficiency

Another parameter to measure the effective power radiated from the system is radiation efficiency. The radiation efficiency of the proposed MIMO system is 92.8% for entire operational frequency range of 2 to 4 GHz as shown in Figure 5.32. The simulated and measured radiation efficiency is plotted together and they are in good agreement.

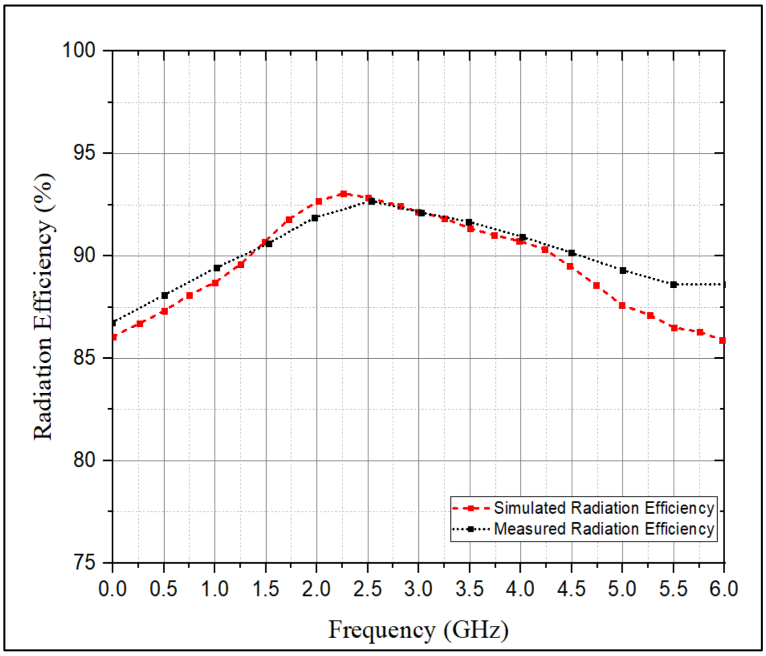

Figure 5.32: Radiation efficiency, measured and simulated, for the proposed antenna.

Radiation Pattern and Co and Cross Polar Plot

Figure 5.33 (a) and 5.33 (b) shows the E-plane and H-plane radiation pattern of the proposed MIMO antenna. The antenna's radiation properties are represented graphically in radiation pattern. It is expressed as a function of space. In short, it gives us an idea about how the antenna radiates electromagnetic energy into the space.

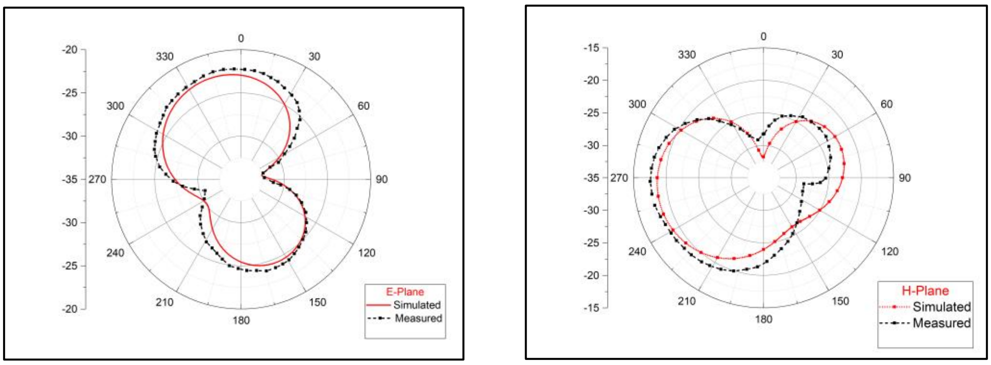

(a) (b)

Figure 5.33: Measured and Simulated Radiation patters for the proposed antenna (Ant IV). (a) *E*-Plane at 3 GHz. (b) *H*-Plane at 3 GHz.

The polarization of the antenna refers to the polarization of the radiated fields when evaluated from far field radiations. In antennas, it is necessary that the polarization of the transmitting and receiving antennas be the same for communication to happen. Co-polarization plot explains the radiation pattern while the transmitting and receiving antennas have some polarization.

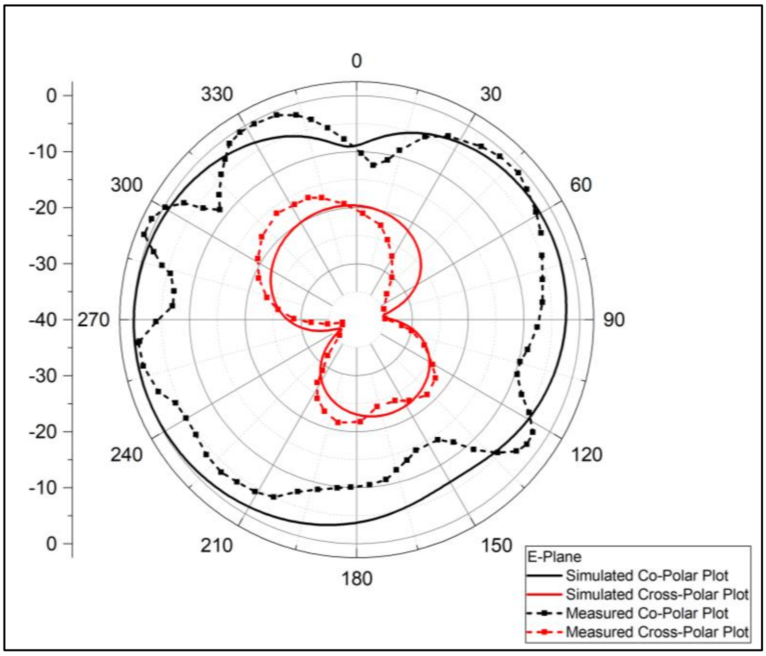

Figure 5.34: Co and Cross polarization for E-plane

Cross polarization refers to the orthogonal radiations. It is desired to reduce cross-polarization. Figure 5.34 and Figure 5.35 shows the Co and Cross polarization for E and H plane respectively.

MIMO Antenna System Performance: Isolation

Mutual coupling refers to the absorption of energy by the adjacent antenna while another antenna in the MIMO system is radiating. This coupling between the elements can influence various parameters including the input impedance and the reflection and radiation characteristics. In this design, the DGS embedded in the ground plane has assisted in achieving the desired bandwidth with reduced mutual coupling. Figure 5.36 shows the simulated and measured values for mutual coupling for all the evolution stages of the proposed design.

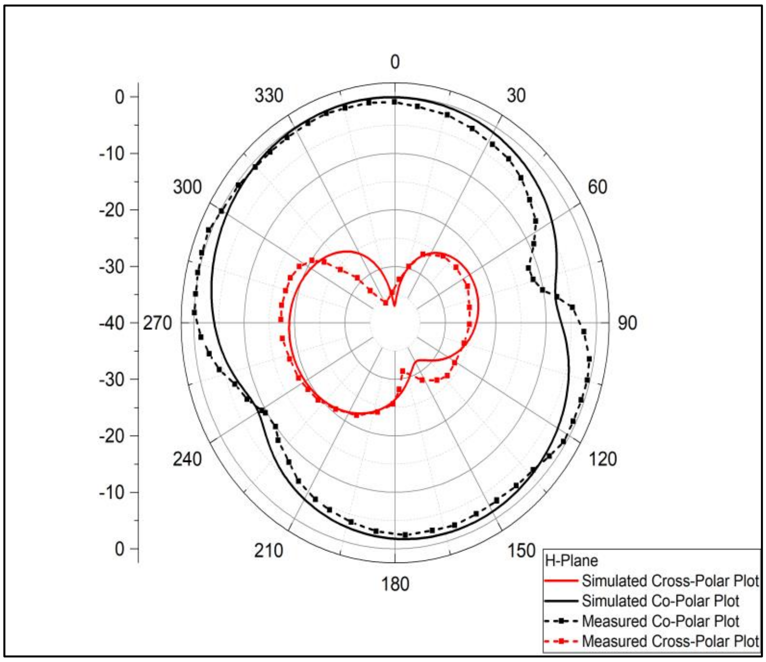

Figure 5.35: Co and Cross polarization for H-plane

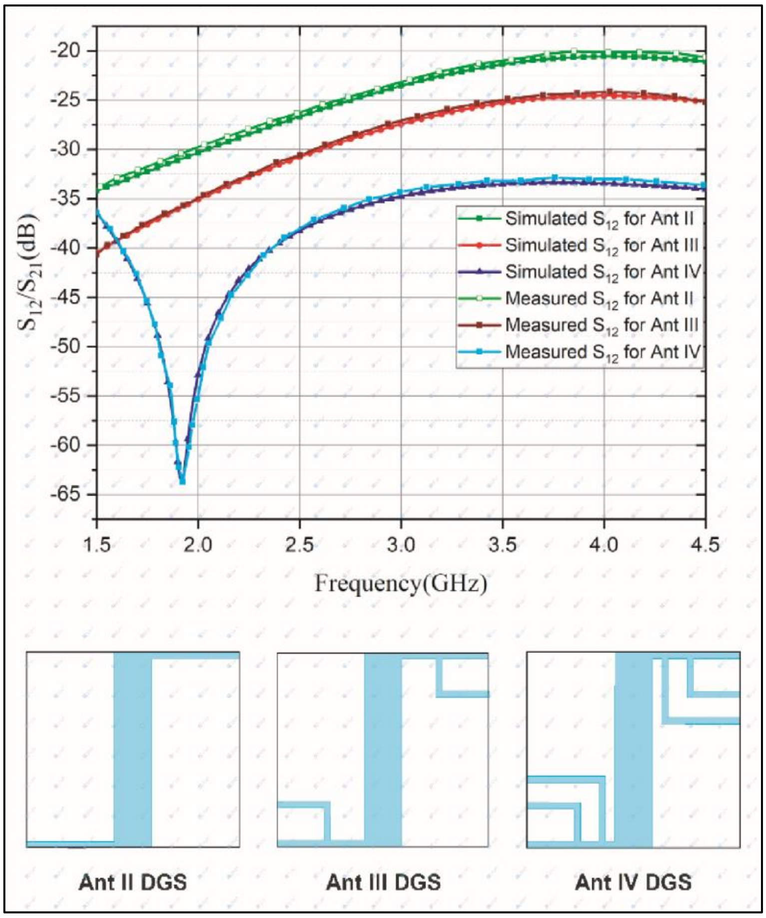

Figure 5.36: Simulated and measured mutual coupling for Ant II, Ant III, and Ant IV.

MIMO Antenna System Performance: ECC

ECC stands for Envelope Correlation Co-efficient and it measures the level of correlation between the MIMO elements. Ideally, expected value of ECC is zero whereas practically, ECC for a MIMO antenna system should be below 0.5 for the system to have acceptable performance. ECC can be calculated from the S-parameters using the following equation (5.3).

$$\mathrm{ECC} = \frac{|S_{11}{}^{*}\, S_{12} + S_{21}{}^{*}\, S_{22}|^2}{(1-|S_{11}|^2-|S_{21}|^2)(1-|S_{22}|^2-|S_{12}|^2)} \tag{5.3}$$

ECC for the designed antenna is shown in Figure 5.37. From the graph, it is observed that ECC for the proposed design is below 0.001.

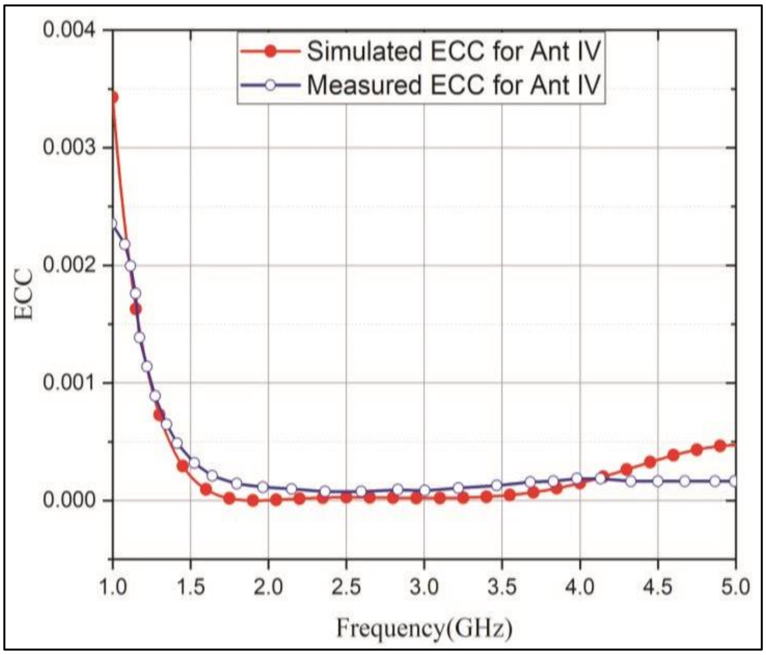

Figure 5.37: Simulated and measured ECC for the proposed MIMO design

MIMO Antenna System Performance: DG

Diversity Gain is a parameter calculated from ECC. The MIMO systems can exploit the phenomenon of multipath propagation and improve the signal quality using a smart receiver. The value of DG is ideally expected to be 10 and practically the desired value is above 9.95. DG can be calculated using equation (5.4) and DG for this design is above 9.99.

$$DG = 10\sqrt{1 - ECC} \tag{5.4}$$

MIMO Antenna System Performance: TARC

TARC of the Total Active Reflection Co-efficient is the measure of the reflected power and the overall power incident on the system. For a 2 element MIMO antenna, TARC can be calculated by the equation (5.5). Figure 5.38 shows the measured and simulated values of DG and TARC for Ant IV.

$$TARC = \sqrt{\frac{(S_{11} + S_{12})^2 \ + (S_{21} + S_{22})^2}{2}} \tag{5.5}$$

Table 5.6 shows the already available similar MIMO antennas in the literature.

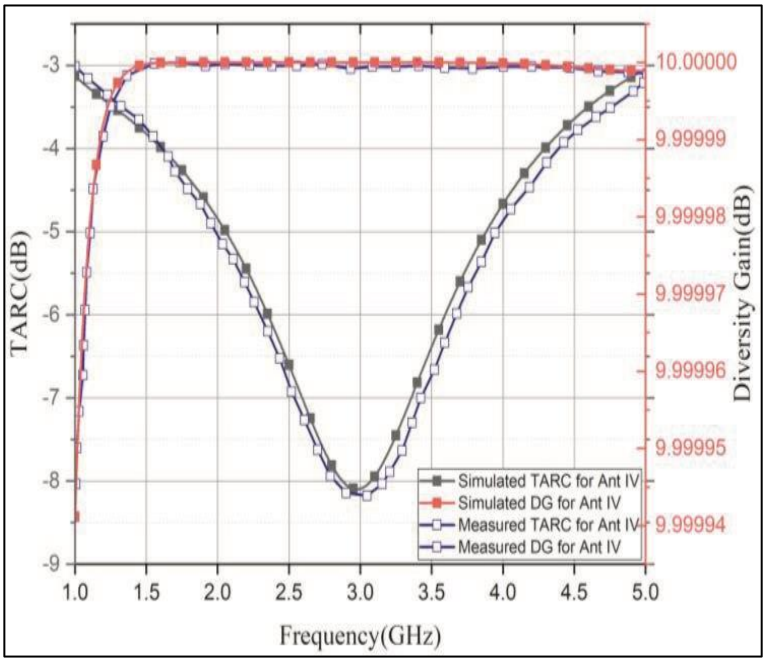

Figure 5.38: Simulated and Measured DG and TARC for the proposed MIMO design.

Table 5.6: Comparative study of the proposed antenna with other similar antennas in literature.

Ref.	Size (mm)	Operating Bandwidth /Frequency	Number of Ports	Gain/ Peak Gain	Efficiency	Isolation Technique and Isolation	ECC
[55]	50 × 61.5	2.35–2.5	3	NA	51–82%	Use of decoupling network < −20	< 0.04
[56]	32 × 28	(2.26–2.58) Hz and (2.58–6.88) GHz	2	5.2dB	Not Mentioned	Double Split Ring Resonator < −24dB	< 0.05
[57]	55 × 65	2.4–2.5	2	4.5dBi at 2.45GHz and 5.3dBi at 5.25GHz	60–65%	Use of decoupling network < −15	< 0.15
[58]	65 ×120 ×1.56	(754–971) MHz, (1.65–1.83) GHz, (2–3.66) GHz, (3.9–4.1) GHz	5	4.9dBi	Not Given	Not Given	< 0.5

		(4.8–5.5) GHz and (5.82–5.93) GHz					
[59]	54.98 ×76 ×1.6	(2.1–4.0) GHz	4	2.83dBi	> 82%	Use of Parasitic element and design of ground plane. < −12dB	< 0.026
[60]	140 × 120	2.25–2.7	4	5.33–6.97dBi	> 57%	Use of Parasitic element < −14dB	< 0.2
[61]	120 × 110	(1.97–3.317) GHz	2	5.4dB	92%	Use of double slit complementary split ring resonator. < −15dB	< 0.5
[62]	25 × 25	(0.66–1.06) GHz and (1.68–2.88) GHz	2	−0.2–3.5dBi	(38–85) %	Using defected ground and grounded branching. < −13.5	< 0.15
[63]	34 × 34	(0.7–3.8) GHz and (3.3–7) GHz	2	Not Mentioned	< 75%	Polarization Diversity. < −20dB	Not Mentioned

[66]	92 ×121.2 ×2	3.5GHz 12.5GHz and 17GHz	4	> 6.34dB	> 81%	Complementary Modified Split Ring Resonator (CMSRR) in the ground. < −18dB	< 0.08
[67]	33 ×57.25 ×1.6	1.89GHz and 2.45GHz	2	> 0.758dB	> 72.12%	Orientation of the elements < −14.2dB	< 0.0471
[68]	27 × 21	(5.19–5.41) GHz and ((7.30–7.66) GHz	2	> 9.38dB	79.8%	Orthogonal Polarization < −22.5dB	< 0.4
[75]	60 × 55	(2.3–23) GHz	4	4.5dBi	(60–90) %	A stub added in the ground plane and the orthogonal placement of the component elements.	< 0.002

						< -20dB	
Proposed Antenna	**15 ×17 ×1.6**	**(2.06GHz –4.04GHz)**	**2**	**2.9dB**	**92.8%**	< -30**dB**	< 0.0002

5.5 CONCLUSION

Two antenna designs are discussed in this chapter.

A planar, log-periodic structured, microstrip patch antenna is designed for IoT applications operating at 2.4 GHz. This antenna can be used in various IoT enabling devices such as ESP8266 module. The size and the performance characteristics are the focal benefit of the proposed structure as most of the IoT applications requires compact, well performing communication module with good gain. This antenna of size $20mm \times 20mm$, built in FR4 substrate of thickness $1.6mm$ and co-planar feed attains a gain of 9.34 dBi and is well suited for mobile device nodes used in IoT applications [87].

A compact, two port MIMO antenna is discussed for IoT applications. The proposed antenna evolved through various stages and the final antenna has an impedance bandwidth between 2.06 GHz to 4.04 GHz with a radiating efficiency of 92.8%. The radiating elements achieves an isolation of above 30 dB and all other MIMO parameters are also in the acceptable range. Compact IoT nodes employed in medium range coverage IoT applications can employ this antenna system to communicate under various WiMAX and WLAN frequencies [88].

CHAPTER 6

WIDEBAND LORA ANTENNA FOR IOT APPLICATIONS

6.1 INTRODUCTION

With the advent of the Internet of Things, the fourth wave of digital revolution is facilitating devices which are connected to internet to sense the world for themselves. IoT provided a brand-new dimension by connecting any device connected to internet (not limiting it to mobile phones and computers) and empowering the devices to exchange information. More than 125 billion such sensor nodes are expected to be connected to form the "things" network in the next few years [89]. So far, IoT devices/sensor nodes are seen to be connected using various existing communication protocols and the selection of the protocol is highly application oriented. Some of the popular communication protocols employed for IoT applications includes NFC (Near Field Communication), Bluetooth, Wi-Fi, LoRaWAN (Long Range Wide Area Network), ZigBee, NB-IoT (Narrow Band IoT) etc. The 10 most popular protocols with their characteristics as expected range of operation, data rate that can be supported and the operational frequency/frequencies. Are summarised in Figure 6.1 [90-98]

LPWAN (Low Power Wide Area Networks) is the name coined for a set of low power and wide area network technologies operating in licensed and unlicensed spectrum. They are widely considered for IoT applications due to their characteristic features like low power consumption, low cost of installation and larger area of coverage when compared to the traditional communication standards [99-100]. NB-IoT, LoRa, ZigBee, Sigfox, LTE-M etc are favoured LPWAN protocols for IoT systems. The common characteristics of LPWAN technologies includes

i. Larger area of coverage
ii. Low bandwidth requirements
iii. Transmits small data packets and
iv. Longer battery life.

Figure 6.1: The popular communication protocols and their characteristics employed in IoT applications.

So, to summarise, LPWAN technologies provides low cost, power efficient systems with wider area of connectivity at the cost of lower data rates. These features are particularly advantageous for IoT systems designed for monitoring purposes such as agriculture monitoring [101], smart cities and buildings [102], medical monitoring systems [103], smart grids and smart power supplies [104] etc. So, LPWAN technologies are handy in applications which requires low bandwidths and larger coverage areas and they are cheaper and draws minimal power. LPWANs are specially designed for millions of low power devices whispering continuously unlike the traditional networks like Ethernet, Wi-Fi, Bluetooth, Cellular and Satellite networks.

In LPWAN technologies, LoRa (Long Range) and Sigfox are two most used communication protocols. They both employ the unlicensed sub-GHz spectrum. The characteristics of LoRa and Sigfox are as summarised in Table 6.1.

The frequency of operation plays an important role in the communication systems. Longer wavelengths generally tend to provide better range of coverage and penetration. For sub-GHz frequencies like 433 MHz, 868 MHz and 915 MHz employed for LoRa technology, they have proven to give a line-of-sight coverage range of about 20 KMs. So, IoT monitoring systems which are to cover wider area and those which requires to transmit only small amounts of data, LPWAN protocols are a good choice.

Table 6.1: Comparative analysis of Sigfox and LoRa LPWAN Technologies

LPWAN Technology	sigfox	LoRa
General Nature	Like cellular networks. Register and get connected to an already existing network with permanently installed receivers, Pay, and use the network.	It is a commercial LPWAN solution for sending and receiving data.
Communication	Mostly meant for up linking data. Downlink capability is limited	Bidirectional data transmission
Data Rates	600/100 bps	50kbps
Maximum messages that can be sent in a day	140 (uplink) and 4 (downlink)	Unlimited
Coverage Area	10 KM (Urban) 40 KM (Rural)	5 KM (Urban) 20 KM (Rural)
Allows private network	No	Yes

Frequency of Operation	Sub-GHz ISM Band	Sub-GHz ISM Band
Packet Size	12 Bytes	User Defined
Cost	Very Low	Low
System Bandwidth	100 KHz	125 KHz
Standardization	Sigfox company and ETSI is standardizing Sigfox based networks	LoRa Alliance

Designing patch antennas for LoRa technology has always been challenging for antenna design engineers as LoRa modules will require small antennas operating at sub-GHz range and as frequency of operation decreases, antenna size tends to increase. The LoRa antenna found in the literature, with their size and characteristics are summarized in Table 6.2.

Table 6.2: A Literature Review of LoRa Antennas

Ref No	Size (mm^2)	Bandwidth/Resonant Frequency	Gain
[95]	100x40	(840-910) MHz and (2.26-2.65) GHz	1.92 dBi and 4.2 dBi
[105]	34x80	(857-880) MHz	1.55 dB
[106]	82.295x105.41	433MHz	2.194 dB
[107]	280x255	433 MHz and 915 MHz	5 dB
Proposed	**34x22**	**(151.9 MHz-1.08 GHz)**	**2.56 dBi**

A miniaturised planar printed antenna is designed here to work for sub-GHz LoRa frequency. The bandwidth of this antenna covers 433 MHz, 868 MHz and 915 MHz and resonates at 433 MHz the designed antenna can be a good contender for IoT surveillance systems.

6.2 ANTENNA DESIGN EVOLUTION AND DIMENSIONS

A double leaf structure is the radiating patch. The cheap and easily available FR4 material of 1.6mm thickness is used as the substrate material. The size of the substrate is *34mm×22mm* and the double leaf structured patch is energized by a 1mm thick microstrip line feed. This structure, with double leaf structured radiating patch fed by a 1mm microstrip line forms Ant 1 as shown in Figure 6.2. No significant bandwidth was obtained for Ant 1.

The ground of Ant 1 was further modified by adding a slot to the ground of Ant 1. This structure is named as Ant 2 and is shown in Figure 6.3. The 1mm thick slot etched to the ground at 3mm from the feeding point improved the performance of the antenna system. The return loss for Ant 1 and Ant 2 is shown in Figure 6.4. The addition of a 1mm slot on the ground plane has improved the return loss over the frequency range of 0.142 GHz to 1.51 GHz.

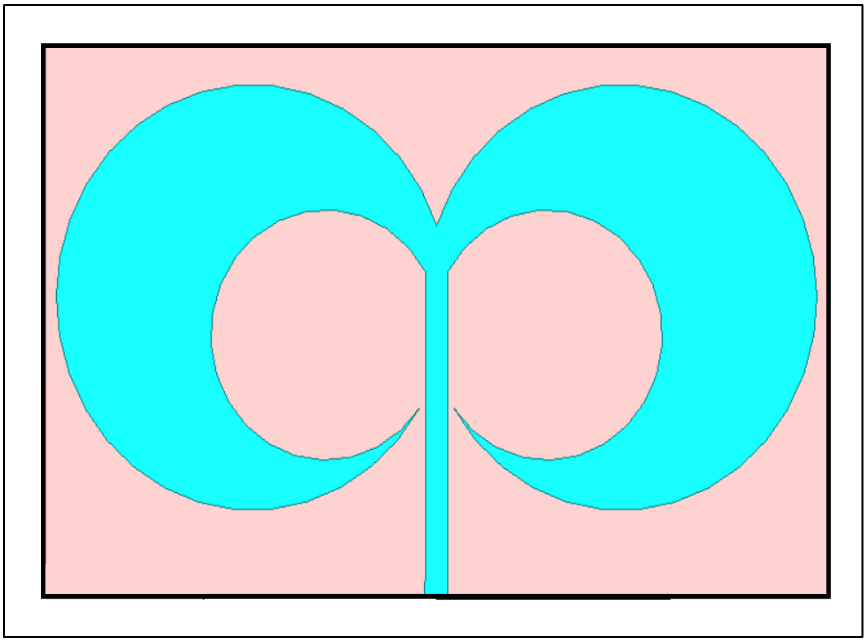

Figure 6.2: The radiating patch of Ant 1.

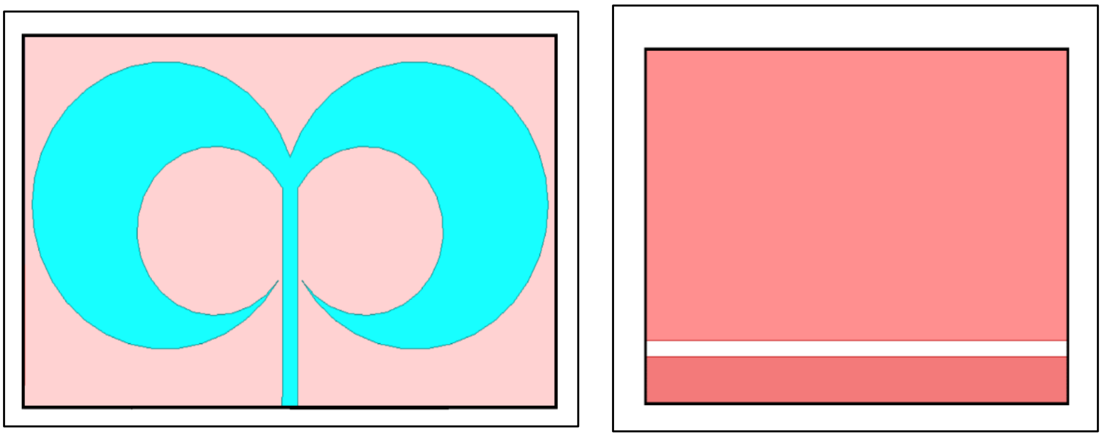

Figure 6.3: The radiating patch and ground plane with 1mm slot of Ant 2.

The ground plane was again altered by adding another 1mm slot at 8mm from the top of the substrate. The radiating structure, along with two 1mm slots on the ground plane is named as Ant 3. The addition of the second slot, further shifted the resonant frequency to the left, now resonating at 433 MHz the evolutionary stages of the final proposed structure are shown in Figure 6.5. Figure 6.6 and Table 6.3 gives a clear picture of the structure and dimensions of the final proposed antenna, Ant 3.

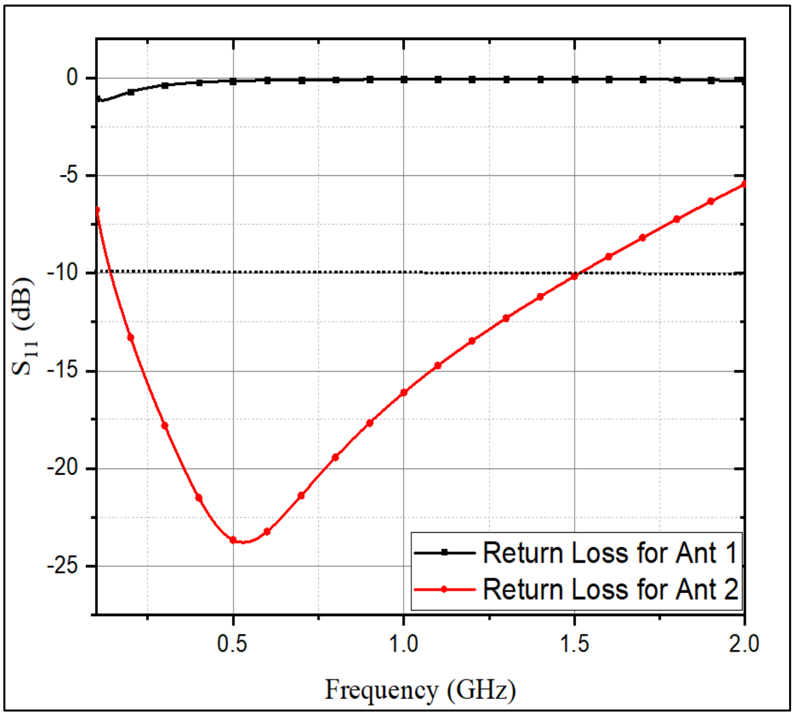

Figure 6.4: Simulated return loss for Ant 1 and Ant 2.

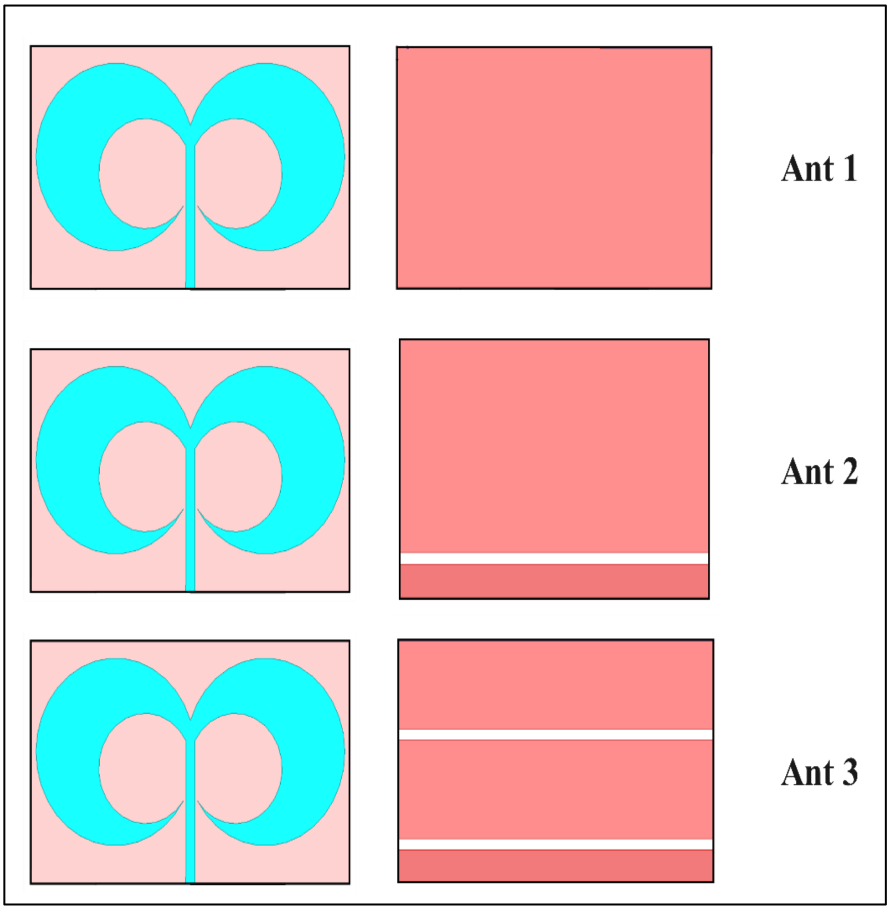

Figure 6.5: Evolutionary stages of the proposed antenna.

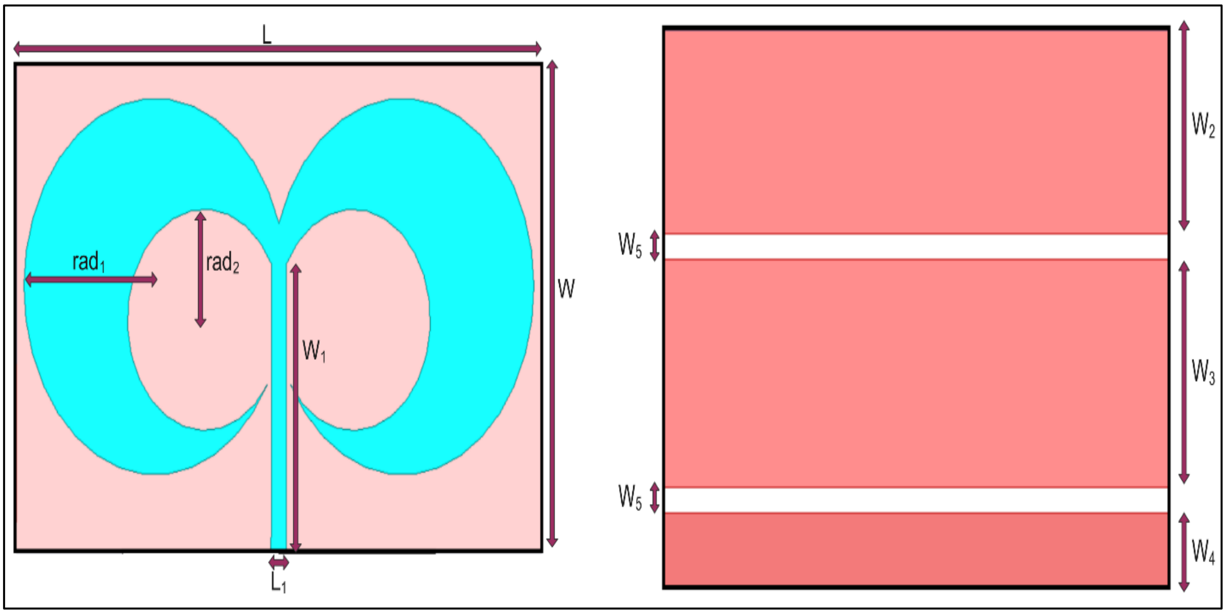

Figure 6.6: Ant 3 radiating structure and DGS with dimensions

Table 6.3: The proposed antenna dimensions

L	34mm	rad_2	5mm
W	22mm	W_2	8mm
L_1	1mm	W_3	9mm
W_1	13mm	W_4	3mm
rad_1	8mm	W_5	1mm

6.3 PARAMETRIC STUDY

The slots implanted on the ground plane caused the 433 MHz resonance and inclusion of 433 MHz, 868 MHz, and 915 MHz; which are the sub-GHz LoRa operational frequencies. Two slots of 1mm each were embedded as defects in the ground plane which altered the current distribution and there by the return loss. The position of the slots and the width of these slots were established by parametric study. The ground plane with the DGS elements under parametric study is given in Figure 6.7. The final evolved antenna, Ant 3, with optimized two slots in the ground plane, resonates at 433 MHz and includes all the three sub-GHz LoRa operational frequencies.

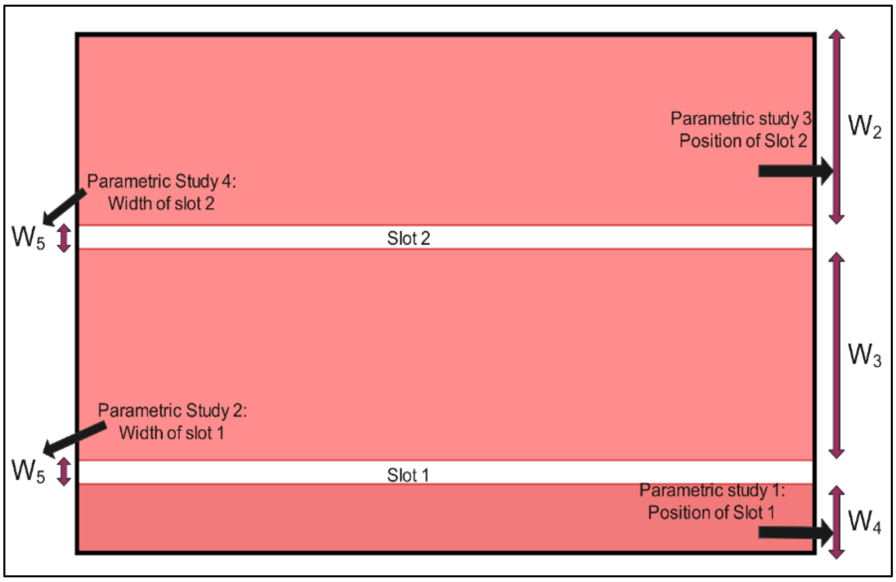

Figure 6.7: Elements under parametric study

6.3.1 Parametric Study on Position of Slot 1

The position of the first slot was optimized by parametric study and it was observed that, at a height of 3mm from the feedline level, the best return loss is attained. Figure 6.8 shows the effect of variations in the slot position from the feedline level.

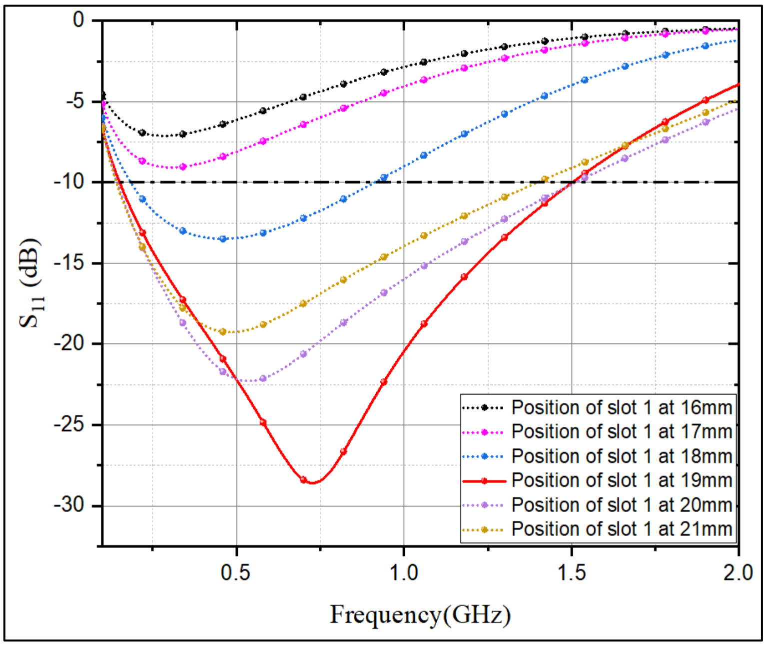

Figure 6.8: Parametric study on the position of slot 1

6.3.2 Parametric Study on Width of Slot 1

The width of slot 1 was also analysed parametrically for optimization. The width was studied for a variation of 1mm to 8mm and was detected that as the width is incremented, the return loss decreases and the bandwidth tends to shift slightly towards the right of the spectrum. The parametric study on width of slot 1 is shown in Figure 6.9.

6.3.3 Parametric Study on Position of Slot 2

A second slot was added to the existing DGS to further optimize the resonant frequency to 433 MHz. The position of this slot 2 was fixed after parametric study. The slot positioned at a height of 8mm from the top plane, the return loss obtained was the best as per this analysis. The outcomes of the parametric analysis in the position of slot 2 is shown in Figure 6.10.

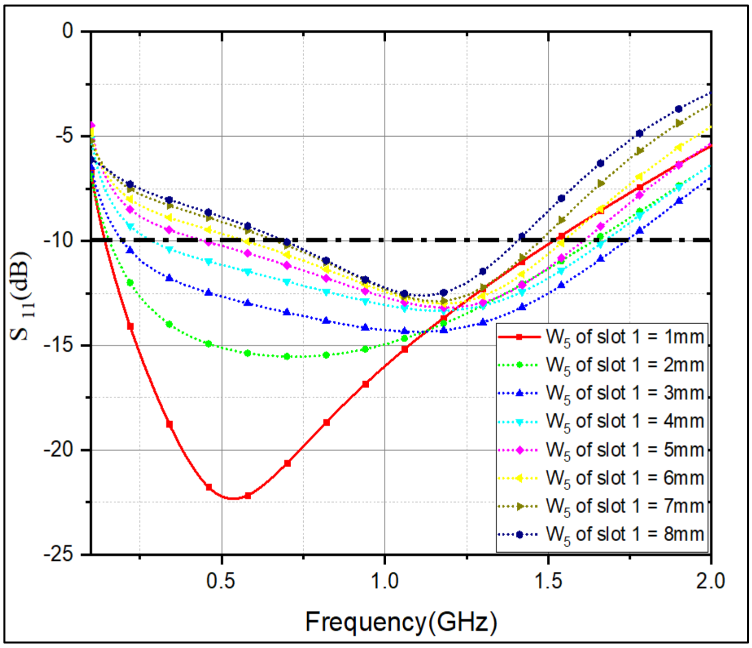

Figure 6.9: Results of parametric study done on width of slot 1

6.3.4 Parametric Study on width of Slot 2

As done for slot 1, width of slot 2 was also investigated for optimization. The difference of the slot width showed a reduction in return loss. For a width of 1mm, a return loss of around 25 dB was attained as shown in Figure 6.11.

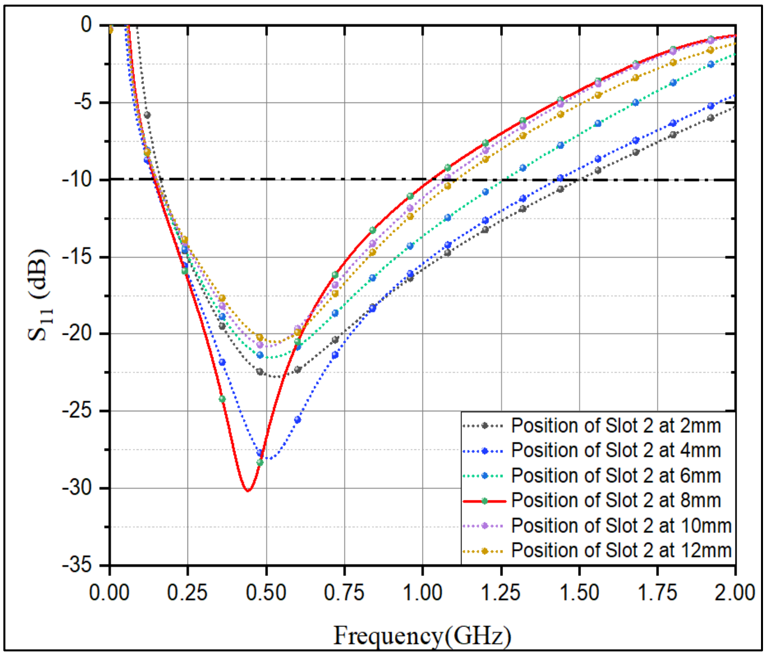

Figure 6.10: Optimizing the position of slot 2 by parametric analysis.

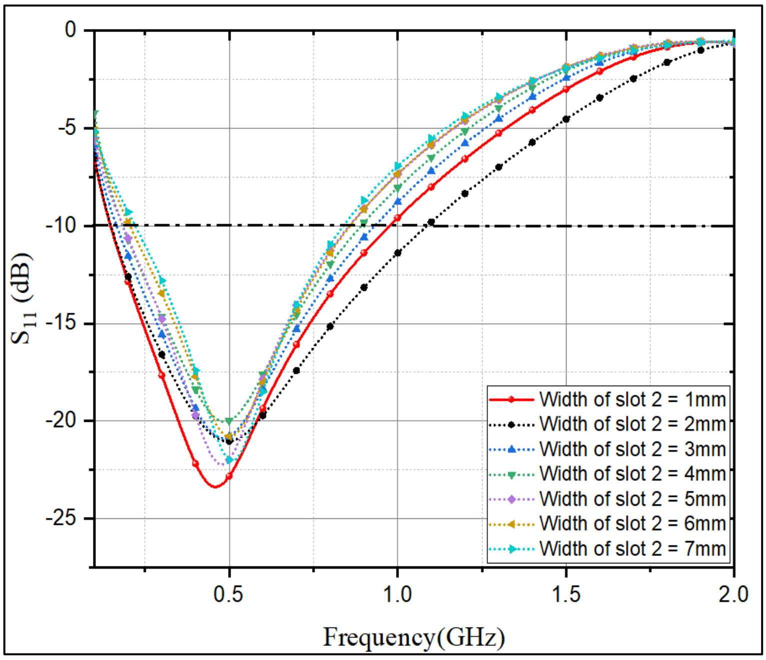

Figure 6.11: Results of parametric study done on the second slot width.

6.4 RESULTS AND DISCUSSIONS

FR4 substrate of size $22\times34mm^2$ is used to host the double leafed structured radiating patch and is simulated in ANSYS HFSS software. The double leafed structured radiating patch alone gave no significate bandwidth. Addition of defects to the ground plane, in the form of two slots, helped in attaining the desired bandwidth. The antenna structure with a solo slot on the ground plane, called Ant 2, gave a bandwidth of 1.37 GHz within the range of 142 MHz to 1.513 GHz. the maximum VSWR of this Ant 2 was 1.92. Addition of the second slot to the existing DGS, modified the bandwidth to 930MHz, tuning the resonating frequency to 433 MHz The VSWR for Ant 3 at 433 MHz is found to be 1.17. Figure 6.12 shows the virtual return loss of Ant 1, Ant 2, and Ant 3.

The finalized antenna, Ant 3, was fabricated and experimentally analysed for its performance. The radiating structure and DGS of fabricated antenna is shown in Figure 6.13.

Figure 6.14 depicts both simulated and measured return loss for Ant 3. Another performance indicator that quantifies the amount of power that has been successfully coupled is the VSWR. Figure 6.15 depicts the simulated VSWR for Ants 2 and 3 as well as the measured VSWR for Ant 3.

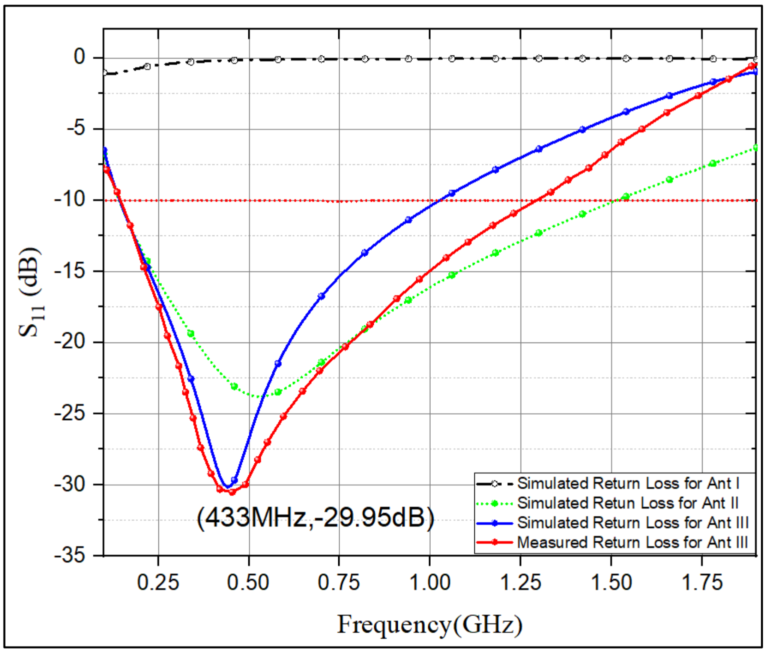

Figure 6.12: Return Loss for Ant 1, Ant 2 and Ant 3

The gain of the antenna is found to be around 2.56 dBi. The gain measures the quantity of power successfully radiating in a specific direction. The measured results and simulated value of gain, which are in respectable agreement, is shown in Figure 6.16.

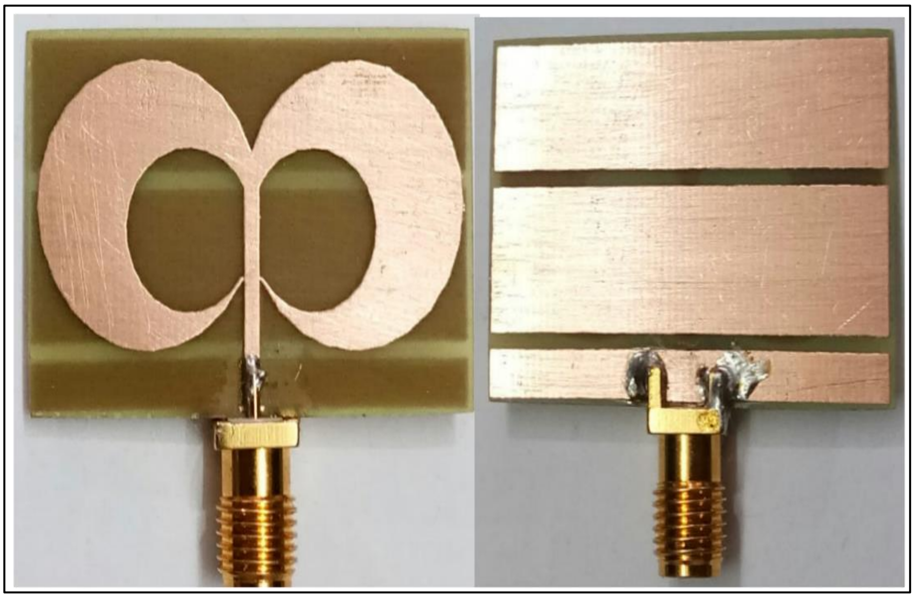

Figure 6.13: Radiating patch and ground plane of fabricated antenna

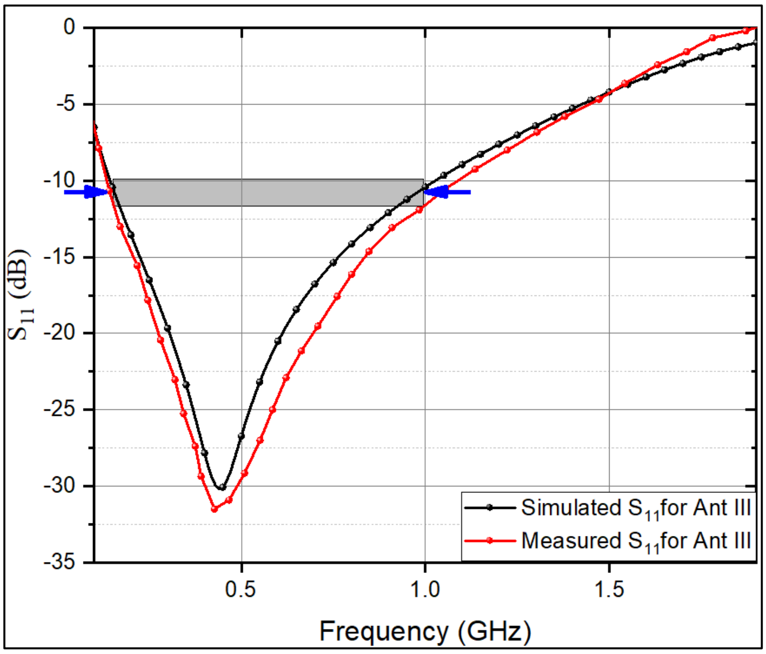

Figure 6.14: Simulated and measured S_{11} for Ant 3

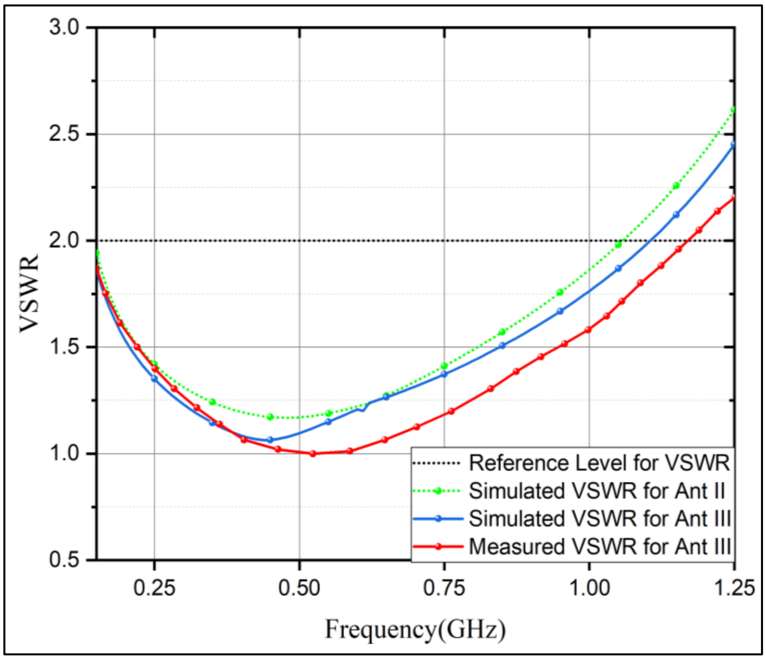

Figure 6.15: Simulated VSWR for Ant 2 and Ant 3 and Measured VSWR for Ant 3

Similarly, the radiation pattern for E-plane and H-Plane at 433 MHz is shown in Figure 6.17 and 6.18 respectively. The radiation efficiency of Ant 3 is observed to be 97% as shown in Figure 6.18.

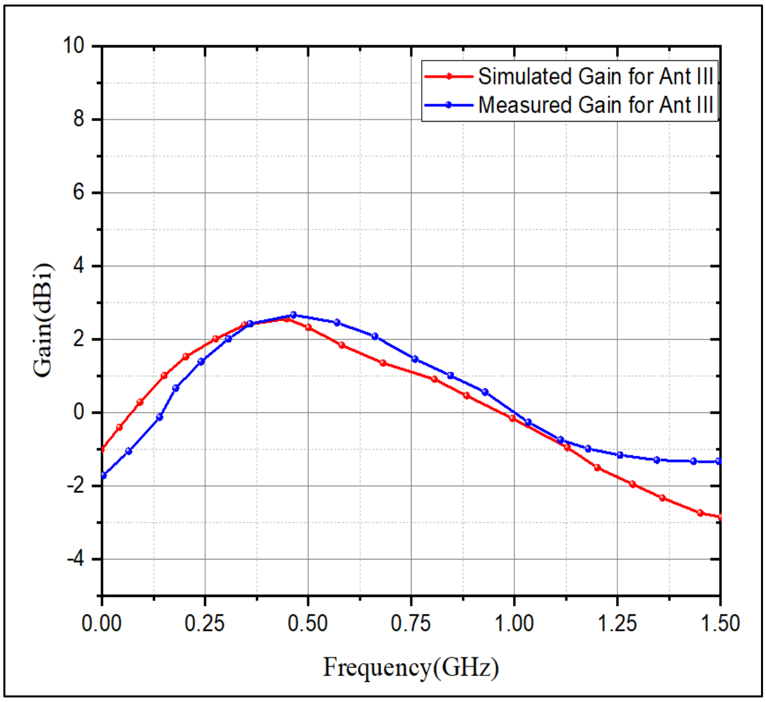

Figure 6.16: Simulated and Measured Gain for Ant 3

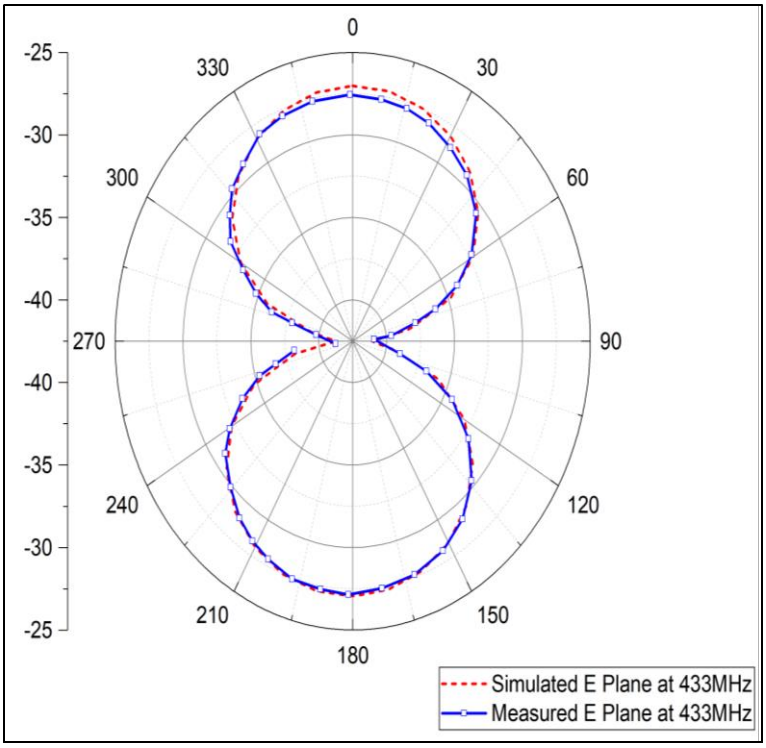

Figure 6.17: E-Plane radiation pattern

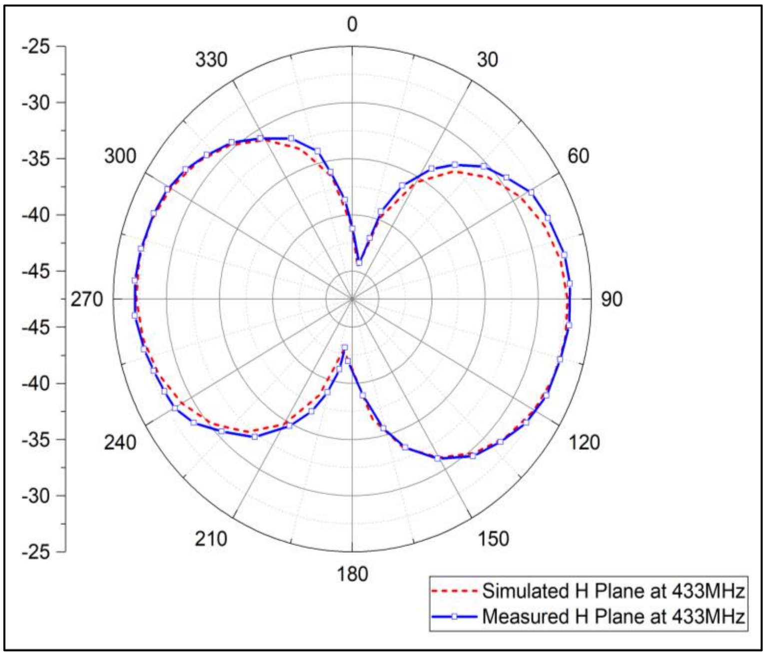

Figure 6.18: H-Plane radiation pattern

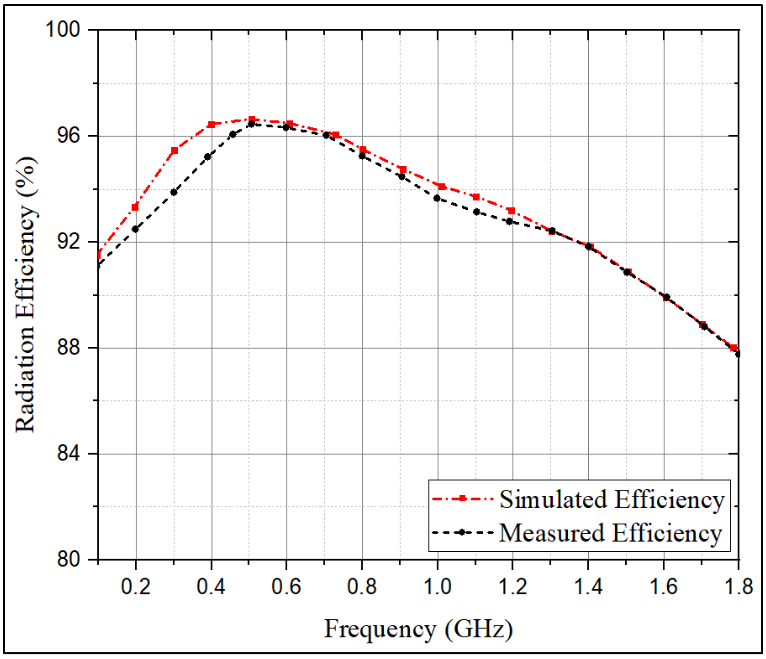

Figure 6.19: Simulated and Measured radiation efficiency.

6.5 CONCLUSION

A compact antenna of size $22\times34mm^2$ is structured and analysed on cheap FR4 substrate. The structure resonated at 433 MHz giving a frequency band of operation of

930 MHz and radiated with an efficiency of 97%. The surveillance applications of IoT under medium range communication can utilize the advantages and properties of the antenna [106].

CHAPTER 7

COMPACT TRI-BAND MIMO FOR IoT APPLICATIONS

7.1 INTRODUCTION

Compared to the traditional communication solutions, MIMO systems are the future of present-day communication technology despite its additional cost and complexity. The three significant features of MIMO, which makes it unique and popular are it beam steering capability, the enhanced data capacity and the diversity characteristics. The major challenge faced in the modern-day MIMO design are in integrating multiple radiating elements in limited space with good isolation and attaining a low correlation between the closely placed antenna elements. Compact, low profile, efficient MIMO antennas are highly preferred for modern wireless and IoT applications.

Modern wireless systems also support multiple applications simultaneously. A compact, low-profile antenna, which can perform over multiple frequency bands, without any change in its structure or dimensions, is highly desired for the present day IoT applications. As IoT systems work over different communication standards, antennas with multiple operating bands can help in reducing the size and hardware complexity to a great extent. A multi-band antenna can act as a single solution to multiple applications working at different frequency bands. To perform over multiple range of frequencies, they will require to be highly efficient with minimum losses.

Various methods are seen in the literature for the design of multi-band antennas. A multiband MIMO can be a complete solution to the data rate and speed requirements, miniaturization and versatility required for the present-day wireless applications including IoT, Mobile communication systems and 5G. Special modifications in the design or use of a combination of regular patches and careful optimization of design dimensions are required to attain multiple operational bandwidths in a MIMO antenna system. The various techniques employed to achieve multiple bands includes

- Addition of parasitic elements
- Insertion of slits and slots
- Careful design of antenna geometry

- Application of DGS

A study and analysis of multiband MIMO antennas found in the recent literature is summarised in Table 7.1.

Table 7.1: Multiband MIMO-Current state of arts.

Ref. No	**No. of Bands/No. of Ports**	**Bandwidth/ Resonant Frequency**	**Isolation**	**Technique used (Multi-banding and Isolation)**	**ECC**	**Size**
[107]	3 / 4	(3.72-3.82) GHz (4.65-4.76) GHz (6.16-6.46) GHz	>-16dB	Slots cut in the square shaped patch	<0.1	32mm*32mm
[108]	3 / 4	(2.29-2.49) GHz (2.85-3.04) GHz (5.61-5.80) GHz	>-18dB	Square shaped CSRR in DGS and use of meta-material	<0.01	106.6mm*106.6mm
[109]	3 / 2	2.9GHz 4.3GHz 7.7GHz	>-26.55dB	DGS and Vias	<0.0001	64mm*30mm
[110]	3 / 4	2.4 GHz 3.66 GHz 5.5 GHz	>-14dB	slots in the DGS and SRR as parasitic element.	-	40mm*40mm
[111]	3 / 4	(2.25-2.41) GHz (3.36-3.65) GHz (4.7-6.25) GHz	>-18dB	Antenna element geometry	<0.001	48mm*48mm
[112]	2 / 2	(2.25-3.15) GHz (4.89-5.95) GHz	>-15dB	Slits in the patch, rectangular stub and DGS	<0.01	50mm*50mm

[113]	2 / 4	(3.3-3.84) GHz (4.61-5.91) GHz	>-15dB	Antenna Geometry	<0.02	14.9mm* 7mm (Single Element)
[114]	2 / 8	(3.3-4.2) GHz (4.8-5) GHz	>-10dB	T-shaped decoupling stubs	<0.12	18.6mm* 7mm
[115]	2 / 4	(3.4-3.6) GHz (4.8-5) GHz	>-16.5 dB	Slits and parasitic patch	<0.01	150mm* 75mm

7.2ANTENNA DESIGN AND DIMENSIONS

The single radiating element of the 2 port MIMO system is as shown in Figure 7.1. Low-cost easily available FR4 substrate is used for the fabrication and High Frequency Structure Simulator (HFSS) software is used for the project design and analysis of the structure. The overall dimension of the designed structure is *40mm×40mm×1.5748mm.*

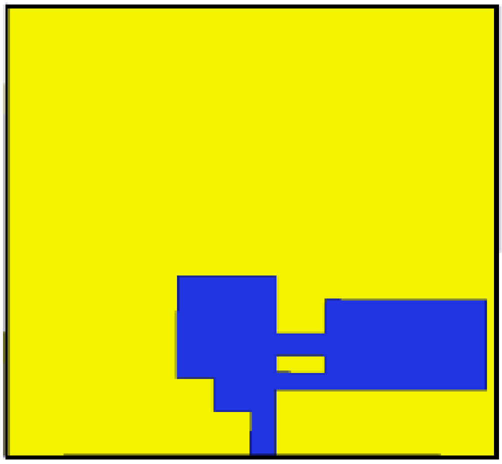

Figure 7.1: The antenna geometry of the radiating single element.

The stepwise development of the radiating structure is shown in Figure 7.2. The design starts from a basic rectangular patch, oriented as an inverted flag, when coupled with the microstrip feedline. The basic patch gave no significant bandwidth over the minimum S-Parameter value of 10 dB return loss. The second step added another rectangular patch to the right side of the first patch. This helped in achieving a single narrow band, (1.922 GHz – 2.009 GHz) resonating at 1.953 GHz with a return loss of 23.71 dB. An additional band is observed around 5 GHz but it is not below 0-10 dB. In the following step, an addition connect was offered to the first and second rectangular patches. This helped in shifting the bandwidth to the right to (2.18 GHz-2.286 GHz) resonating at 2.235 GHz with -36.244 dB. A shift is observed in the additional bandwidth seen in step two but the return loss could not be enhanced in this step. In step 4, a square slot of *3mm×3mm* was cut in the right corner of the first rectangular patch. This provided an enhanced return loss to the additional operation band. The final resonating element has dual operational bandwidths, (2.207 GHz-2.28 GHz) and (4.849 GHz-5.249 GHz) resonating at 2.235 GHz and 5.04 GHz respectively. The picture of the evolution steps is summarised in Figure 7.2.

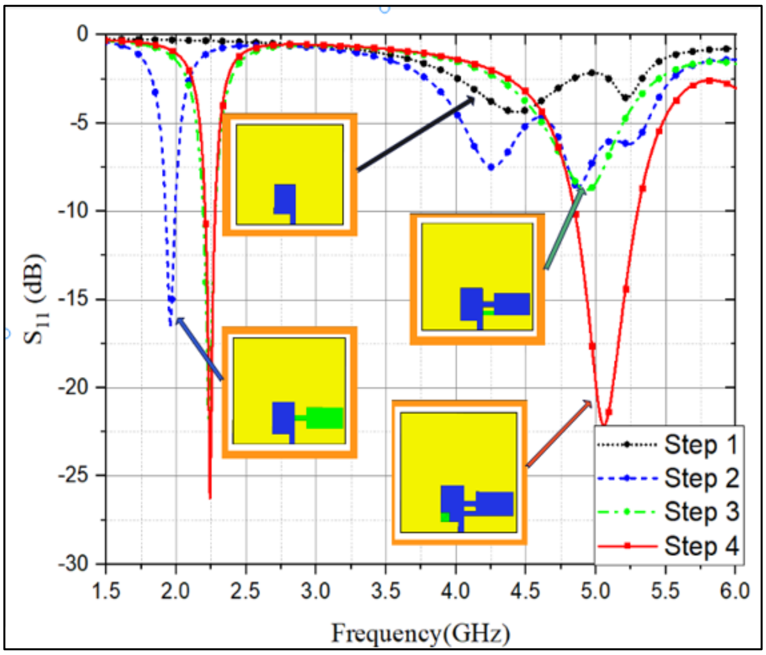

Figure 7.2: Evolution of the basic radiating element

Parametric study is conducted on every element added in each step of progress to the final radiating element. In step 2, the length and position of the second rectangular patch added is optimzed through parametric study as shown on 7(a). The results of the study on step two is given in Figure 7.3 (b) and Figure 7.3 (c).

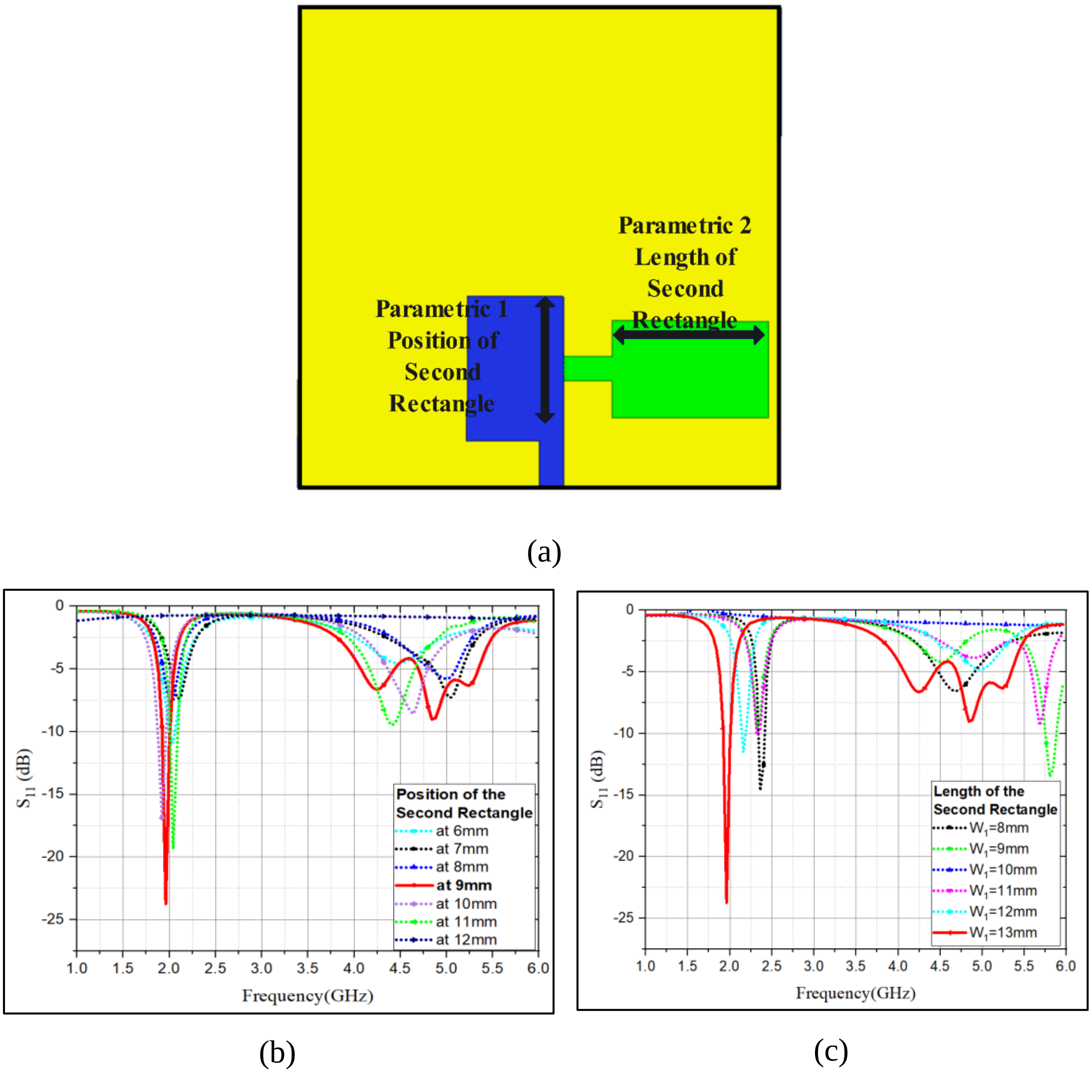

Figure 7.3: Parametric study done on step 2. (a) Antenna dimensions where parametric study is applied (b) Parametric analysis results on position of the second rectangle. (c) Parametric study results on length of the second rectangle.

In step 3 of the design of radiating element, a rectangular stub is used make an extra connection with the first and second rectangular patch. The width of this patch is set under parametric study to conclude that the best return loss characteristics is attained at 2.4 GHz when the width is the stub is 1.5mm. The diagrammatic representation of the parametric analysis done on step 3 is shown in Figure 7.4.

In the final step of the design, a slot is embedded in the first rectangular patch. Embedding this slot resulting in dual operational bands. The foremost band ranged between 2.207 GHz- 2.28 GHz and the second band from 4.84 GHz to 5.24 GHz. the length and width of the slot embedded is again optimized through parametric study. Figure 7.5 (a) shows the parameters investigated under this study, Figure 7.5(b) shows the parametric analysis on length of the slot and Figure 7.5 (c) shows the parametric study on the width of the slot.

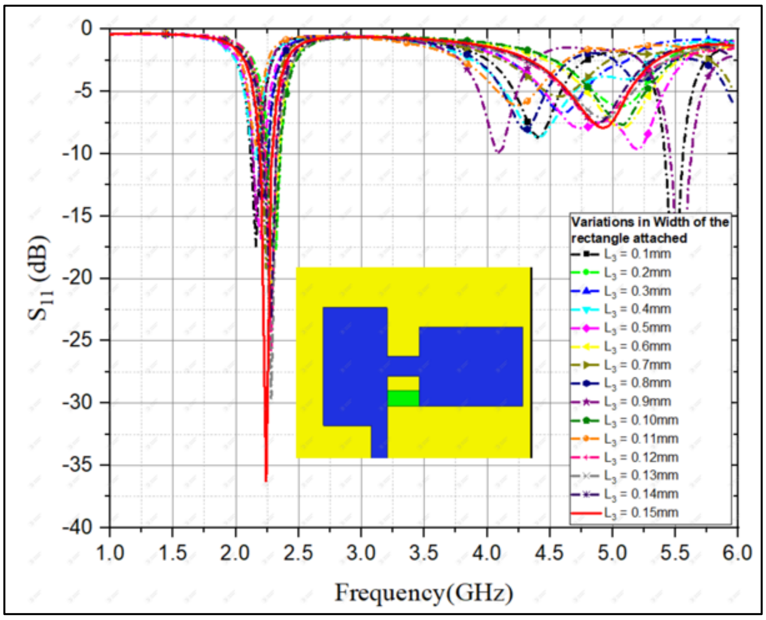

Figure 7.4: Parametric study done on the rectangular stub width connecting the two rectangular patches.

The radiating element was thus designed. Further, a 2-element MIMO system was designed as shown in Figure 7.6. Individual radiating elements were organized in an FR4 substrate of size *40mm*40mm.*

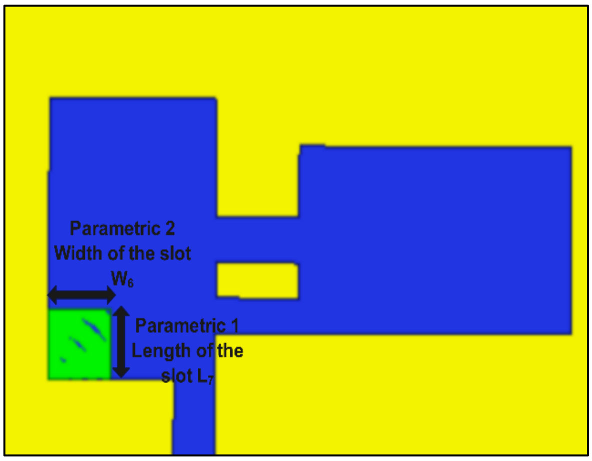

(a)

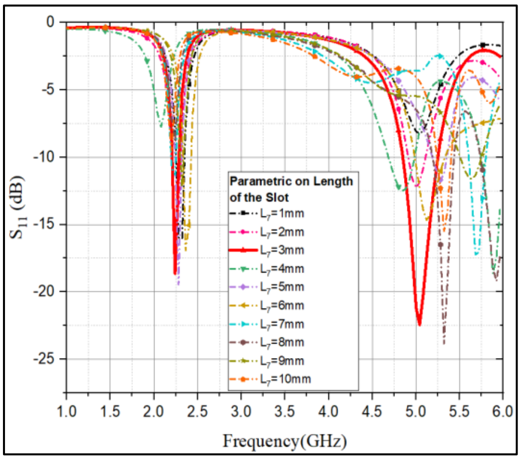

(b)

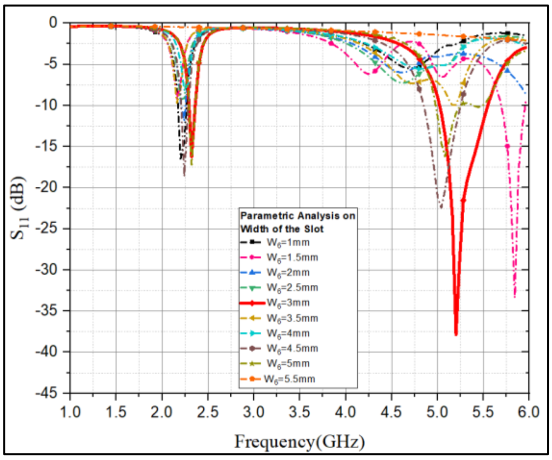

(c)

Figure 7.5: Parametric Analysis done on the slot on the rectangular radiating patch. (a) Figure showing the parameters under study for optimization. (b) Parametric analysis results on length of the slot. (c) Parametric study results on width of the slot.

The MIMO antenna with tri-band evolved through three stages, Stage 1 is named Ant_I and is shown in Figure 7.6(a). In the next stage two element MIMO is configured by placing the elements orthogonally to use antenna utilization to enhance isolation. This antenna is names as Ant_II and is shown in 7.6(b). In stage 3, a CSRR is embedded into the ground plane to achieve the third band of resonance and improve isolation. Stage 3, with CSRR in DGS, is named as Ant_III as shown in Figure 7.6(c).

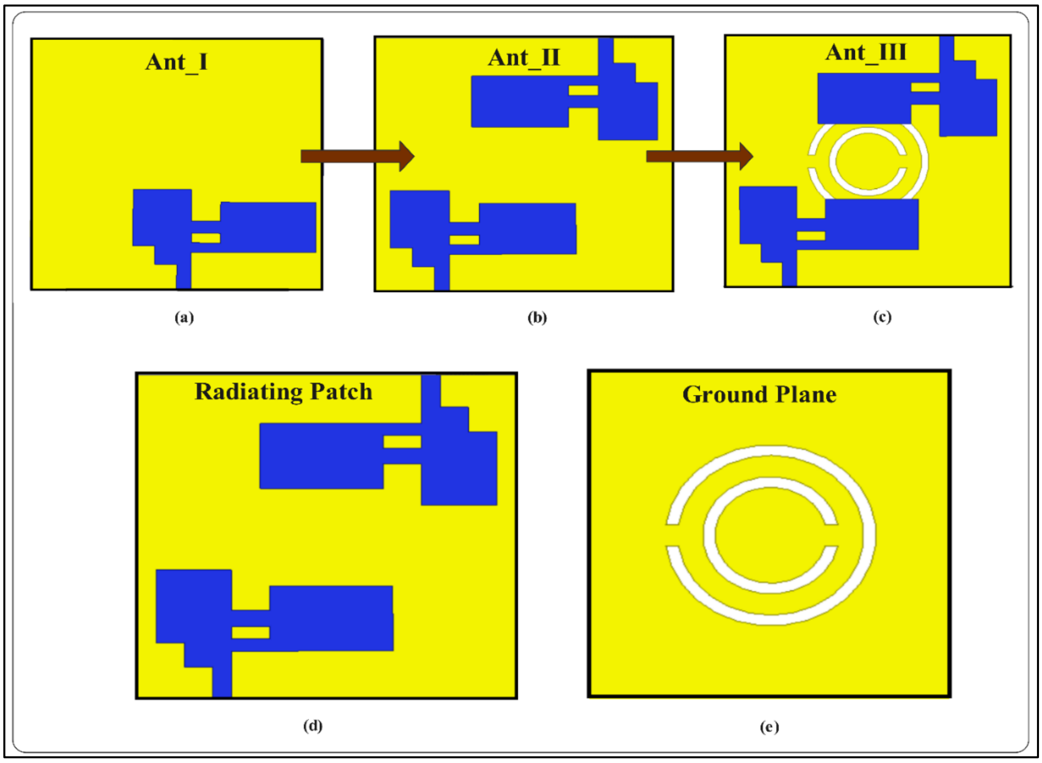

Figure 7.6: Evolution of the Dual-port Tri-band MIMO antenna. (a) Radiating single element as Ant_I. (b) Orthogonally placed 2-element MIMO, Ant_II. (c) Two-element MIMO with CSRR in DGS, Ant_III. (d) Radiating plane of the proposed antenna. (e) Ground plane of the proposed antenna.

CSRR is used as an effective method to achieve compactness while designing for a particular frequency. CSRR can be excited by means of an axial time varying electric field or by means of a magnetic field applied to the plane of antenna. Under ideal conditions, i.e., a perfectly conducting and zero-thickness metallic surface, it can be demonstrated that the resonance frequency of the CSRR is identical to the resonance frequency of the SRR (provided identical dimensions and substrate are considered). Indeed, the capacitance of the CSRR, C_c, is the capacitance of a disk of radius r_o-$c/2$ surrounded by a ground plane at a distance c of its edge. The inductance is given by the parallel connection of the two inductances of the metallic strips connecting the inner and outer metallic regions of the CSRR. These inductive values are given by $L_o/2$, where $L_o = 2\pi r L_{pul}$, with L_{pul} being the per unit length inductance. Due to change in equivalent inductance and capacitance of the ground plane, effective current distribution of ground plane changes resulting in the appearance of a new ISM band

(5.119 GHz – 5.353 GHz). The CSRR parameters include the average ring of radius r_o, i.e., the mean radius of the ring, and ring width c as shown in Figure 7.7.

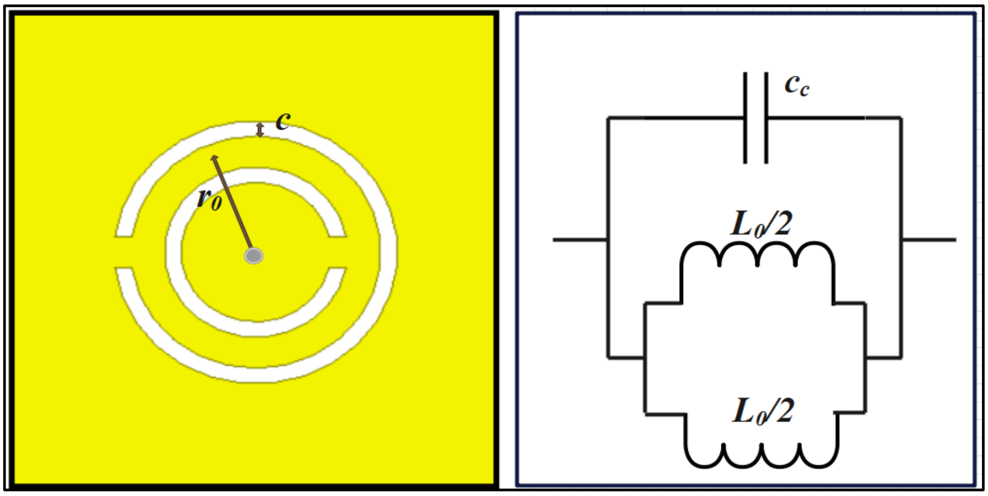

Figure 7.7 CSRR dimensions and its equivalent circuit

The final top and bottom view of the antenna is shown in Figure 7.6 (d) and (e) respectively. The optimized design dimensions are summarised in Figure 7.8 and Table 7.2. The 2-element MIMO was then fabricated as shown in Figure 7.11.

Table 7.2: Optimized dimensions of the patch and DGS of the proposed MIMO antenna

W	W_1	W_2	W_3	W_4	W_5	W_6	W_7	
40mm	13mm	17mm	4mm	2mm	3mm	3mm	8mm	
L	L_1	L_2	L_3	L_4	L_5	L_6	L_7	L_8
40mm	8mm	2.54mm	1.55mm	1.5mm	6mm	4mm	3mm	9mm
R_1	R_2	R_3	R_4	SW				
4.5mm	5.5mm	7.5mm	8.5mm	2mm				

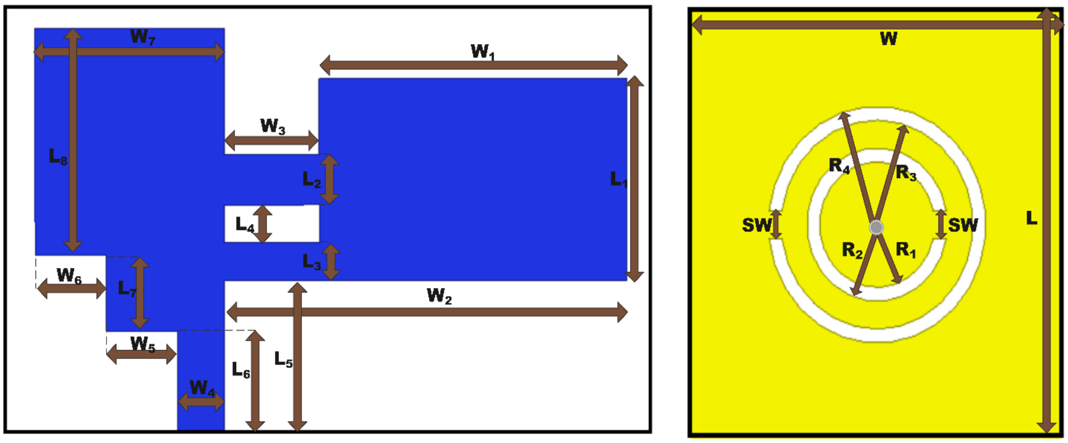

Figure 7.8: Design Dimensions for the Radiating Structure and DGS.

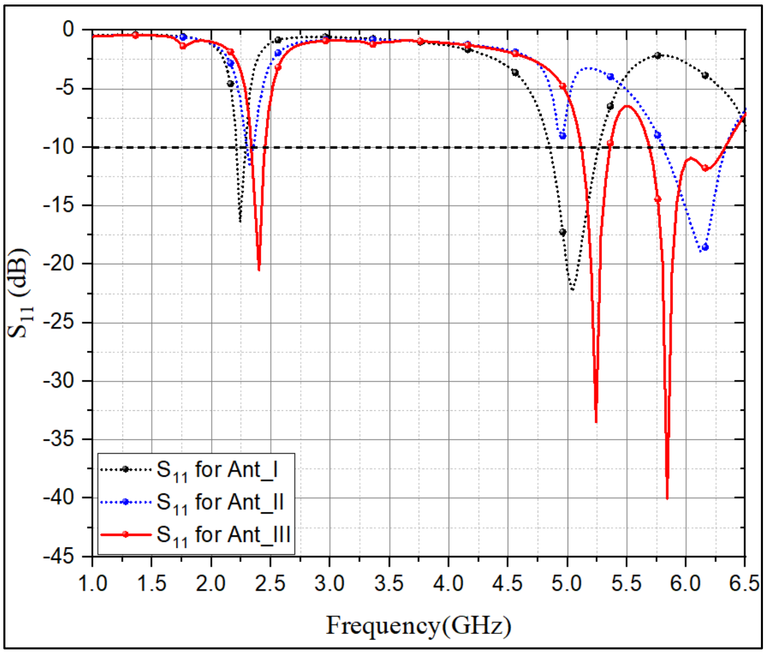

Figure 7.9: S_{11} evolutional stages of the compact two-element tri-band MIMO.

Figure 7.9 picturises the operational bandwidths and isolation achieved in each stage of evolution. Ant_I show two operational bandwidths, 2.207 GHz to 2.28 GHz, resonating at 2.235 GHz (-18.48 dB) and 4.84 GHz to 5.04 GHz, resonating at 5.04 GHz (-22.31 dB). Ant_II is the orthogonally placed 2-element MIMO system with two bands of 2.299 GHz to 2.360 GHz and 5.806 GHz to 6.334 GHz. The return loss of the second band, originally present in the simulation results of Ant_I was reduced below the reference level of -10dB. So, the two bands of Ant_II resonated at 2.32 GHz (-11.45

dB) and 6.121 GHz (-18.879 dB) respectively. The addition of CSRR as a DGS to Ant_II attained enough return loss (>10 dB) for the second band of Ant_I. Ant_III, therefore has three bands of operation as 2.336 GHz to 2.449 GHz, resonating at 2.39 GHz (-20.17 dB), 5.696 GHz to 6.29 GHz, resonating at 5.84 GHz (-40.03 dB) similar to that of Ant_II and the third additional band (as in Ant_I) 5.119 GHz to 5.353 GHz, resonating at 5.235 GHz (-33.16 dB).

Figure 7.10 shows the isolation amongst the elements in Ant_II (without CSRR) and Ant_III (with CSRR). For the Band 1 (2.336 GHz – 2.449 GHz), the isolation ranges between 15.97 dB to 18.87 dB in Ant_II and 24.05 dB to 25.94 dB in Ant_III. At the first resonance (2.39 GHz), the isolation in Ant_II is 16.32 dB and in Ant_III is 24.05 dB. For the second band (5.119 GHz – 5.353 GHz), the isolation ranges between 32.94 dB to 36.54 dB in Ant_II and 41.36 dB to 25.38 dB in Ant_III. At the second resonance (5.235 GHz), the isolation in Ant_II is 35.32 dB and in Ant_III is 28.06 dB. For the Band 3 (5.696 GHz – 6.29 GHz), the isolation ranges between 16.84 dB to 27.34 dB in Ant_II and 32.32 dB to 41.28 dB in Ant_III. At the third resonance (5.84 GHz), the isolation in Ant_II is 24.7 dB and in Ant_III is 37 dB.

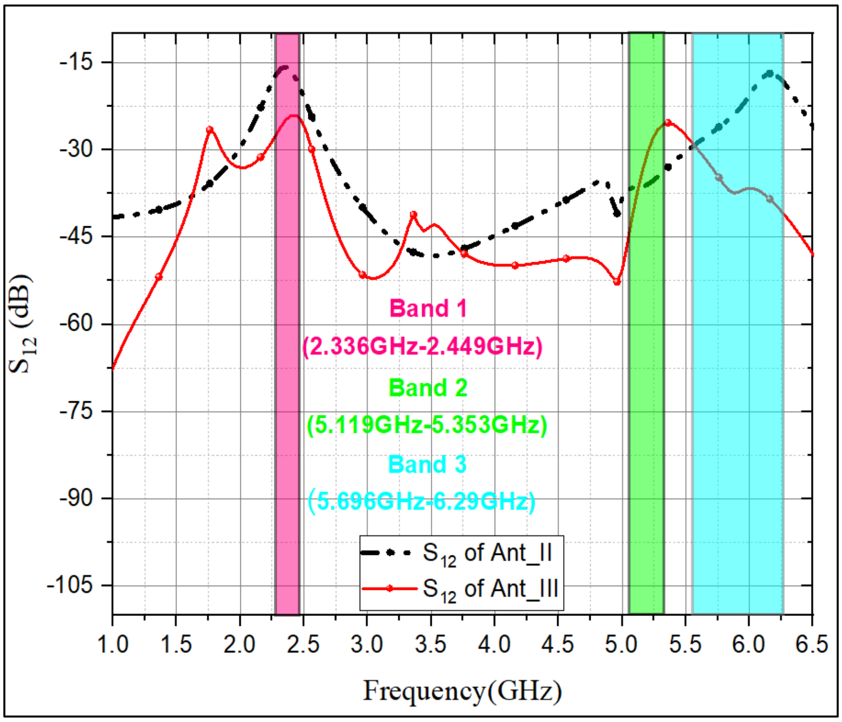

Figure 7.10: Isolation of Ant_II and Ant_III

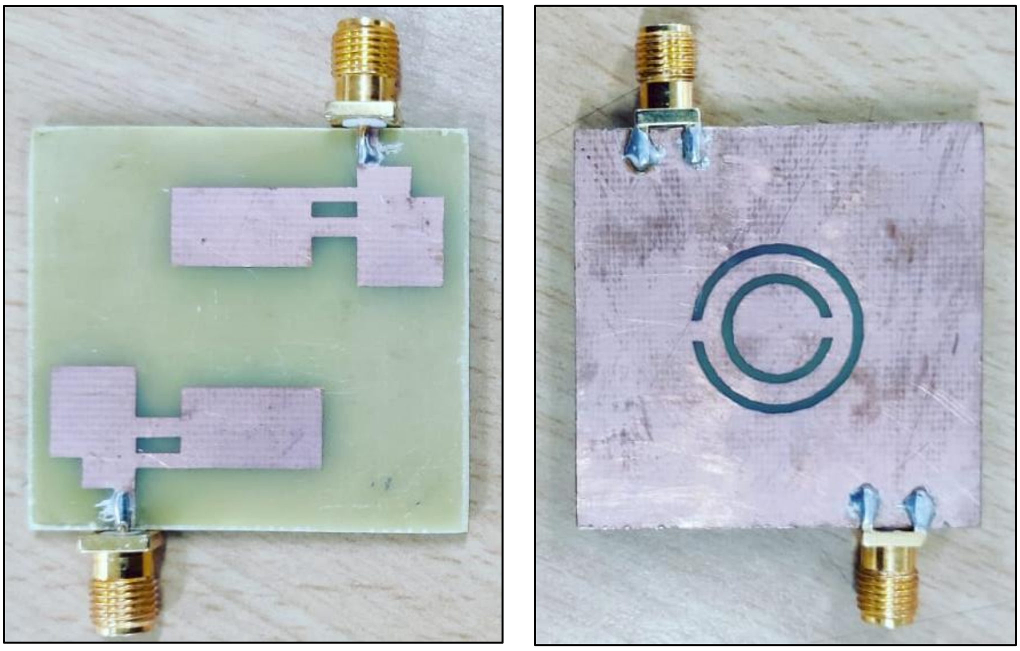

Figure 7.11: An image of the final antenna, Radiating surface (Top-View) and Ground plane (Bottom-View) of the proposed tri-band MIMO.

7.3 RESULTS AND DISCUSSIONS

A dual-element, tri-band MIMO antenna is designed and fabricated for measurements. The antenna offers three versatile frequencies of operation in the Sub-6 GHz band for various WLAN and IoT applications. The return loss for the antenna was measured by a VNA and the results seems to satisfactorily match with the software results. The performance of the MIMO antenna was also studied under an anechoic chamber to determine gain and the radiation characteristics. Slight deviations are observed between the simulated and measured values which might be possibility due to minute error occurred during the fabrication, soldering process or testing set up.

7.3.1 Parametric Study

A set of parametric study was conducted to attain best possible seclusion between the radiating elements and to accomplish all three bands of operation.

Orientation of the antenna elements

The element orientation in the substrate was carefully optimized to achieve maximum isolation. Figure 7.12 shows the different orientations investigated.

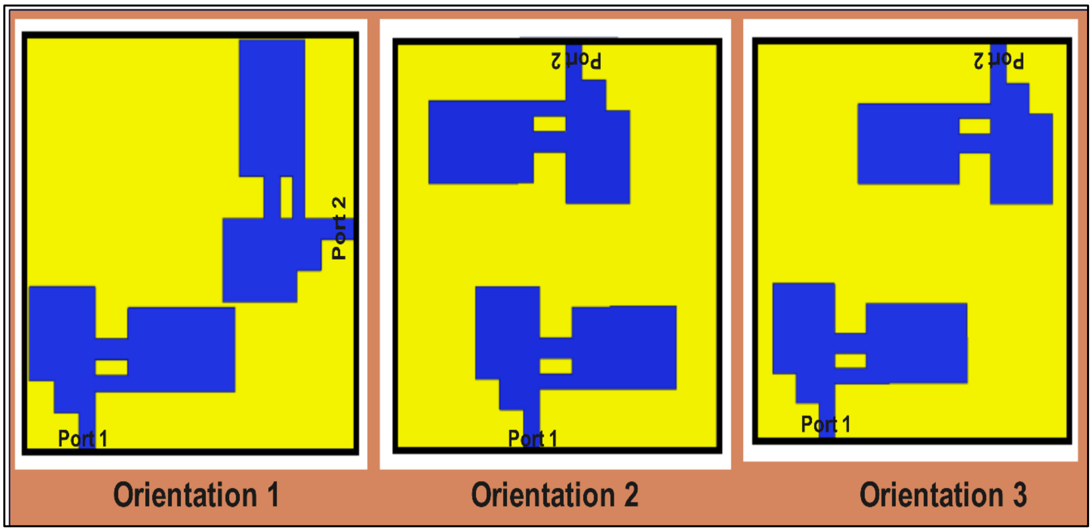

Figure 7.12: Variations in orientations applied.

The antenna elements were placed at 90˚ with respect to one another (orientation 1), at 180˚ with each other (orientation 2) and at 180˚ and moved to the corners to keep them maximum apart from each other (orientation 3). The orientation 1 gave good isolation at the lower band but isolation was above 10 dB for the second band and between 15 dB to 20 dB for the third band. Orientation 2, meanwhile provided good isolation to band 3. Orientation 3 attained lowest isolation for all the three resonant frequencies as shown in Figure 7.14.

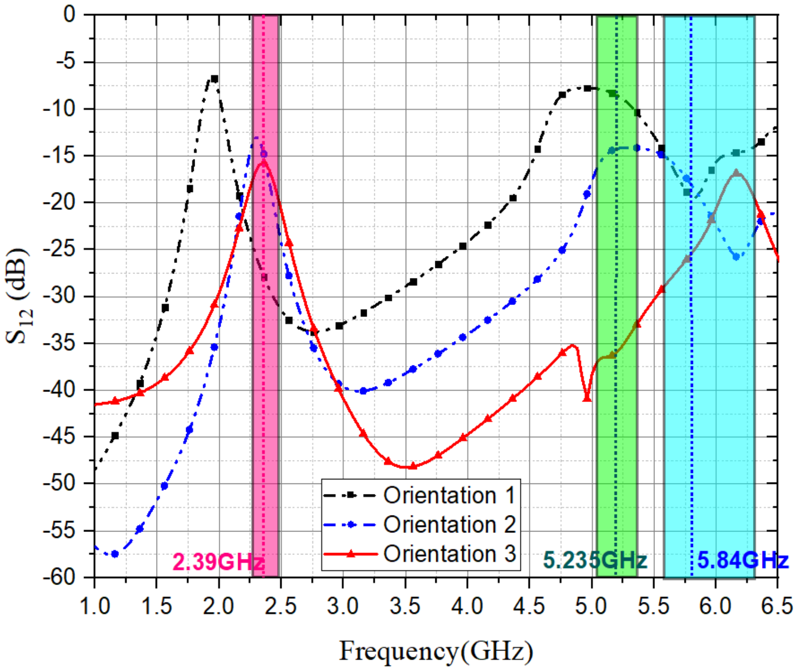

Figure 7.13: S_{12} (dB) achieved for different orientations

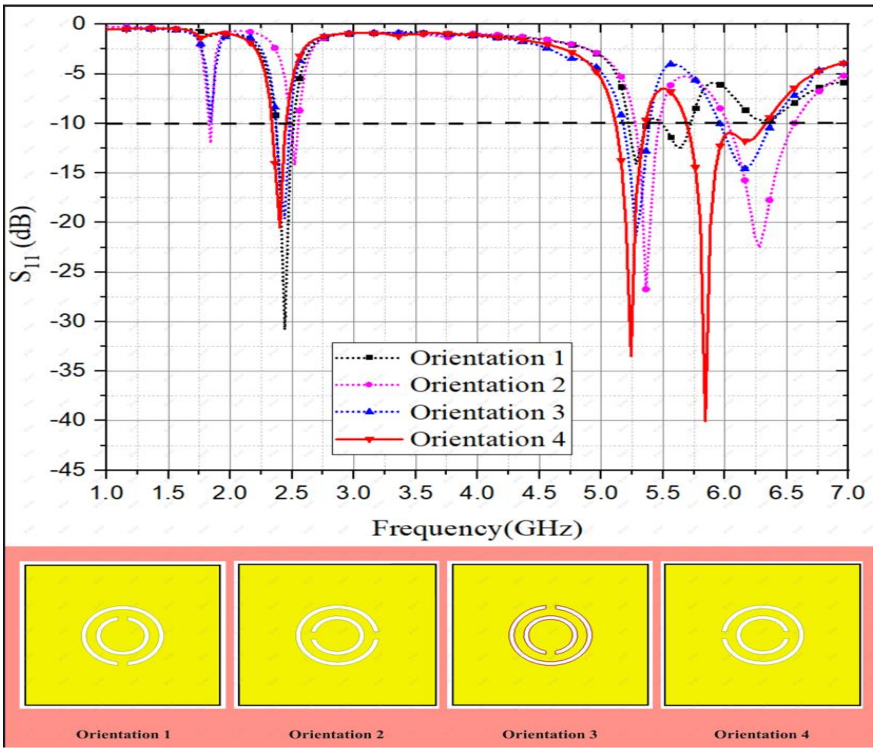

Figure 7.14: The distinction in S_{11} for various orientations of CSRR DGS.

The orientation of the CSRR in the ground plane of the MIMO antenna also influences the performance as shown in Figure 7.15. Orientation 1 provides three operating bands but the return loss is very less for band 2 and 3. The orientation 2 gives slightly shifted version of the bandwidths towards the right with an additional resonance at 1.8 GHz. The resonant frequencies in orientation 2 are 1.88GHz, 2.55 GHz, 5.39 GHz, and 6.31 GHz. The third orientation attains a band at 1.8GHz but not enough to have a return loss beyond 10 dB. The first lower band resonates at 2.43 GHz, the second at 5.28 GHz and the third band at 6.1 GHz. The orientation of CSRR as in orientation 4 optimizes the resonant frequencies to 2.38 GHz, 5.23 GHz and 5.84 GHz. Figure 7.16 shows the variations in S_{12} according to the orientation of CSRR in the ground plane. At some points it is seen that the isolation for orientation 4 is less compared to other orientation by orientation 4 shows better isolation than all other orientations for the operating bandwidths.

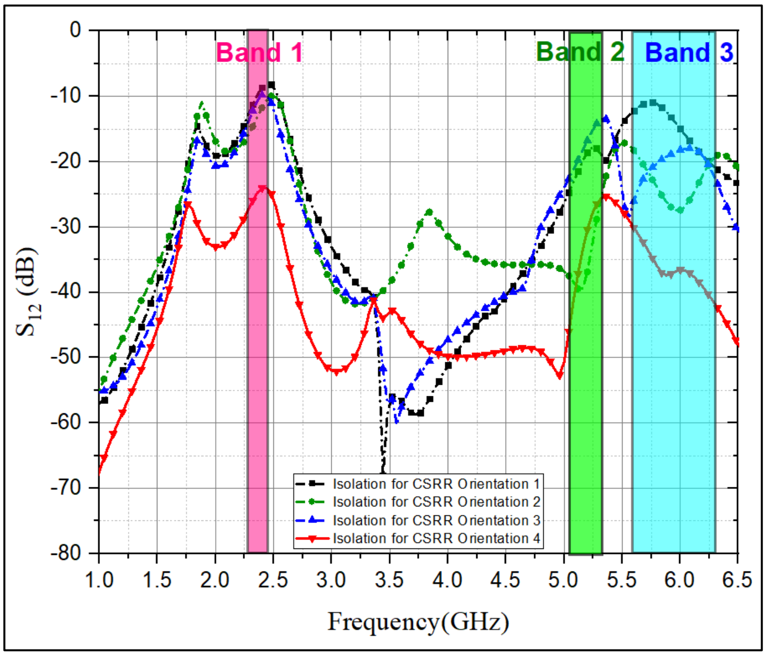

Figure 7.15: Isolation for different orientation of CSRR in the ground plane

The other parameters of CSRR, investigated parametrically are shown in Figure 7.16 (a). The includes the rectangular slot width cut for the CSRR (Figure 7.16 (b)), the width of the rings of the CSRR (Figure 7.16 (c)) and the distance or spacing between the rings of the CSRR, (Figure 7.16 (d)). After the parametric analysis, Slot width of CSRR is fixed at 2mm, and the width of CSRR and spacing between the rings of CSRR, are fixed at 1mm.

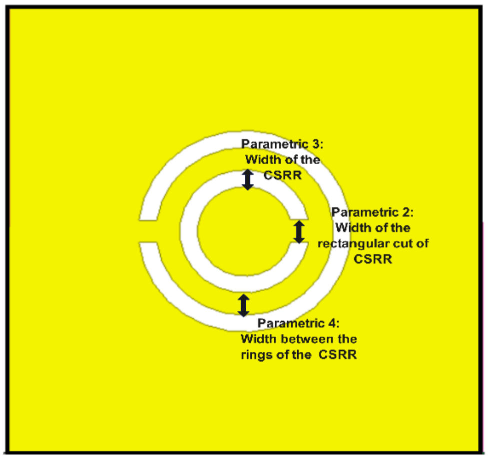

(a)

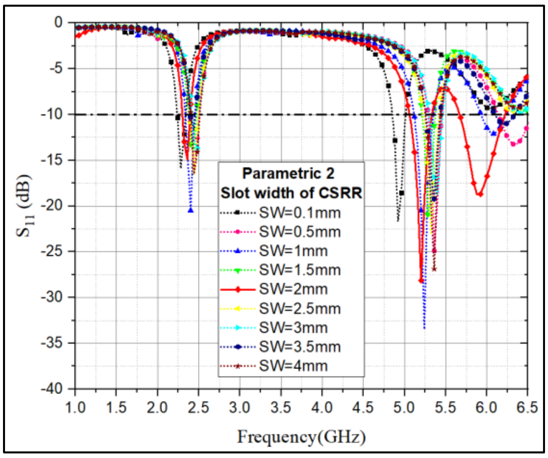

(b)

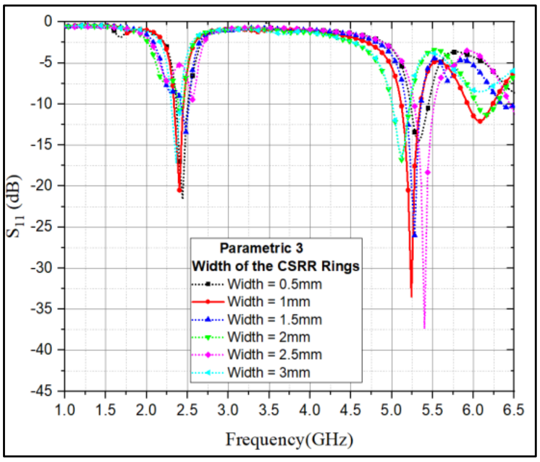

(c)

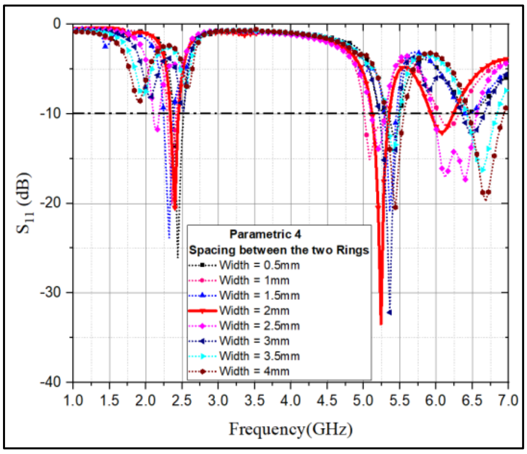

(d)

Figure 7.16: Parametric study on CSRR. (a) Parameters under investigation (b) Slot Width of CSRR. (c) Width of CSRR rings. (d) Spacing between the CSRR rings.

7.3.2 Antenna Parameters

The simulated and measured values of the antenna parameters for the proposed antenna is discussed below.

S-Parameters

The simulated and measured S-parameters are in good agreement with each other. Figure 7.17 shows the summary of both return loss and isolation values for the proposed antenna and all the s-parameters are in good agreement other than foe very slight variation in the return loss which might be due to slight fabrication errors or device calibration.

Gain, Efficiency and Radiation Pattern

The gain and radiation pattern of the proposed MIMO antenna is measured in an anechoic chamber with the help of a particular antenna measurement setup. The Figure 7.18 shows the plot of simulated and measured gain and radiation efficiency. Both these parameters explain how well the designed antenna performs. The maximum gain attained by the antenna is 7.17 dBi at 5.28 GHz. It is observed that the gain is lower at lower frequencies. This is because the antenna becomes smaller with respect to the wavelength at lower frequencies. Gain at 2.4 GHz is 1.893 dBi and at 5.84 GHz, gain attained is 6.71 dBi. The radiation efficiencies are 65.74% (2.4 GHz), 84.75% at 5.28 GHZ and 92.3% at 5.84 GHz.

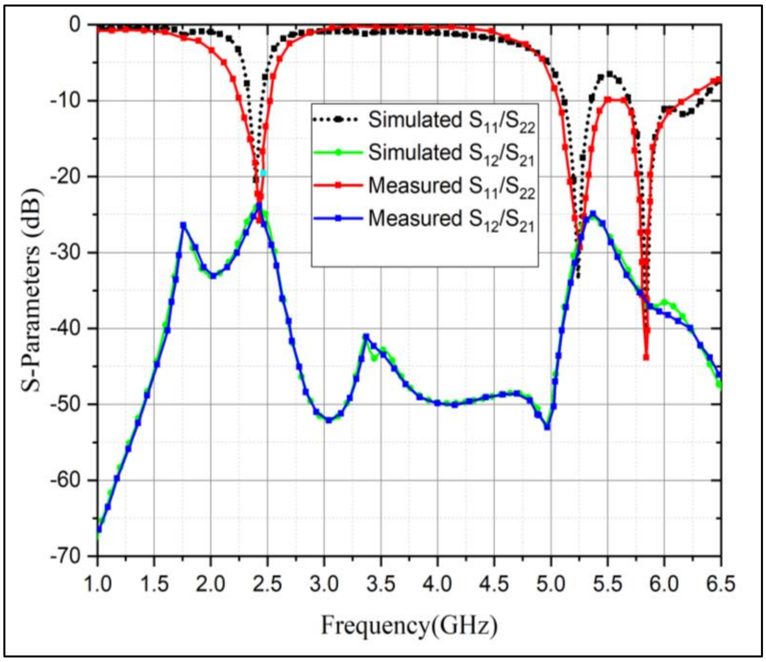

Figure 7.17: Simulated and Measured S-Parameters for the proposed antenna

The radiation pattern for the E-Plane and H-Plane at all the three resonant frequencies are as shown in the Figure 7.19. Figure 7.19(a) is the radiation pattern at 2.4 GHz, Figure 7.19(b) is the pattern for 5.2 GHz and Figure 7.19(c) is the radiation pattern at 5.8 GHz.

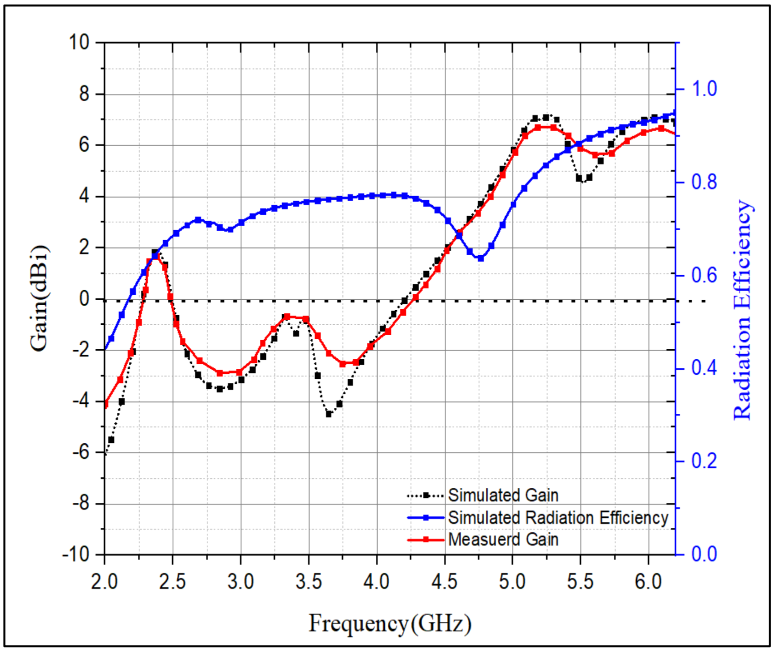

Figure 7.19 : Gain and Radiation Efficiency for the proposed MIMO antenna

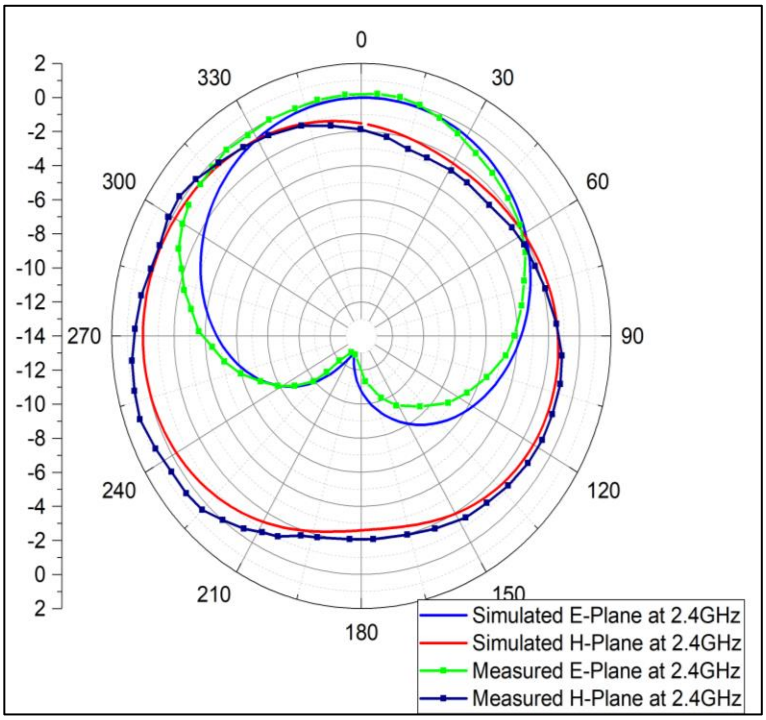
0
30
60
90
120
150
180
210
240
270
300
330
2
0
-2
-4
-6
-8
-10
-12
-14
-12
-10
-8
-6
-4
-2
0
2
Simulated E-Plane at 2.4GHz
Simulated H-Plane at 2.4GHz
Measured E-Plane at 2.4GHz
Measured H-Plane at 2.4GHz

(a)

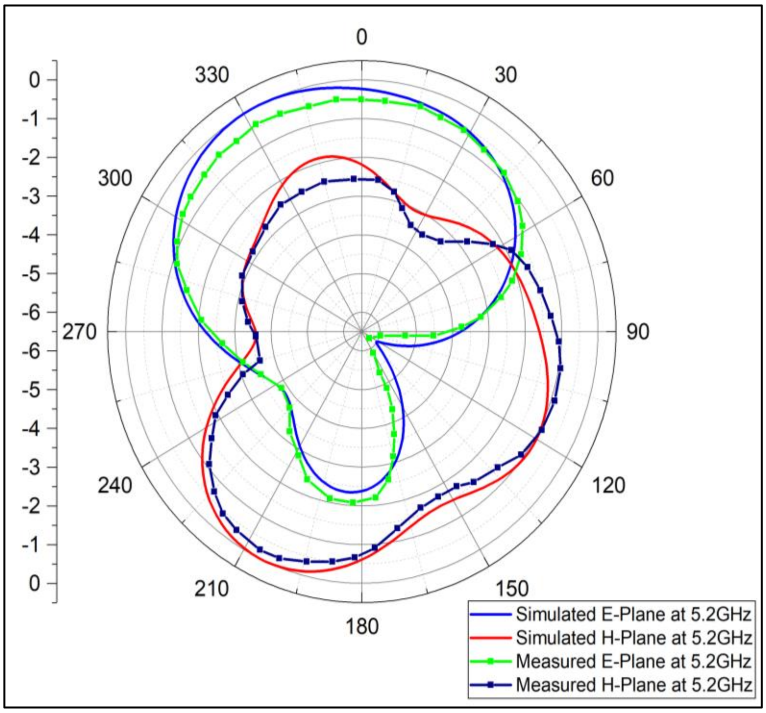
0
30
60
90
120
150
180
210
240
270
300
330
0
-1
-2
-3
-4
-5
-6
-6
-5
-4
-3
-2
-1
0
Simulated E-Plane at 5.2GHz
Simulated H-Plane at 5.2GHz
Measured E-Plane at 5.2GHz
Measured H-Plane at 5.2GHz

(b)

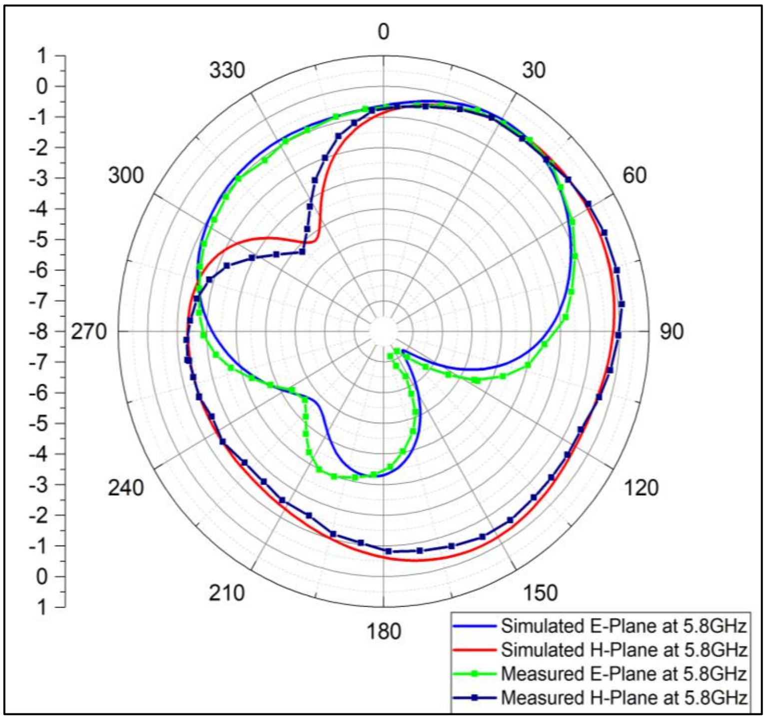

(c)

Figure 7.19: E-Plane and H-Plane radiation patterns. (a) at 2.4GHz, (b) at 5.2GHz and (c) at 5.8GHz

7.3.3 MIMO Diversity Parameters

MIMO antennas are analysed with a set of diversity parameters as the "Envelope Correlation Co-efficient" (ECC), the "Diversity Gain" (DG), "Total Active Reflection Co-efficient" (TARC), and "Channel Capacity Loss" (CCL). Each of these has be evaluated below for the designed dual-element, tri-band MIMO antenna.

Envelope Correlation Co-efficient

When multiple antennas are used simultaneously, the correlation between the received signals helps in analysing the performance of the system. The far field radiation characteristics helps in evaluating ECC by the following Equation (7.1).

$$ECC = \left| \frac{\iint_{4\pi} S_i\,(\theta,\emptyset).S_j^*\,(\theta,\emptyset)d\Omega}{\sqrt{\iint_{4\pi} S_i\,(\theta,\emptyset).S_i^*\,(\theta,\emptyset)d\Omega \iint_{4\pi} S_j\,(\theta,\emptyset).S_j^*\,(\theta,\emptyset)d\Omega}} \right|^2 \text{------------(7.1)}$$

The far field radiation characteristics of port i and port j are represented as S_i and S_j. Ideally the preferred value of ECC is 0 and the acceptable value is below 0.5 for well performing MIMO antenna.

Diversity Gain

The diversity gain is another parameter of interest in MIMO systems. DG is easily calculated from ECC using Equation (7.2). The DG needs to be very close to 10 dB for the operating bands in a well performing MIMO.

$$DG = 10\sqrt{1 - ECC} \text{--(7.2)}$$

The ECC and DG plot for the proposed MIMO is shown in Figure 7.20. Both the measured and simulated ECC are well below 0.15 for this MIMO antenna and the DG for the operating bands are close to 10. Table 7.3 summarizes the ECC and DG values for all the three operational bands.

Table 7.3: Summarised ECC and DG

Band of Operation	**1**	**2**	**3**
Frequency of Operation	2.39 GHz	5.23 GHz	5.84 GHz
ECC	0.029	0.0014	0.0007
DG	9.99	10	10

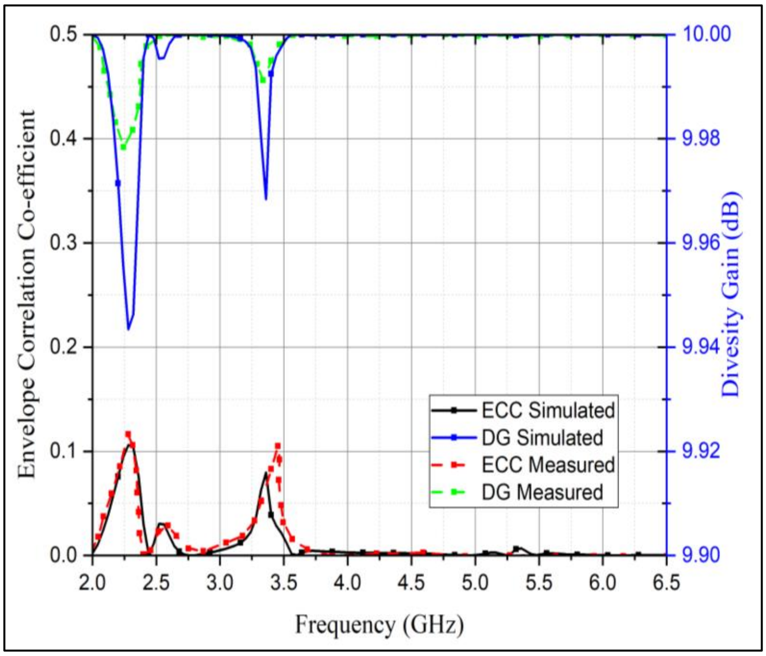

Figure 7.20: Simulated and Measured ECC and DG for the proposed antenna

Channel Capacity Loss

CCL is the parameter used to measure the information transmission rate of the wireless channel and CCL needs to be less than 0.5bits/sec/Hz for a good communication system. The channel capacity loss for a system is calculated from the Equation (7.3).

$$CCL = -log_2\, det(\varphi^R) \text{-------------------(7.3)}$$

Where, φ^R is the performance of the MIMO antenna and is given as in Equation (7.4)

$$\varphi^R = \begin{matrix} \rho_{ii} & \rho_{ij} \\ \rho_{ji} & \rho_{jj} \end{matrix} \text{ ---------------------------(7.4)}$$

The CCL values are 0.34bits/sec/Hz for 2.39 GHz, 0.108bits/sec/Hz for 5.23 GHz and 0.261bits/sec/Hz for 5.84 GHz. The plot of simulated and measured CCL is shown in Figure 7.21(a).

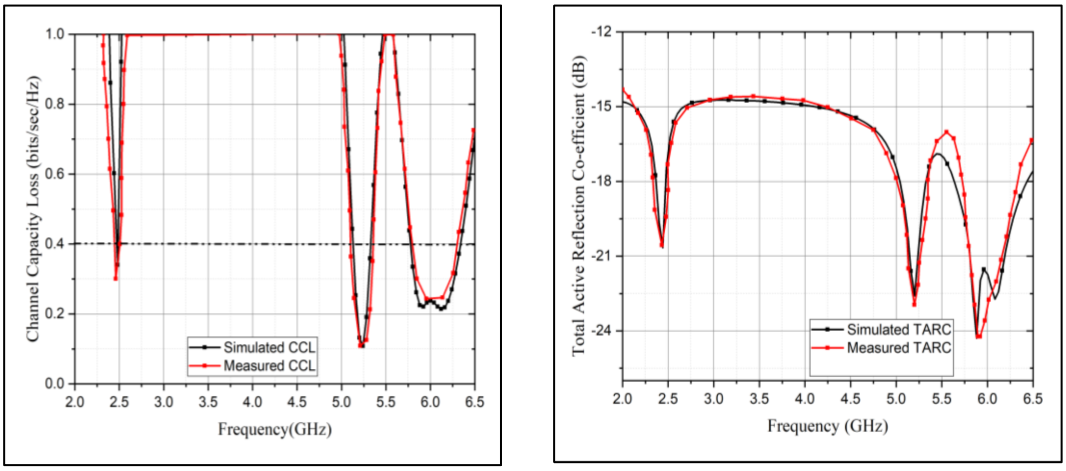

(a) (b)

Figure 7.21: Diversity Parameters of Proposed MIMO. (a) Simulated and Measured CCL. (b) Simulated and Measured TARC

Total Active Reflection Co-efficient

TARC is another major parameter to study the performance of a MIMO antenna system. TARC studies the diversity performance while multiple antennas are working simultaneously. TARC, in other words, can be considered as the return loss of a MIMO antenna system. TARC can be calculated from the formulation given as Equation (7.5).

$$_a^t\Gamma = \sqrt{\frac{|S_{11}+S_{12}\, e^{j\theta}|^2+|S_{11}+S_{12}\, e^{j\theta}|^2}{2}} \text{------------------------------(7.5)}$$

Where θ = the variance in phase among the excitation signals.

For a well performing MIMO antenna, TARC is expected to be less than 0 dB. In this antenna, TRAC is below -18 dB for the operational bandwidths which concludes that the proposed MIMO has good diversity performance. The software simulated and experimentally measured TARC is depicted in Figure 7.21(b).

7.4. CONCLUSION

The chapter studies a two-element, tri-band MIMO antenna with a microstrip line feed. The antenna is low profile and compact and built of FR4 substrate of size *40mm*40mm.* The identical radiating patches with the CSRR embedded in the DGS provides three versatile operating frequencies of 2.4 GHz, 5.2 GHz, and 5.8 GHz. This antenna displays decent isolation and steady gain and radiation characteristics and can be used for IEEE 802.11 a/b/g applications and other IoT systems connected to the above frequencies of operation. This 2-element tri-band MIMO antenna can support various IoT modules operating at 2.4 GHz, 5.2 GHz, and 5.8 GHz [116].

CHAPTER 8

CONCLUSION AND FUTURE SCOPE

8.1 INTRODUCTION

Communication is an attribute ever-present in the human evolution. The evolving world of technologies have always demanded continuous enhancement and refinement of communication technologies. Internet has taken the communication standards into an entirely new era. The modern-day communication includes connecting people to devices and devices to devices all over the world. The new gadgets like smart meters, smart watches, Alexa, smart homes and many more are all examples of the modern IoT implementations.

IoT systems are basically made of powerful sensors/chain of sensors, high end processors, cloud system and gateways and application specific communication protocols to support any or every communication between these modules and the end users.

Antennas are an inevitable part of any wireless communication system, and microstrip antennas are the preferred choice for many IoT applications owing to its low profile, compact nature, and flexible and designable characteristics.

This thesis studies and aims at designing microstrip patch antennas which are compact in size and holds good range and radiation characteristics for the communication modules supporting modern IoT applications. The aim of this chapter is to conclude and summarise the work carried out over the period of study and to put up some suggestions on the future scope of research in this field of study. This final chapter of this 8-chapter thesis summarises the work done and the intended application.

8.2 CONCLUSION

This research is focused in designing, fabricating, and testing of microstrip antennas for IoT enabled devices and modules for various wireless applications. The major factors and benchmarks kept under consideration includes

- Size of the antenna structure
- Operational frequency of the system
- Performance parameters like return loss and gain
- Radiation characteristics to study the coverage area and radiation pattern and,
- The isolation between the antenna elements in case of MIMO antenna design.

Chapter 1 of this report explains the current scenario of digital communication and how IoT systems are dependent on microstrip antennas. The importance of highly effective communication module in an IoT system is discussed. The objectives of this study and the organization of this thesis is summarised in this chapter. Chapter 2 studies the basics of antennas, the electromagnetic spectrum, microstrip antennas and their ad vantages and disadvantages are explained. The DGS techniques and MIMO antennas are explained in the latter sections of this chapter.

A detailed literature study of IoT antennas found in the literature for last 5-7 years are reviewed and summarized in Chapter 3. Both the monopole antennas and the MIMO antenna systems proposed for various IoT applications are studied and summarised in this chapter. The antennas are designed and simulated in software and then fabricated. The simulation software, HFSS, and the steps of simulation is explained in Chapter 4 along with other measurement devices and set ups including Vector Network Analyzer, Spectrum Analyzer and Anechoic chamber.

Four microstrip antennas are designed which can be used to operate with various IoT enabling devices with different IoT communication protocols widely used in IoT applications. The antennas in this thesis are designed and simulated with HFSS simulator software and has employed various antenna designing techniques like DGS and MIMO to attain the desired characteristics.

The first antenna is a compact monopole antenna of size *20mm×20mm,* in a log-periodic like structure, and fed by a slotted co-planar feeding system. As discussed in section 5.3, this antenna resonates around one of the most versatile frequencies of 2.4 GHz with a gain of 9. 34 dBi. The antenna is fabricated and can easily be integrated with modules like ESP8266 for various IoT applications. In this same chapter, Chapter 5, another log-periodic structured, dual-port MIMO antenna is discussed in section 5.4. This structure is of size *15mm×17mm* built on FR4 substrate and provides a wide band of operation of 2 GHz. DGS technique is employed in this system to attain the chosen frequency range of operation and to enhance isolation between the elements. This antenna operates between 2.06 GHz and 4.04 GHz with a maximum gain of 2.9 dBi and an isolation of more than 30 dB amongst the operating elements. This MIMO antenna system is proposed for the IoT applications using WLAN and WiMAX frequencies.

Chapter 6 of the thesis proposes a sub-GHz antenna of size *22mm×34mm*, bandwidth of 930 MHz and radiation efficiency of 97%. The radiating patch of this antenna is double-leaf structured. DGS is employed to attain the desired frequency of resonance, 433 MHz, which is used by LoRa communication protocol. LoRa protocols are generally used in applications requiring a coverage area of 10KM-15KM. The other LoRa operating frequencies in sub-GHz range are 868 MHz and 915 MHz, which also comes under the operational bandwidth of the proposed antenna. The antenna can be integrated with LoRa module at sub-GHz frequencies which enables IoT applications.

Chapter 7 discusses a 2-element tri-band MIMO antenna, which can support various IoT modules operating at 2.4 GHz, 5.2 GHz and 5.8 GHz. Here again, the technique of defected ground is employed by embedding a CSRR in the DGS of this tri-band antenna. This antenna offers stable gain and good isolation between antenna elements.

All proposed antenna structures are compact and has good radiational characteristics. They can easily be integrated with modules like ESP8266 operating at various frequency ranges to enable different IoT applications.

8.3 FUTURE SCOPE

This thesis includes study and design of various compact antenna, both monopole and 2-eleement MIMO structures, for application in IoT enabling devices. The designed antennas are to use as external antenna. Some enhancements which done be done in future includes

- Study and implementing various power harvesting antenna techniques to attend to the power limitations faced by the deployed and un-attenable nodes.
- Gain enhancements may be achieved by employing array antennas
- Metamaterials and their properties and fractal antennas could be exploited to attain better performing compact antennas
- Antennas could be designed with polarization purity to enhance the reception at the receiver side.
- This study has used MIMO with 2-elements. More elements can be included in the MIMO structure to further enhance the performance.

Bibliography

[1] Sanjay Kumar Pal. 2008. 21st Century Information Technology Revolution. Ubiquity 2008, June, Article 9 (June 2008), 1 page. DOI: https://doi.org/10.1145/1403922.1399619

[2] Handong Zhang and Lin Zhu, "Internet of Things: Key technology, architecture and challenging problems," 2011 IEEE International Conference on Computer Science and Automation Engineering, 2011, pp. 507-512, doi: 10.1109/CSAE.2011.5952899.

[3] Gameiro, A., Castanheira, D., Sanson, J. et al. Research Challenges, Trends and Applications for Future Joint Radar Communications Systems. Wireless Personal Communications 100, 81–96 (2018). https://doi.org/10.1007/s11277-018-5614-8

[4] N. Alam, P. Vats and N. Kashyap, "Internet of Things: A literature review," 2017 Recent Developments in Control, Automation & Power Engineering (RDCAPE), 2017, pp. 192-197, doi: 10.1109/RDCAPE.2017.8358265.

[5] Ashton, Kevin. "That 'internet of things' thing." RFID journal 22.7 (2009): 97-114.

[6] Z. Zhang, M. C. Y. Cho, C. Wang, C. Hsu, C. Chen and S. Shieh, "IoT Security: Ongoing Challenges and Research Opportunities," 2014 IEEE 7th International Conference on Service-Oriented Computing and Applications, 2014, pp. 230-234, doi: 10.1109/SOCA.2014.58.

[7] Luigi Atzori, Antonio Iera, Giacomo Morabito, The Internet of Things: A survey, Computer Networks, Volume 54, Issue 15, 2010, Pages 2787-2805, ISSN 1389-1286, https://doi.org/10.1016/j.comnet.2010.05.010.

[8] G. Kortuem, F. Kawsar, V. Sundramoorthy and D. Fitton, "Smart objects as building blocks for the Internet of things," in IEEE Internet Computing, vol. 14, no. 1, pp. 44-51, Jan.-Feb. 2010, doi: 10.1109/MIC.2009.143.

[9] K. Lee and K. Tong, "Microstrip Patch Antennas—Basic Characteristics and Some Recent Advances," in Proceedings of the IEEE, vol. 100, no. 7, pp. 2169-2180, July 2012, doi: 10.1109/JPROC.2012.2183829.

[10] Pal, S. K (2008). 21st Century Information Technology Revolution. Ubiquity Volume 9, Issue 24 (June 17 - 23, 2008).

[11] Arya, A. K., Kartikeyan, M. V., &Patnaik, A. (2010). Defected ground structure in the perspective of microstrip antennas: a review. Frequenz, 64(5-6), 79-84.

[12] Khandelwal, M. K., Kanaujia, B. K., & Kumar, S. (2017). Defected ground structure: fundamentals, analysis, and applications in modern wireless trends. International Journal of Antennas and Propagation, 2017.

[13] Park, J. S. (2003). An equivalent circuit and modeling method for defected ground structure and its application to the design of microwave circuits. Microwave Journal, 46(11), 22-33.

[14] Weng, L.H., Guo, Y., Shi, X., & Chen, X. (2008). An Overview on Defected Ground Structure. Progress in Electromagnetics Research B, 7, 173-189.

[15] Garg, C., &Kaur, M. (2014).A review of defected ground structure (DGS) in microwave design. International Journal of Innovative Research in Electrical, Electronics, Instrumentation and Control Engineering, 2(3), 1285-1290.

[16] Xiao, J. K., Zhu, Y. F., & Fu, J. S. (2019). DGS lowpass filters extend wide stopbands. Semiconductors..

[17] Verma, S., Rano, D., &Hashmi, M. S. (2017, November). A novel miniaturized band stop filter using fractal type defected ground structure (DGS). In 2017 IEEE Asia Pacific Microwave Conference (APMC) (pp. 799-802). IEEE.

[18] Kumar, A., &Kartikeyan, M. V. (2017). Design and realization of microstrip filters with new defected ground structure (DGS). Engineering Science and Technology, an International Journal, 20(2), 679-686.

[19] Dhurvey, Prof.Prashant. (2015). Bandwidth Enhancement for PIFA Antenna Using Circular Slot in Radiating Patch and Ground Plane for Wireless Communication. International Journal of Advanced Research in Electrical, Electronics and Instrumentation Engineering. 4. 6929-6934. 10.15662/ijareeie.2015.0408015.

[20] Rajawat, A., Singhal, P. K., Gupta, S. H., Jain, C., Tomar, P., &Kapur, K. (2018). Gain enhancement of microstrip patch antenna using H-shaped defected ground structure. In Progress in Intelligent Computing Techniques: Theory, Practice, and Applications (pp. 517-526). Springer, Singapore.

[21] Panda, R. A., Tripathy, C. M., Sahu, K. C., & Mishra, D. (2019, March). Perturbed Triangular Patch Antenna with DGS for K Band Application. In 2019 International Conference on Vision Towards Emerging Trends in Communication and Networking (ViTECoN) (pp. 1-5). IEEE.

[22] Belekar, V. M., Mukherji, P., &Pote, M. (2017, March). Improved microstrip patch antenna with enhanced bandwidth, efficiency and reduced return loss using DGS. In 2017 International Conference on Wireless Communications, Signal Processing and Networking (WiSPNET) (pp. 2471-2474). IEEE.

[23] L. Daza and S. Misra, "Fundamentals of Massive MIMO (Marzetta, T., et al; 2016) [Book Reviews]," in IEEE Wireless Communications, vol. 25, no. 1, pp. 9-9, February 2018, doi: 10.1109/MWC.2018.8304383.

[24] Sharawi, M. S. (2014, February). Printed MIMO antenna systems: performance metrics, implementations and challenges.In Forum for Electromagnetic Research Methods and Application Technologies (FERMAT) (Vol. 1, pp. 1-11).

[25] Vikram, N. (2016, March). Design of ISM band RFID reader antenna for IoT applications. In *2016 International Conference on Wireless Communications, Signal Processing and Networking (WiSPNET)* (pp. 1818-1821). IEEE.

[26] Labade, R. P., Tambe, A. R., & Poddar, A. K. (2017, November). Semicircular multiband ACS feed antenna for IoT. In *2017 IEEE Asia Pacific Microwave Conference (APMC)* (pp. 779-782). IEEE.

[27] Jha, K. R., Mishra, G., & Sharma, S. K. (2017, July). An octahedron shaped planar antenna for IoT applications. In *2017 IEEE International Symposium on Antennas and Propagation & USNC/URSI National Radio Science Meeting* (pp. 2447-2448). IEEE.

[28] Hassan, S. A., Samsuzzaman, M., Hossain, M. J., Akhtaruzzaman, M., & Islam, T. (2017, December). Compact planar UWB antenna with 3.5/5.8 GHz dual band-notched characteristics for IoT application. In *2017 IEEE International Conference on Telecommunications and Photonics (ICTP)* (pp. 195-199). IEEE.

[29] Masius, A. A., Wong, Y. C., & Lau, K. T. (2018). Miniature high gain slot-fed rectangular dielectric resonator antenna for IoT RF energy harvesting. *AEU-International Journal of Electronics and Communications*, *85*, 39-46.

[30] Naidu, P. V., & Kumar, A. (2018). ACS-fed e-shaped dual band uniplanar printed antenna for modern wireless communication applications. *Radioelectronics and Communications Systems*, *61*(3), 87-93.

[31] Saha, T. K., Knaus, T. N., Khosla, A., & Sekhar, P. K. (2018). A CPW-fed flexible UWB antenna for IoT applications. *Microsystem Technologies*, 1-7.

[32] Arun, V., & Marx, L. K. (2018). Internet of Things controlled reconfigurable antenna for RF harvesting. *Defense Science Journal*, *68*, 566-571.

[33] Mao, Y., Guo, S., & Chen, M. (2018). Compact dual-band monopole antenna with defected ground plane for Internet of things. *IET Microwaves, Antennas & Propagation*, *12*(8), 1332-1338.

[34] Shafique, K., Khawaja, B. A., Khurram, M. D., Sibtain, S. M., Siddiqui, Y., Mustaqim, M., ... & Yang, X. (2018). Energy harvesting using a low-cost rectenna for Internet of Things (IoT) applications. *IEEE access*, *6*, 30932-30941.

[35] Sanil, N., Venkat, P. A. N., & Ahmed, M. R. (2018, August). Design and performance analysis of multiband microstrip antennas for IoT applications via satellite communication. In *2018 Second International Conference on Green Computing and Internet of Things (ICGCIoT)* (pp. 60-63). IEEE.

[36] Kumar, P., Ghivela, G. C., & Sengupta, J. (2019, July). Optimized N-sided polygon shaped microstrip patch antenna for UWB application. In *2019 10th International Conference on Computing, Communication and Networking Technologies (ICCCNT)* (pp. 1-7). IEEE.

[37] Park, K., Joung, J., Lim, S., & Lee, H. L. (2019). A compact crossed inverted-V antenna with a common reflector for polarization diversity in the IoT. *Electronics*, *8*(6), 637.

[38] Islam, M. S., Islam, M. T., Ullah, M. A., Beng, G. K., Amin, N., & Misran, N. (2019). A modified meander line microstrip patch antenna with enhanced bandwidth for 2.4 GHz ISM-band Internet of Things (IoT) applications. *IEEE Access*, *7*, 127850-127861.

[39] Vamseekrishna, A., Madhav, B. T. P., Anilkumar, T., & Reddy, L. S. S. (2019). An IoT controlled octahedron frequency reconfigurable multiband antenna for microwave sensing applications. *IEEE Sensors Letters*, *3*(10), 1-4.

[40] Khalili, H. F., Lemey, S., Caytan, O., Deckmyn, T., Agneessens, S., Ginste, D. V., & Rogier, H. (2019). Biodegradable dual semicircular patch antenna tile for smart floors. *IEEE Antennas and Wireless Propagation Letters*, *18*(2), 368-372.

[41] Piao, H., Zahid, M. Z., Jin, Y., & Qu, L. (2019). Compact loop-type antenna with ground-mode tuning for dual-band IoT applications. *Journal of Electromagnetic Waves and Applications*, *33*(11), 1453-1462.

[42] de Cos Gómez, M. E., Álvarez, H. F., González, C. G., Valcarce, B. P., Olenick, J., & Las-Heras, F. (2019, March). Ultra-thin compact flexible antenna for IoT applications. In *2019 13th European Conference on Antennas and Propagation (EuCAP)* (pp. 1-4). IEEE.

[43] Burtowy, M., Rzymowski, M., & Kulas, L. (2019). Low-profile ESPAR antenna for RSS-based DoA estimation in IoT applications. *IEEE Access*, *7*, 17403-17411.

[44] Ramesh, G. P., & Kumar, N. M. (2020). Design of RZF antenna for ECG monitoring using IoT. *Multimedia Tools and Applications*, *79*(5), 4011-4026.

[45] Elijah, A. A., & Mokayef, M. (2020). Miniature microstrip antenna for IoT application. *Materials Today: Proceedings*, *29*, 43-47.

[46] Olan-Nuñez, K. N., Murphy-Arteaga, R. S., & Colín-Beltrán, E. (2020). Miniature patch and slot microstrip arrays for IoT and ISM band applications. *IEEE Access*, *8*, 102846-102854.

[47] Singh, P. P., Goswami, P. K., Sharma, S. K., & Goswami, G. (2020). Frequency reconfigurable multiband antenna for IoT applications in WLAN, Wi-Max, and C-band. *Progress In Electromagnetics Research C*, *102*, 149-162.

[48] Kirtania, S. G., Younes, B. A., Hossain, A. R., Karacolak, T., & Sekhar, P. K. (2021). CPW-fed flexible ultra-wideband antenna for IoT applications. *Micromachines*, *12*(4), 453.

[49] Rashid, T., Hasan, M. N., & Mazumdar, P. S. (2021, February). An L-slot Compact Antenna for Medical, Wearable Device and IoT Applications. In *2021 International Conference on Information and Communication Technology for Sustainable Development (ICICT4SD)* (pp. 100-104). IEEE.

[50] Abdulkawi, W. M., Sheta, A. F. A., Elshafiey, I., & Alkanhal, M. A. (2021). Design of Low-Profile Single-and Dual-Band Antennas for IoT Applications. *Electronics*, *10*(22), 2766.

[51] Sabban, A. (2022). Wearable circular polarized antennas for health care, 5G, energy harvesting, and IoT systems. *Electronics*, *11*(3), 427.

[52] Patnaik, A., & Kartikeyan, M. V. (2022). Compact dual and triple band antennas for 5G-IOT applications. *International Journal of Microwave and Wireless Technologies*, *14*(1), 115-122.

[53] Sreelekshmi, S., & Sankar, S. P. (2022). A square ring and single split resonator based wearable antenna for Microwave energy harvesting for IoT nodes. *Sustainable Energy Technologies and Assessments*, *52*, 102217.

[54] Moutaouakil, A., Jabrane, Y., Reha, A., & Koumina, A. (2022). Design, Realization and Measurements of Printed Patch Antenna with Circular Slots for UWB and IoT Applications. *Journal of Information Technology Management*, *14*(4), 57-68.

[55] Kim, D. W. and S. Nam, “Systematic design of a multiport MIMO antenna with bilateral symmetrybased on characteristic mode analysis,” *IEEE Transactions on Antennas and Propagation*, Vol. 66, No. 3, 1076–1085, 2017.

[56] Yu, K., Y. Li, and X. Liu, “Mutual coupling reduction of a MIMO antenna array using 3-D novelmeta-material structures,” *The Applied Computational Electromagnetics Society Journal (ACES)*, 758–763, 2018.

[57] Kiem, N. K. and D. N. Chien, “A transmission line decoupling technique for enhancement ofport isolation of dual-band MIMO antennas,” *Journal of Electromagnetic Waves and Applications*, Vol. 32, No. 10, 1195–1211, 2018.

[58] Jha, K. R., B. Bukhari, C. Singh, G. Mishra, and S. K. Sharma, “Compact planar multistandardMIMO antenna for IoT applications,” *IEEE Transactions on Antennas and Propagation*, Vol. 66, No. 7, 3327–3336, 2018.

[59] Chouhan, S., D. K. Panda, V. S. Kushwah, and P. K. Mishra, “Octagonal-shaped wideband MIMOantenna for human interface device and S-band application,” *International Journal of Microwave and Wireless Technologies*, Vol. 11, No. 3, 287–296, 2019.

[60] Moradi, A., R. Ngah, and M. Khalily, “Polarized diversity compact planar MIMO antenna forwireless access point applications,” *Progress In Electromagnetics Research C*, Vol. 91, 115–127, 2019.

[61] Rezapour, M., J. Rashed-Mohassel, A. Keshtkar, and M. Naser-Moghadasi, “Isolation enhancementof rectangular dielectric resonator antennas using wideband double slit complementary split ring resonators,” *International Journal of RF and Microwave Computer-Aided Engineering*, Vol. 29, No. 7, e21746, 2019.

[62] Hu, W., L. Qian, L. Wen, X. Yang, and Y. Yin, “Compact dual-band antenna based on CRLH-TLfor WWAN/LTE terminal applications,” *International Journal of RF and Microwave ComputerAided Engineering*, Vol. 29, No. 4, e21587, 2019.

[63] Sanad, M. and N. Hassan, “Orthogonally polarized MIMO LTE/5G terminal antennas for handsetsand IoT applications,” *2019 IEEE Radio and Wireless Symposium (RWS)*, 1–4, IEEE, January 2019.

[64] Chouhan, S., D. K. Panda, and V. S. Kushwah, “Modified circular common element four-portmultiple-input-multiple-output antenna using diagonal parasitic

element," *International Journal of RF and Microwave Computer-Aided Engineering*, Vol. 29, No. 2, e21527, 2019.

[65] Kumar, P., S. Urooj, and A. Malibari, "Design and implementation of quad-element super-widebandMIMO antenna for IoT applications," *IEEE Access*, Vol. 8, 226697–226704, 2020.

[66] Kumar, N. and R. Khanna, "A compact multi-band multi-input multi-output antenna for 4G/5Gand IoT devices using theory of characteristic modes," *International Journal of RF and Microwave Computer-Aided Engineering*, Vol. 30, No. 1, e22012, 2020.

[67] Maurya, N. K. and R. Bhattacharya, "Design of compact dual-polarized multiband MIMO antennausing near-field for IoT," *AEU — International Journal of Electronics and Communications*, Vol. 117, 153091, 2020.

[68] Dkiouak, A., A. Zakriti, and M. El Ouahabi, "Design of a compact dual-band MIMO antennawith high isolation for WLAN and X-band satellite by using orthogonal polarization," *Journal of Electromagnetic Waves and Applications*, Vol. 34, No. 9, 1254–1267, 2020.

[69] Palanisamy, P., & Subramani, M. (2021). Design of metallic via based octa-port UWB MIMO antenna for IoT applications. *IETE Journal of Research*, 1-11.

[70] Thiruvenkadam, S., Parthasarathy, E., Palaniswamy, S. K., Kumar, S., & Wang, L. (2021). Design and performance analysis of a compact planar MIMO antenna for IoT applications. *Sensors*, *21*(23), 7909.

[71] Chattha, H. T., Ishfaq, M. K., Khawaja, B. A., Sharif, A., & Sheriff, N. (2021). Compact multiport MIMO antenna system for 5G IoT and cellular handheld applications. *IEEE Antennas and Wireless Propagation Letters*, *20*(11), 2136-2140.

[72] Mathur, R., & Dwari, S. (2021). Frequency and port reconfigurable MIMO antenna for UWB/5G/WLAN band IoT applications. *International Journal of RF and Microwave Computer-Aided Engineering*, *31*(7), e22692.

[73] Ramasamy, R., Rajkumar, R., Sellapillai, S., Babu, M. V., & Kumar, C. V. (2021, November). A Compact UWB MIMO Antenna for IoT Applications. In *2021 Innovations in Power and Advanced Computing Technologies (i-PACT)* (pp. 1-5). IEEE.

[74] Sharma, D., Kanaujia, B. K., & Kumar, S. (2021). Compact multi-standard planar MIMO antenna for IoT/WLAN/Sub-6 GHz/X-band applications. *Wireless Networks*, *27*(4), 2671-2689.

[75] Khurshid, A., J. Dong, M. S. Ahmad, and R. Shi, "Optimized super-wideband MIMO antennawith high isolation for IoT applications," *Micromachines*, Vol. 13, No. 4, 514, 2022.

[76] Nagendra, R., & Swarnalatha, S. (2022). Design and performance of four port MIMO antenna for IOT applications. *ICT Express*, *8*(2), 235-238.

[77] https://www.ansys.com/en-in/products/electronics/ansys-hfss

[78] Kafle, V. P., Y. Fukushima, and H. Harai, "Internet of things standardization in ITU and prospective networking technologies," IEEE Communications Magazine, Vol. 54, No. 9, 43–49, 2016.

[79] Chouhan, S., D. K. Panda, and V. S. Kushwah, "Modified circular common element four-port multiple-input-multiple-output antenna using diagonal parasitic element," International Journal of RF and Microwave Computer-Aided Engineering, Vol. 29, No. 2, e21527, 2019.

[80] Nashuha, S. H., Lee, G. H., Kumar, S., Choi, H. C., & Kim, K. W. (2020). Ultra-wideband trapezoidal log-periodic antenna integrated with an elliptical lens. *Electronics*, *9*(12), 2169.

[81] Modasiya, S. S., & Rathod, J. M. (2020). Design of Modified Wideband Log Periodic Microstrip Antenna with Slot for Navigational Application. In Advances in Electrical and Computer Technologies (pp. 997-1006). Springer, Singapore.

[82] Panda, R. A., Panda, M., Nayak, P. K., & Mishra, D. (2019, January). Log periodic implementation of butterfly shaped patch antenna with gain enhancement technique for

X-band applications. In International Conference on Intelligent Computing and Communication Technologies (pp. 20-28). Springer, Singapore.

[83] Diallo, Kadidiatou, et al. "Efficient dual-band pifa antenna for the internet of things (iot)." 2018 IEEE Conference on Antenna Measurements & Applications (CAMA). IEEE, 2018.IEEE.

[84] Wang, Wensong, et al. "Compact Broadband Four-Port MIMO Antenna for 5G and IoT Applications." 2019 IEEE Asia-Pacific Microwave Conference (APMC). IEEE, 2019.

[85] Gandhimohan, J., and T. Shanmuganantham. "Coplanar waveguide fed triangular/circular patch antenna in UWB range for BAN." 2017 IEEE Applied Electromagnetics Conference (AEMC). IEEE, 2017.Electromagnetics Conference (AEMC). IEEE, 2017.

[86] Manouare, Ahmed Zakaria, et al. "Miniaturized triple wideband CPW-fed patch antenna with a defected ground structure for WLAN/WiMAX applications." Journal of Microwaves, Optoelectronics and Electromagnetic Applications 15.3 (2016): 157-169.

[87] Roges, R., Malik, P. K., & Sharma, S. (2021, June). A compact CPW-fed log-periodic antenna for IoT applications. In 2021 International Conference on Communication, Control and Information Sciences (ICCISc) (Vol. 1, pp. 1-5). IEEE.

[88] Roges, R., Malik, P. K., Sharma, S., & Gehlot, A. (2022). A Compact Two-Port MIMO Antenna with Suppressed Mutual Coupling for IoT Applications. Progress In Electromagnetics Research B, 96, 19-38.

[89] Otoum, Y., Liu, D., & Nayak, A. (2019). DL-IDS: a deep learning–based intrusion detection framework for securing IoT. *Transactions on Emerging Telecommunications Technologies*, e3803.

[90] Al-Sarawi, S., Anbar, M., Alieyan, K., & Alzubaidi, M. (2017, May). Internet of Things (IoT) communication protocols. In *2017 8th International conference on information technology (ICIT)* (pp. 685-690). IEEE.

[91] Elhadi, S., Marzak, A., Sael, N., & Merzouk, S. (2018). Comparative study of IoT protocols. *Smart Application and Data Analysis for Smart Cities (SADASC'18)*.

[92] Chahid, Y., Benabdellah, M., & Azizi, A. (2017, November). Internet of things protocols comparison, architecture, vulnerabilities and security: State of the art. In *Proceedings of the 2nd International Conference on Computing and Wireless Communication Systems* (pp. 1-6).
[93] Roges, R., & Malik, P. K. (2021). Planar and printed antennas for Internet of Things-enabled environment: Opportunities and challenges. *International Journal of Communication Systems*, *34*(15), e4940.
[94] Routray, S. K., & Mohanty, S. (Eds.). (2021). *Principles and Applications of Narrowband Internet of Things (NBIoT)*. IGI Global.
[95] Reha, A., Tarbouch, M., & El Amri, A. (2019, June). A Dual Band Compact PIFA Antenna for Internet of Things Networks Sigfox, Lorawan And Zigbee. In *Colloque sur les Objets et systèmes Connectés*.
[96] Tiwari, P., & Malik, P. K. (2021). Design of Planer Wide Band Micro-Strip Patch Antenna for 5G Wireless Communication Applications. In *Proceedings of Second International Conference on Computing, Communications, and Cyber-Security* (pp. 109-120). Springer, Singapore.
[97] Aldahdouh, K. A., Darabkh, K. A., & Al-Sit, W. (2019, March). A survey of 5G emerging wireless technologies featuring LoRaWAN, Sigfox, NB-IoT and LTE-M. In *2019 International Conference on Wireless Communications Signal Processing and Networking (WiSPNET)* (pp. 561-566). IEEE.
[98] Borkar, S. R. (2020). Long-term evolution for machines (LTE-M). In *LPWAN Technologies for IoT and M2M Applications* (pp. 145-166). Academic Press.
[99] Chaudhari, B. S., Zennaro, M., & Borkar, S. (2020). LPWAN technologies: Emerging application characteristics, requirements, and design considerations. *Future Internet*, *12*(3), 46.
[100] Mekki, K., Bajic, E., Chaxel, F., & Meyer, F. (2019). A comparative study of LPWAN technologies for large-scale IoT deployment. *ICT express*, *5*(1), 1-7.
[101] Singh, R. K., Aernouts, M., De Meyer, M., Weyn, M., & Berkvens, R. (2020). Leveraging LoRaWAN technology for precision agriculture in greenhouses. *Sensors*, *20*(7), 1827.
[102] Al Homssi, B., Al-Hourani, A., Magowe, K., Delaney, J., Tom, N., Ying, J., ... & Gomez, K. M. (2020). A Framework for the Design and Deployment of Large-Scale

LPWAN Networks for Smart Cities Applications. *IEEE Internet of Things Magazine*, *4*(1), 53-59.

[103] Olatinwo, D. D., Abu-Mahfouz, A., & Hancke, G. (2019). A survey on LPWAN technologies in WBAN for remote health-care monitoring. *Sensors*, *19*(23), 5268.

[104] Reddy, G. P., & Kumar, Y. P. (2020). Future Wireless Communication Technologies for Smart Grids: A LPWAN Prospective. *Future*.

[105] Trinh, L. H., Nguyen, T. Q. K., Phan, D. D., Tran, V. Q., Bui, V. X., Truong, N. V., & Ferrero, F. (2017, October). Miniature antenna for IoT devices using LoRa technology. In 2017 International Conference on Advanced Technologies for Communications (ATC) (pp. 170-173). IEEE.

[106] Roges, R., Malik, P. K., & Sharma, S. (2022, April). A compact wideband antenna with DGS for IoT applications using LoRa technology. In 2022 10th International Conference on Emerging Trends in Engineering and Technology-Signal and Information Processing (ICETET-SIP-22) (pp. 1-4). IEEE.

[107] Mushtaq, A., Gupta, S. H., & Rajawat, A. (2020, February). Design and performance analysis of LoRa LPWAN antenna for IoT applications. In 2020 7th international conference on signal processing and integrated networks (SPIN) (pp. 1153-1156). IEEE.

[108] Rohan, C., Audet, J., & Keating, A. (2021). Small Split-Ring Resonators as Efficient Antennas for Remote LoRa IOT Systems—A Path to Reduce Physical Interference. Sensors, 21(23), 7779.

[109] Krishnamoorthy, R., Desai, A., Patel, R., & Grover, A. (2021). 4 Element compact triple band MIMO antenna for sub-6 GHz 5G wireless applications. Wireless Networks, 27(6), 3747-3759.

[110] Aminu-Baba, M., Rahim, M. K. A., Zubir, F., Iliyasu, A. Y., Jahun, K. I., Yusoff, M. F. M., ... & Lin, I. K. C. (2021). A compact triband miniaturized MIMO antenna for WLAN applications. AEU-International Journal of Electronics and Communications, 136, 153767.

[111] Pasumarthi, S. R., Kamili, J. B., & Avala, M. P. (2020). Design of tri-band MIMO antenna with improved isolation using DGS and Vias. Wireless Personal Communications, 110(3), 1523-1532.

[112] Rajeshkumar, V., & Rajkumar, R. (2021). SRR loaded compact tri-band MIMO antenna for WLAN/WiMAX applications. Progress In Electromagnetics Research Letters, 95, 43-53.

[113] Naidu, P. V., Dhanekula, M. B., Almustafa, K. M., Kumar, A., Meerja, K. A., & Akkapanthula, S. H. (2021). Design and performance analysis of MAZE shaped quad port ACS fed tri band MIMO antenna for V2V and multi band applications. AEU-International Journal of Electronics and Communications, 134, 153676.

[114] Dou, Y., Chen, Z., Bai, J., Cai, Q., & Liu, G. (2021). Two-port CPW-fed dual-band MIMO antenna for IEEE 802.11 a/b/g applications. International journal of antennas and propagation, 2021.

[115] Huang, J., Dong, G., Cai, Q., Chen, Z., Li, L., & Liu, G. (2021). Dual-band MIMO antenna for 5G/WLAN mobile terminals. Micromachines, 12(5), 489.

[116] Roges, R., Malik, P. K., Sharma, S., Arora, S. K., & Maniraguha, F. (2023). A Miniaturized, Dual-Port, Multiband MIMO with CSRR DGS for Internet of Things Using WLAN Communication Standards. Wireless Communications and Mobile Computing, 2023.

Appendix-A

Acronyms and Abbreviations

Acronyms	**Description**
3D	Three Dimensional
3GPP	3rd Generation Partnership Project
4G	4th Generation
5G	5th Generation
ACS	Asymmetric Coplanar Strip
AI	Artificial Intelligence
AMPS	Advanced Mobile Phone Service
AoC	Antenna on Chip
bps	Bits per Second
BW	Bandwidth
CP	Circular Polarization
CPW	Coplanar Waveguide
CSRR	Complimentary Split Ring Resonator
DG	Diversity Gain
DGS	Defected Ground Structure
DL	Deep Learning
DoA	Direction of Arrival
DRA	Dielectric Resonator Antenna
ECC	Envelope Correlation Coefficient
ECG	Electrocardiogram
EDGE	Enhanced Data for Global Evolution
EM	Electromagnetic
ENIAC	Electronic Numerical Integrator and Computer
FDTD	Finite Difference Time Domain
FEM	Finite Element Method
FR4	Flame Retardant 4
GHz	Giga Hertz

GPS	Global Positioning System
GUI	Graphical User Interface
HFSS	High Frequency Structure Simulator
IC	Integrated Circuit
IEEE	Institute of Electrical and Electronics Engineers
IoT	Internet of Things
ISM	Industrial Scientific and Medical
KHz	Kilo Hertz
LHCP	Left Hand Circular Polarized
LoRa	Long Range
LPDA	Log-Periodic Antenna
LPWAN	Low-Power Wide-Area Network
LTE	Long Term Evolution
M2M	Machine to Machine
MEG	Mean Effective Gain
MIMO	Multiple Input Multiple Output
MISO	Multiple Input Single Output
ML	Machine Learning
MoM	Method of Moments
MPA	Microstrip Patch Antenna
NodeMCU	Node Microcontroller Unit
PC	Personal Computer
PCB	Printed Circuit Board
PIFA	Planar Inverted-F Antenna
PIN Diode	Positive-Intrinsic Negative Diode
RADAR	Radio Detection and Ranging
RF	Radio Frequency
RFID	Radio Frequency Identification
RHCP	Right Hand Circular Polarized
RL	Return Loss
SAR	Specific Absorption Rate

SISO	Single Input Single Output
SIMO	Single Input Multiple Output
SMA	Sub-Miniature Version A
SNR	Signal to Noise Ratio
SRR	Split Ring Resonator
TARC	Total Active Reflection Co-efficient
TV	Television
UHF	Ultra-High Frequency
UMTS	Universal Mobile Telecommunications System
UWB	Ultra-Wide band
VLSI	Very Large-Scale Integration
VNA	Vector Network Analyzer
VSWR	Voltage Standing Wave Ratio
Wi-Fi	Wireless Fidelity
WiMAX	Worldwide Interoperability for Microwave Access
WLAN	Wireless Local Area Network

Appendix-B

List of Symbols

H	Efficiency
г	reflection coefficient
ε_r	relative permittivity
$\tan \delta$	loss tangent
λ	Wavelength
c	Speed of light
f_r	Resonating frequency
λ_g	Guided wave length

Appendix-C

List of Publications

[1] Roges, R., & Malik, P. K. (2021). Planar and printed antennas for Internet of Things-enabled environment: Opportunities and challenges. *International Journal of Communication Systems*, *34*(15), e4940.

[2] Roges, R., Malik, P. K., Sharma, S., & Gehlot, A. (2022). A Compact Two-Port MIMO Antenna with Suppressed Mutual Coupling for IoT Applications. *Progress In Electromagnetics Research B, 96*, 19-38.

[3] Roges, R., Malik, P. K., Sharma, S., Arora, S. K., & Maniraguha, F. (2023). A Miniaturized, Dual-Port, Multiband MIMO with CSRR DGS for Internet of Things Using WLAN Communication Standards. *Wireless Communications and Mobile Computing*, *2023*.

[4] Bhardwaj, S., Roges, R., Malik, P. K., & Agarwal, S. (2022). Introduction to Internet of Things-enabled printed antenna. In *Printed Antennas: Design and Challenges* (pp. 1-13). CRC Press.

Appendix-D

List of Conferences

[1] Roges, R., Malik, P. K., & Sharma, S. (2021, June). A compact CPW-fed log-periodic antenna for IoT applications. In *2021 International Conference on Communication, Control and Information Sciences (ICCISc)* (Vol. 1, pp. 1-5). IEEE.

[2] Roges, R., Malik, P. K., & Sharma, S. (2022, April). A compact wideband antenna with DGS for IoT applications using LoRa technology. In *2022 10th International Conference on Emerging Trends in Engineering and Technology-Signal and Information Processing (ICETET-SIP-22)* (pp. 1-4). IEEE.